NASA TECHNICAL TRANSLATION

NASA TT F-625

NASA TT F-625

ASTROMETRICAL RESEARCH

Edited by V. P. Shcheglov,
Uzbek SSR Academy of Sciences

"FAN" Press, Tashkent, 1969

NATIONAL AERONAUTICS AND SPACE ADMINISTRATION • WASHINGTON, D. C. • NOVEMBER 1971

NASA TT F-625

ASTROMETRICAL RESEARCH

Edited by V. P. Shcheglov

Uzbek SSR Academy of Sciences

Translation of "Astrometricheskiye Issledovaniya"
"FAN" Press, Tashkent, 1969

NATIONAL AERONAUTICS AND SPACE ADMINISTRATION

For sale by the Clearinghouse for Federal Scientific and Technical Information
Springfield, Virginia 22151 – CFSTI price $3.00

The collection is made up of papers concerned with research on star clusters and proper motions of certain nova-like stars to establish the exact time and to obtain catalogues of right ascensions of stars.

The collection will be of interest to scientists working in the field of photographic astronomy and time.

TABLE OF CONTENTS

INVESTIGATION OF FIVE DIFFUSE STAR CLUSTERS

Kh. Z. Ishmukhamedov

ABSTRACT. This paper discusses the results of an investigation of the diffuse star clusters NGC 1502, NGC 2422, NGC 7380, NGC 7788, and 7790. Three criteria are used in determining whether a star is a cluster member. These criteria are:

1. the position of the star in the color-stellar magnitude diagrám, [V, (B - V)];
2. its position in the two-color diagram, [(U - B), (B - V)];
3. the star's proper motion.

The proper motion criterion was applied by means of Ebbighausen's method. In those cases where the interstellar absorption was found to vary from point to point across a cluster, the individual color excesses of the stars were considered.

Basing his work on the above criteria, the author found that 38 stars were definite members of the cluster NGC 7788. For the cluster NGC 7790, 30 stars satisfied the three criteria for cluster membership. A Cepheid variable, CF Cas, and an eclipsing variable, QX Cas, were found to be members of this cluster. The cluster NGC 2422 was found to have 45 definite members, one of which is a giant star. In the case of the cluster NGC 1502, 35 stars were found to be members. Finally, in the case of the cluster NGC 7380, 25 stars turned out to be definite cluster members.

In addition the author calculated the absolute proper motions and tangential velocities of these clusters corrected for the solar motion. Then using the known radial velocities, the total space peculiar velocities of the clusters in question were calculated.

In the present paper the results are presented for an investigation of /3* the diffuse star clusters NGC 1502, NGC 2422, NGC 7380, NGC 7788, and NGC 7790 as well as their proper motions determined on the basis of a catalogue of proper motions of the stars of these clusters and in their vicinity [1-3]. In the regions of the clusters NGC 7788 and NGC 7790 the proper motions of the stars were first determined by the author of the present paper. The proper motions of 146 stars in the region of the cluster NGC 1502 were determined

* Numbers in the right margin indicate pagination in the foreign text.

previously by Hopmann [4]. However, the observational material used by him was obtained with various instruments, which naturally affected the accuracy of the results. In the region of the cluster NGC 7380 the proper motions of the stars were determined by Li Hen [5], but in his paper there is no list of the members of the cluster and the proper motion of the cluster was not determined.

The proper motions of 2942 stars to the 16th photographic magnitude are presented in papers [1-3] in the five regions of the sky containing the investigated stellar clusters. All five clusters are provided with three-color photometric data determined by Sandage (NGC 7799), Becker (NGC 7788), and Hoag and others (NGC 2422, NGC 1502, NGC 7380).

Method of selection of the stellar members of a cluster. The method of selecting members of a cluster from the stars of the background plays a significant role in determining the proper motions of a diffuse star cluster, since even in the central parts of these clusters a significant number of background stars can be projected.

At present the choice of the members of a cluster is carried out with the aid of proper motions and photometric characteristics of the stars in a given region of the sky. Although many star clusters have been thoroughly investigated photometrically, the same cannot be said regarding their proper motions. To carry out the selection of the members of a cluster we used a method worked out at the Pulkov Observatory [20].

According to this method, the membership of each star in a cluster is determined on the basis of three criteria: the criterion of proper motions and two photometric criteria for which the position of a star in the color-stellar magnitude diagram [V, (B - V)] and in the two-color diagram [(U - B), (B - V)] serve. /4

The method proposed by Ebbighausen [6] is used to exhibit the membership of a star in the cluster based on its proper motion; in addition, in the case of selection in regions of the sky where the value of the interstellar absorption varies from point to point we included the individual color excesses of the stars.

It is known from papers [7,8] that in the regions of the sky containing star

clusters NGC 7788, NGC 7790, and NGC 2422 the interstellar absorption is a constant. Therefore for each of these regions they constructed a color-stellar magnitude diagram [V, (B - V)] and a two-color diagram [(U - B), (B - V)] without taking into account the individual color excesses of the stars: the stars situated on the main sequence or in the giant and supergiant regions were taken as probable cluster members.

For stars in regions of the sky with the stellar clusters where the interstellar absorption is not constant and for stars which have UBV photometry they first found V and the color index (B - V) corrected for reddening and the total interstellar absorption of light and then constructed from them the color-stellar magnitude diagram. Thereupon they calculated the value of the total interstellar absorption in the V region from the formula

$$A_V = 3E_{(B - V)},$$

where

$E_{(B - V)}$ is the color excess in the (B - V) color index.

In contrast to the observed V and (B - V), the values corrected for reddening and total interstellar absorption of light are denoted as V_0 and $(B - V)_0$. They carried out the selection of cluster members from the $[V_0, (B - V)_0]$ diagram and the individual color excesses of the stars. They did not consider the star as a probable cluster member if its color excess stood out sharply among the color excesses of the stars closest to it, differing from the average value of the color excesses by an amount larger than the amplitude of variation of $E_{(B - V)}$ over the total area of the cluster.

With the aid of cluster members thus selected they carried out the final selection of the stars of the cluster. For this, according to Ebbighausen, they constructed a vector diagram from the components of the proper motions of the selected stars. Along the X-axis they plotted μ_x, and along the Y-axis, μ_y. Then as is well known, the members of the cluster should form a compact group around some point whose coordinates evidently should correspond to the average value of the proper motions of all the stars of this group. For selection of the cluster stars in the first approximation by proper motion of the cluster we assume the coordinates of this point, then describe around it three concentric circles having radii corresponding to $r_1 = \sqrt{2}\,\sigma$, $r_2 = 2\sigma$, $r_3 = 2\sqrt{2}\,\sigma$

(σ is the mean square error of a single proper motion of a star).

The stars whose proper motions corresponded to points within the first circle were considered to be the most probable cluster members; the stars corresponding to points located between the first two circles were considered probable members of the clusters. And finally the stars whose proper motions corresponded to points situated between the second and third circles were considered as probably belonging to the background. Evidently all stars whose proper motions in the vector diagram corresponded to points located beyond the limits of the circle of radius $r_3 = 2\sqrt{2}\,\sigma$, should belong to the background.

The application of both methods of selection gave us the possibility of more certainly distinguishing cluster members. /5

Clusters NGC 7788 and NGC 7790. The clusters in question are projected on the celestial sphere not far from one another. On a photograph taken with a normal astrograph the distance between centers of these clusters was equal to 14 mm. Their equatorial coordinates are the following (epoch 1950.0):

for NGC 7788, we have $\alpha = 23^h54^m.2$, $\delta = +61°07'$,
for NGC 7799, we have $\alpha = 23^h55^m.9$, $\delta = +60°57'$.

The proper motions of the stars of these clusters are indicated in the paper [1].

The accuracy of the proper motions of the stars is characterized by their probable errors. For the clusters in question they are:

$$\varepsilon_x = \pm 0''.0018 \quad \text{and} \quad \varepsilon_y = \pm 0''.0020$$

The observational material for the regions under discussion is given in Table 1 of the paper [1].

The photometric data of the stars in the region of the cluster NGC 7788 are contained in the papers [8-10 and others]. K.A. Barkhatova [9] presents the results of photographic determinations of V and (B - V) for 98 stars and (U - B) for 24 stars. I. E. Alekseyev [10] determined from photographs obtained at the Shternberg Astronomical Institute photographic magnitudes for 113 stars and their connection with the B system in the region of the diffuse star clusters NGC 7788 and NGC 7790. As a standard for obtaining the photographic magnitudes of the stars he used 40 stars from the region of NGC 7790, whose magnitudes were determined by Sandage [11] as a result of photographic and photoelectric observations

on the UBV system.

Three-color photometry on the UBV system for stars in the region of the cluster NGC 7788 was carried out by Becker [8]. In all he measured 113 stars of which accurate three-color photometry was carried out for 63 stars (the remaining 50 were too faint to obtain ultraviolet magnitudes). On the basis of these measurements Becker carried out a selection of cluster members from the background stars. As a result 60 stars appeared to be members and two stars, doubtful members of the cluster. In addition, the constancy of the value of the interstellar absorption was established by him. Below are presented some data from this paper, where the true distance modulus, i.e. corrected for the effect of reddening and total interstellar absorption, is denoted by (m - M); the distance from the sun in parsecs by R, and the average color excess in the region of the cluster by $E_{(B-V)}$:

m - M	R	$E_{(B-V)}$	Cluster diameter		Diameter of the nucleus	
			apparent	linear	apparent	linear
$11^m.91$	2410	$0^m.28$	9'	6.3 pc	3'	2.1 pc

We measured 67 stars from Becker's list (46 faint stars were not obtained on our photographs). The color-stellar magnitude diagram is shown in Figure 1 and in Figure 2, the two-color diagram for members of the cluster NGC 7788 based on the photometric data of Becker. The [V, (B - V)] and [(U - B), (B - V)] diagrams are constructed for the 67 stars measured. According to their position 19 stars deviate significantly from the main sequence.

Thus according to the photometric criterion, 48 stars can be taken to be probable members of the cluster. Among them we carried out the selection of cluster members by Ebbighausen's method [6]. The vector diagram is given in Figure 3, where the radii of the three concentric circles were obtained as follows: /6

$$r_1 = 0.^{\circ}0040, \quad r_2 = 0.^{\circ}0056, \quad r_3 = 0.^{\circ}0079.$$

As a result of the selection, it was clear that on the basis of proper motions only 38 stars could be cluster members. Stars 69 and 108 (numbers according to Becker) deviated considerably from the main sequence on the

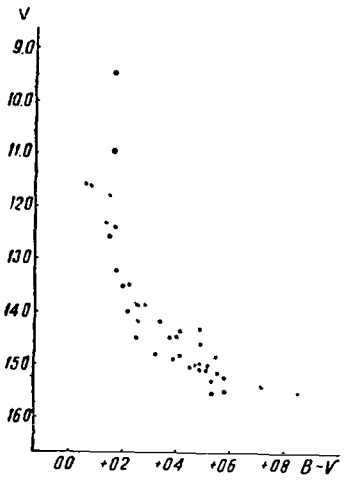

Figure 1.

[(U - B), (B - V)] diagram, although on the [V, (B - V)] diagram and the vector diagram one could assign them as cluster members with assurance. The (U - B) color indices of these stars are probably determined with insufficient accuracy. On this assumption we incorporated them into the list of cluster members (Table 1). The remaining 10 stars (28, 39, 42, 47, 52, 53, 74, 95, 102, and 110) according to the proper motion criterion cannot be cluster members.

In Table 1 the number of the stars according to Ishmukhamedov's catalogue [1] are denoted by $No._I$, the number in Becker's catalogue [8] by $No._B$; m_I is the photographic stellar magnitude from the paper [1]; m_B is the photovisual magnitude: CI_B is the color index; μ_x, μ_y are the annual proper motion. The proper motions of the stars are presented in this paper to four decimal places without rounding off. Therefore in what follows we will use the proper motions of the stars without rounding off.

The probable members of the cluster NGC 7788 are given in Table 2.

The stars located within the limits of the apparent boundaries of the cluster which according to the proper motion criterion can be cluster members are entered here. These stars are denoted by circles on Figure 3.

The relative proper motion of the cluster NGC 7788 is obtained as the average value of μ_x and μ_y of the definitely selected cluster members, i.e. stars included in Table 2. It turned out to be:

$\bar{m}$	$\bar{\mu}_x$	$\bar{\mu}_y$	n
$14^m.2$	$-0''.0008$	$-0''.0002$	38
	$\pm 0''.0007$	$\pm 0''.0003$	

where

$\bar{m}$ is the average stellar magnitude of the cluster members;

n is the number of cluster members; and the probable errors of μ_x and μ_y are shown under their values.

They were determined from the deviations from the average value of the proper motions of the cluster calculated from separate pairs of plates.

Sandage [11] carried out photometry on the UBV system of the stars in the region of the cluster NGC 7790 with the aid of photoelectric and photographic observations. He determined U, B, and V magnitudes for 22 stars and B and V for 78 stars. According to this work the interstellar absorption in the region occupied by the cluster has a constant value equal on the average to $\overline{A}_V = 1^m.56$. /7

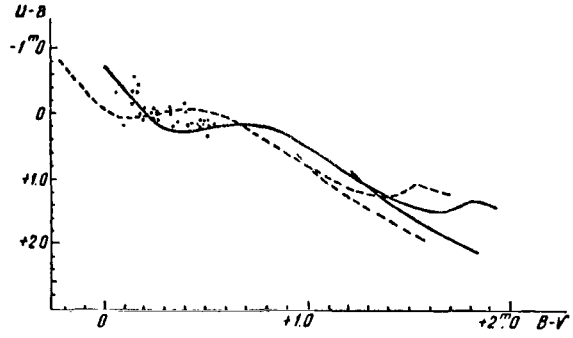

Figure 2.

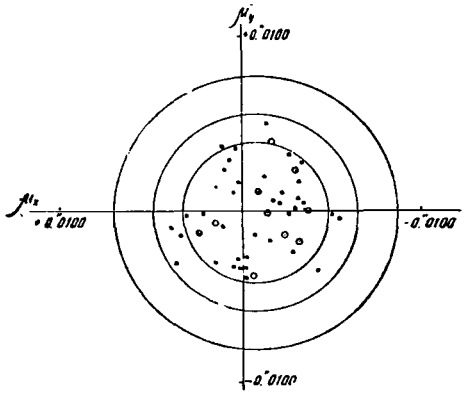

Figure 3.

In addition, for seven stars of the cluster in question he gives $E_{(B-V)}$, the individual color excesses, $M_V(S_p)$, the spectroscopic absolute stellar magnitude, (m - M), the apparent distance moduli, and S_p, the spectral type (Table 3).

The results of a discussion based on UBV photometric data for 106 diffuse star clusters are presented in the paper [7]. We present below some data from the paper [7] for the cluster NGC 7790:

m - M	R	$E_{(B-V)}$	$(B-V)_T$	S_p
$12^m.8 \pm 0^m.3$	3600	$0^m.52$	$-0^m.18$	B 4

where

$(B-V)_T$ is the point on the color-stellar magnitude diagram where the main sequence of the star cluster turns to the right;

S_p is the spectral type of the stars lying at the point $(B-V)_T$.

The remaining notations are the same as in Table 1. The turning point $(B-V)_T$

is determined as the color index $(B - V)_0$ of the earliest main sequence stars among the cluster members corrected for reddening and expresses the evolutionary effect in the color-stellar magnitude diagram.

From $(B - V)_T$ and the spectral class of the stars lying at the point $(B - V)_T$ the cluster NGC 7790 appears to be rather young. In this same region are situated the four variable stars CE Cas_a, CE Cas_b, CF Cas, and QX Cas. The first three of them are Cepheids, and the remaining one is an eclipsing variable. On our photographs the images of the Cepheids CE Cas_a and CE Cas_b were blended so that it was not possible to determine their individual brightnesses. Therefore the proper motion of star 705 given in our catalogue cannot be considered reliable.

TABLE 1

No.$_I$	No.$_B$	m_I	m_B	CI_B			
				$B-V$	$U-B$	μ_x	μ_y
351	21	$15^m.5$	$15^m.11$	$0^m.52$	$+0^m.19$	$+0''.0010$	$-0''.0010$
372	59	15.1	14.86	0.42	+ 26	+ 1	− 29
379	54	16.0	15.42	0.73	—	− 2	− 28
384	34	13.6	13.58	0.21	− 05	− 32	+ 6
391	55	16.0	15.54	0.54	—	− 1	− 33
394	2	12.6	12.62	0.15	− 04	− 35	+ 3
395	12	15.7	15.26	0.58	− 04	− 34	+ 27
396	13	15.6	15.14	0.56	—	− 7	− 15
400	56	15.7	15.32	0.53	—	− 13	+ 19
402	36	14.6	14.54	0.25	+ 17	+ 3	+ 36
404	1	9.5	9.49	0.16	− 30	+ 9	+ 22
405	7	15.4	15.00	0.51	+ 17	− 18	+ 5
406	11	14.8	14.52	0.37	+ 20	− 49	− 2
412	10	11.5	11.63	0.05	− 29	+ 21	− 2
413	5	12.3	12.34	0.14	− 28	− 15	+ 49
420	38	16.0	15.52	0.59		− 27	+ 32
428	50	13.3	13.24	0.25	00	− 22	+ 4
429	61	15.5	15.08	0.53	+ 41	+ 30	− 4
433	48	14.1	14.03	0.22	+ 09	− 23	+ 9
435	62	14.3	14.19	0.26	+ 04	− 2	− 40
440	112	14.7	14.39	0.46	+ 25	− 32	+ 16
445	40	14.4	14.21	0.34	+ 24	− 29	− 26
446	91	15.3	14.85	0.55	+ 21	00	− 34
459	91	15.3	14.85	0.55	+ 26	− 55	− 5
461	90	16.0	14.78	0.33	+ 01	+ 13	+ 13
464	73	13.6	13.49	0.22	+ 10	− 27	− 3
467	74	14.3	14.18	0.25	+ 06	+ 33	− 16
471	67	14.7	14.29	0.50	+ 31	+ 10	+ 36
476	69	14.8	14.50	0.40	− 11	+ 4	− 33
481	94	15.1	14.88	0.40	+ 05	+ 4	+ 10
482	97	14.0	13.88	0.28	+ 19	+ 6	+ 28
483	71	11.0	10.98	0.17	− 53	− 16	+ 19
484	88	15.3	15.01	0.46	+0.26	+ 01	+ 15
489	99	14.0	13.89	0.26	+ 02	+ 14	− 31
497	85	14.9	14.57	0.49	+ 33	− 31	+ 1
381	108	11.6	11.64	0.08	+ 13	+ 16	− 23
468	68	11.8	11.86	0.15	− 47	− 41	− 35
505	101	12.5	12.49	0.18	+ 04	+ 36	− 32

The Cepheid CE Cas and the eclipsing variable QX Cas (corresponding to stars 750 and 840 in our catalogue) were investigated by Sandage [11]. His period and amplitude of brightness variation for the Cepheid CF Cas were found to be the same as in an earlier paper [12]. The amplitude of brightness variation in the V system amounts to $0^m.5$ for the star QX Cas. The period of brightness variation cannot be determined from Sandage's observations.

Kraft [13] presents spectral and photometric data for eight stars in the region of the cluster NGC 7790. On the basis of the data for CF Cas he considers it to be a cluster member.

We constructed the color-stellar magnitude diagram and the two-color diagram from the photometric data of Sandage [11]. Based on the photometric indications, 35 stars, for which he constructed the vector diagram using their proper motions, appeared to be members of the cluster. As a result of the selection 30 stars appeared to be cluster members; they are presented in Table 4, where the numbers of the stars according to Sandage's list [11] are denoted by $No._S$; m_I is the photographic stellar magnitude [1]; V is the photovisual stellar magnitude; (B - V) and (U - B) are the color indices [11]; S_p is the spectral type [11]; $M_V(S_p)$ is the absolute stellar magnitude; and μ_x, μ_y are the annual proper motions expressed in $0''.0001$. According to the position of stars 750 and 840 on the [V, (B - V)] and [(U - B), (B - V)] diagrams, and particularly in the vector diagram, they appear to be cluster members.

/9

TABLE 2

No.$_1$	m_1	μ_x	μ_y
338	$15^m.4$	−0.0015	−0.0002
375	14.1	− 32	− 19
377	14.1	− 24	− 16
398	11.7	− 31	+ 22
399	11.7	− 10	+ 10
424	15.5	+ 23	− 14
436	14.9	− 18	+ 38
454	15.6	+ 14	− 14
493	13.8	− 06	− 38
535	15.3	− 37	00

TABLE 3

№$_S$	№$_I$	S_p	$M_V(S_p)$	V	$m-M$	$E_{(B-V)}$
A	692	B 2 III—IV	$-3^m.2$	$11^m.08$	$14^m.28$	$0^m.51$
D	724	B 9 III	−2.0	12.59	14.59	—
B	768	B 5 IV	−2.2	12.79	14.99	50
O	811	B 9 IV	−1.0	13.54	14.54	51
40	796	B 8 IV	−1.7	13.07	14.77	34
95	784	B 5 IV	−2.2	12.67	14.89	46
99	789	B 7 IV	−1.8	13.34	15.14	50

Stars 886, 232, 835, 847, and 889 appeared in the vector diagram beyond the limit of the circle having radius r_3; we assigned them to the list of background stars. Based on proper motion and position in the sky, there are still six stars which can be considered cluster members, but on the color-stellar magnitude diagram they deviated from the main sequence. We do not have available other photometric data besides that described above, so we cannot categorically state that these stars belong to the cluster; they are given in Table 5.

The color-stellar magnitude diagram and the two-color and vector diagrams based on the proper motions of the stars of the cluster NGC 7790 are presented in Figures 4, 5, and 6, respectively. The relative proper motion of the cluster NGC 7790 was obtained as the average of μ_x and μ_y for the individual stars from Table 4. It was found to be:

$\bar{m}$	$\bar{\mu}_x$	$\bar{\mu}_y$	Number of stars
$14^m.0$	-0".0008	-0".0004	30
	±0".0007	±0".0006	

/10

Here the probable error is presented and $\bar{m}$ is the average stellar magnitude of the cluster members.

TABLE 4

№ I	№ S	m_I	V	$B-V$	$U-V$	S_p	$M_V(S_p)$	μ_x	μ_y
670	88	$15^m.2$	$14^m.89$	$0^m.45$	$-0^m.19$			+0".0005	+0".0013
691	86	14.3	14.02	0.45				— 6	— 3
692	*A*	12.2	11.8	0.24	—0.63	*B*2 V	—3.2	— 25	— 17
699	87	13.9	13.68	0.37	—0.21			+ 22	— 13
702	*J*	13.6	13.30	0.46	+0.36			— 7	— 23
724	*D*	12.8	12.68	0.31		*B*9 III	—2.0	+ 1	0
731	63	15.1	14.84	—0.39	—0.03			— 40	— 17
736	62	13.6	13.32	0.41	+0.10			+ 15	+ 16
741	*B*	12.6	12.16	0.41	+0.02			— 22	— 14
744	61	15.0	14.67	0.44	—0.13			— 14	— 7
756	*Q*	14.1	13.81	0.42	—0.07			+ 8	— 26
757	*x*	15.0	14.62	0.46	—0.08			— 19	— 12
758	82	15.6	15.18	0.52				+ 14	+ 13
759	24	15.6	15.32	0.42				— 10	— 6
772	*R*	14.3	14.14	0.35	—0.05			— 9	— 11
768	*E*	13.0	12.78	0.36	—0.07	*B*5 IV	—2.2	— 21	— 29
784	95	12.8	12.67	0.33	—0.11	*B*5 IV	—2.2	— 3	+ 19
789	99	13.6	13.34	0.40	+0.03	*B*7 IV	—1.8	— 9	+ 32
790	55	13.2	13.06	0.34	+0.02			— 27	+ 23
796	40	13.2	13.07	0.26	—0.01	*B*8 IV	—1.7	— 29	+ 4
806	52	13.31	13.13	0.33	—0.04			+ 31	— 8
811	*O*	13.7	13.54	0.36		*B*9 IV	—1.0	— 16	+ 1
814	*v*	14.9	14.56	0.44	0.00			— 2	— 48
831	36	13.9	13.66	0.40	0.00			+ 8	— 6
857	*H*	13.5	13.13	0.47	+0.42			+ 9	— 13
800	51	15.1	14.82	0.40	—0.04			+ 8	— 6
860	*U*	15.0	14.52	0.58	—0.24			— 34	— 39
750	*CF Cas*	12.0	11.14	1.24	0.87	*G*0	—3.2	— 24	+ 3
840	*QX Cas*	9.7	10.41	0.28	—0.63	*B*1	—3.6	+ 16	+ 17
813	*M*	13.6	13.32	0.38				— 47	+ 23

Cluster NGC 2422. The diffuse stellar cluster NGC 2422 (equatorial coordinates $\alpha_{1950.0} = 07^h33^m.9$, $\delta_{1950.0} = -14°24'$) is situated in the constellation Puppis. The accuracy of the proper motions obtained by us for the stars in the region of this cluster is equal in x to $\varepsilon_x = \pm 0''.0031$ and in y, $\varepsilon_y = \pm 0''.0035$, and the radii of the concentric circles on the vector diagram of the proper motions corresponding to them have the following values:

$$r_1 = 0''.0069,\ r_2 = 0''.0098,\ r_3 = 0''.0138$$

TABLE 5

№I	№S	m_I	V	B−V	μ_x	μ_y
243	39	$13^m.4$	$13^m.36$	$0^m.16$	−0.0046	+0.0001
767	P	14.3	13.60	0.80	+ 29	+ 3
797	L	13.8	13.23	0.72	+ 13	+ 31
838	G	13.5	13.02	0.62	− 20	+ 20
872	K	14.7	12.98	1.72	+ 2	+ 13
890	4	14.8	13.17	1.66	+ 36	− 2

Photometric investigations of the stars in the region of the cluster NGC 2422 are described in the papers [14, 16]. Zug [14] determined the photographic magnitudes and color indices for 43 stars in the cluster and its vicinity and for 32 stars, individual color excesses. Then based on them he carried out a selection of cluster members. It turned out that one star whose spectral class was KO does not appear to be a cluster member. For the remaining 31 stars, Zug obtained the average value of the color excess in the region of the sky occupied by the cluster. /11

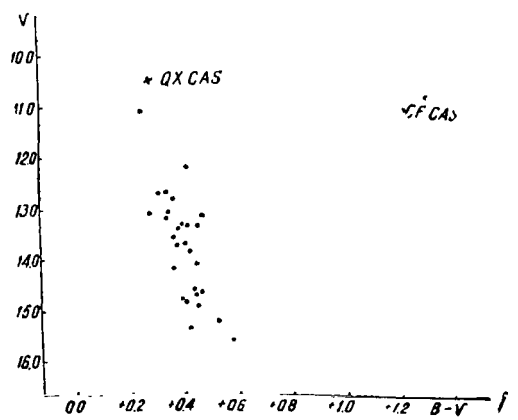

Figure 4

In order to apply the three-color photometry on the UBV system to stars of the southern sky Lynga [15] determined the quantities V, (B - V), and (U - B) of stars in five southern regions of the sky with diffuse star clusters, among which was NGC 2422, for which he presents a stellar map of the region and three-color photometry of 21 stars. The color indices

were obtained by a photoelectric method with the 60-inch Rockfeller reflector of the Boyden Observatory in South Africa.

In the paper [7] are described the results of a photometric investigation of stars in 106 diffuse star clusters. We present below some data from this paper for NGC 2422:

m - M	R	$E_{(B-V)}$	$(B-V)_T$	S_p
$8^m.4 \pm 0^m.2$	480	$0^m.08$	$-0^m.18$	B4

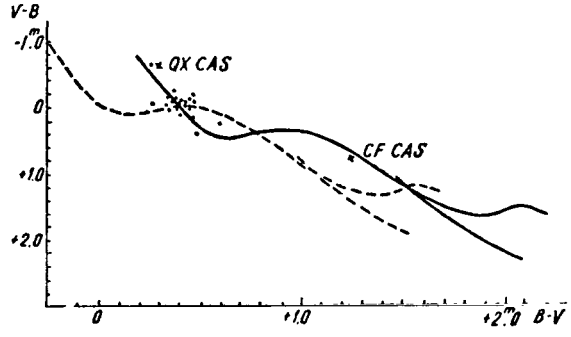

Figure 5.

According to [7], the interstellar absorption in the region of the sky occupied by the cluster is constant and has the following value: $A_V = 0^m.24$.

In the catalogue of the Washington Observatory [16], three-color photometry is presented for 95 stars scattered over a large part of the sky in the cluster NGC 2422 and around it. It includes stars to magnitude $14^m.2$ in the V system. Therefore to select cluster members from background stars according to the photometric criterion, we took the three-color photometry presented in [16]. Of the 95, we measured 75 stars. According /12

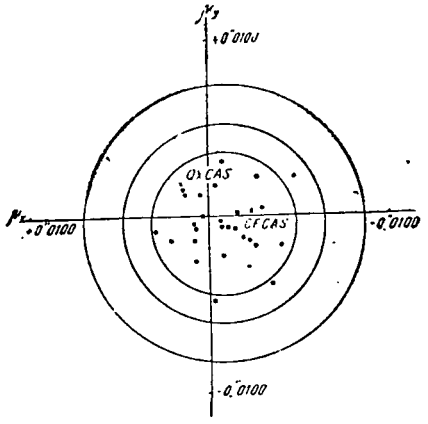

Figure 6.

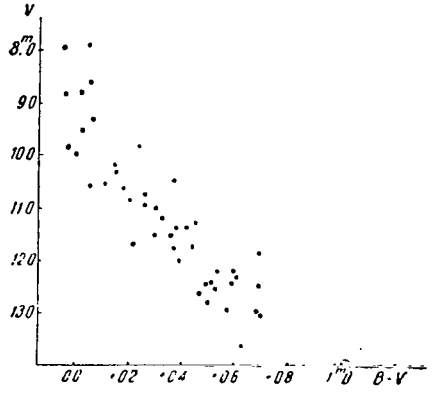

Figure 7.

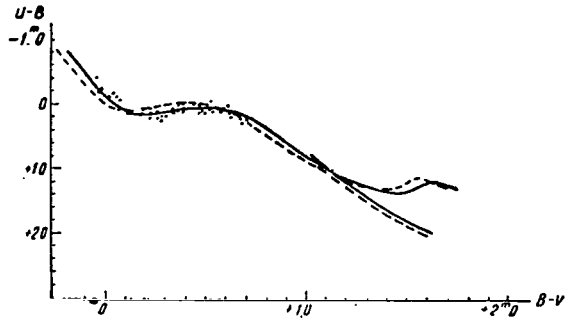

Figure 8.

to the two-color diagram and the color-stellar magnitude diagram constructed by us for cluster members, one can take 53 stars; 20 stars deviated from the main sequence, and stars 266 and 270 (according to our catalogue) were situated in the giant region. The color-stellar magnitude diagram and the two-color diagram are presented in Figures 7 and 8, respectively.

The final selection of cluster members was carried out on the basis of the proper motions of 55 stars. In all, there turned out to be 45 cluster members. One of them (star 266) is a giant. Star 270 was situated on the vector diagram outside the circle of radius r_2 and we assigned it to the background. The vector diagram for cluster members of NGC 2422 is shown in Figure 9, where stars 266 and 270 are denoted by crosses.

A list of the cluster members is given in Table 6; $No._I$, $No._W$, and $No._Z$ /13 are the star numbers from the papers [2],[16], and [14], respectively; the remaining designations are the same as those used in similar preceding tables.

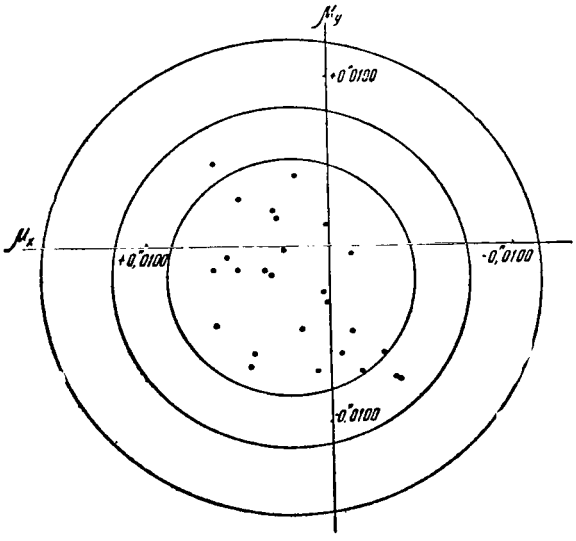

Figure 9.

The relative proper motion of the cluster was obtained as the average of μ_x and μ_y for the individual stars from Table 6:

$\bar{m}$	$\bar{\eta}_x$	$\bar{\mu}_y$	Number of stars
$11.^m3$	$-0".0025$	$-0".0025$	45
	$\pm 0".0003$	$\pm 0".0003$	

Here and in the regions of NGC 1502 and NGC 7380 the internal probable errors are presented.

The investigation of the proper motions of 138 stars to the $12.^m1$ photographic magnitude in the given region

is described in the paper [17]. Three pairs of plates with a difference of epoch of around 60 years obtained with the 30-cm refractor (f = 5732 mm) of the Bonn Observatory served as the observational material in it. The average error of the proper motions of the stars was found to be ±0".0019 in x and ±0".0024 in y, and 36 stars appeared to be cluster members, two of which the author assigns as doubtful cluster members. In addition, the absolute proper motion of the cluster was calculated in this paper based on the selected cluster members: $\mu_x = -0".0096$, $\mu_y = 0".0024$.

Notwithstanding the fact that in our investigations one pair of plates with a smaller difference in epoch (42.1 years) than in the paper [17] was used, the values of the absolute proper motion of the cluster in our paper and in [17] almost coincide:

$$\mu_x = -0".0064, \quad \mu_y = -0".0008.$$

Cluster NGC 1502. The equatorial coordinates of the diffuse star cluster /14
NGC 1502 are as follows:

$$\alpha_{1950.0} = 04^h03^m.4, \quad \delta_{1950.0} = +62^\circ12'.$$

It is located in the constellation Camelopardus. The accuracy of the proper motions obtained for the stars in the region of the cluster is characterized by the probable errors:

$$\varepsilon_x = \pm 0'.0031, \quad \varepsilon_y = \pm 0'.0035.$$

The average photographic stellar magnitude of the cluster stars is $\bar{m} = 12^m.1$. The radii of the concentric circle on the vector diagram of proper motions calculated on the basis of the probable errors are equal, respectively, to: /15
$r_1 = 0".0069$, $r_2 = 0".0098$, $r_3 = 0".0138$. The photometric investigations in the region of the sky under discussion are presented in the papers [14] and [16].

Zug [14] determined the photographic magnitudes and color indices for 50 stars. Using the spectral classification of Trumpler, he also determined the individual color excesses for 31 stars on the basis of which he carried out

TABLE 6

№I	№W	№Z	m_I	V	$B-V$	$U-B$	μ_x	μ_y	Sp
221	8		$10^m.4$	$10^m.31$	$0^m.26$	$0^m.16$	$-0''.0024$	$-0''.0039$	
234	21		7.8	7.91	0.05		— 20	— 26	
258	49	37	12.0	11.66	0.44	0.03	+ 19	— 37	
271	56		12.8	12.40	0.52	0.08	— 41	— 16	
272	64		13.1	12.76	0.49	0.10	— 1	— 107	
274	11	21	10.5	10.58	0.06	0.08	+ 35	— 37	A3
275	10		10.6	10.60	0.19	0.14	— 45	— 44	
284	15		11.1	10.98	0.30	0.17	— 36	+ 28	
285	17		12.2	12.00	0.39	0.09	— 91	+ 2	
291	52		12.6	12.12	0.60	0.04	— 91	— 22	
292	13	24	10.9	10.81	0.22	0.16	— 33	0	A2
297	48	34	11.7	11.64	0.22		— 53	+ 20	
311	18		13.0	12.61	0.47	0.15	+ 48	— 22	
320	9	26	10.5	10.52	0.11	0.13	— 47	— 35	AI
323	38	28	11.0	10.89	0.27	0.23	— 28	— 19	
325	23	10	8.5	8.62	0.06	—0.09	+ 45	— 1	B8
328	26	9	9.2	9.26	0.06	—0.13	— 81	+ 22	
334	65	43	13.2	12.79	0.50	0.16	— 31	— 67	
339	28	15	9.4	9.54	0.03	—0.14	— 23	— 10	B9
340	70		13.6	12.99	0.70	0.23	— 26	+ 16	
354	29	14	9.8	9.74	0.24	0.21	— 22	— 34	
368	60		12.9	12.53	0.53	0.13	+ 4	— 48	
355	78		14.1	13.58	0.63	0.04	— 87	— 67	
370	6		18.7	8.83	0.02	—0.09	— 21	+ 39	
373	37	25	10.8	10.72	0.27	0.27	— 17	— 63	
377	42	32	10.6	11.37	0.42	0.13	— 72	+ 32	
385	7	11	18.6	8.84	—0.04	—0.15	— 86	+ 18	B9
386	54	40	12.8	12.28	0.61	0.11	— 84	— 64	
392	53	42	12.6	12.16	0.54	0.00	— 98	— 70	
394	46	35	11.7	11.52	0.36	0.11	— 8	+ 11	
402	57	41	12.9	12.40	0.59	0.04	+ 7	— 23	
401	19		13.4	12.92	0.57	0.12	— 29	— 31	
405	50	36	12.0	11.73	0.37	0.08	— 36	— 14	O
410	33	23	10.2	10.15	0.22	0.08	— 40	— 69	A2
415	30	13	9.6	9.82	—0.02	—0.13	— 47	— 38	B9
421	16	23	12.4	11.76	0.71	0.17	+ 53	— 21	
423	39		11.3	11.16	0.33	0.08	— 5	— 9	
425	40	30	11.6	11.23	0.47	0.04	— 2	— 44	
446	22	5	7.7	7,95	—0.04	—0.42	— 78	— 5	B8
460	44	31	11.6	11.44	0.31	0.22	— 39	— 81	A5
469	32	16	9.8	9.98	0.00	0.04	+ 38	+ 39	
476	58		13.0	12.45	0.69	0.30	— 35	— 71	
481	69		13.5	12.96	0.68	0.21	+ 3	— 82	
542	43		11.6	11.38	0.38	0.38	— 4	— 52	
266	4	7	9.0	7.99	1.12	1.12	— 13	+ 14	KO

a selection of cluster members. In all, three stars of late spectral class appeared to be background stars based on the color excess. According to Zug, the average color excess in the region of the sky occupied by the cluster NGC 1502 appeared to be equal to $0^m.80$.

Three-color UBV photometry of the stars in the region of the cluster NGC 1502 was carried out by A. A. Hoag, H. L. Johnson, B. Iriarte, R. I. Mitchell, K. L. Hallam, and S. Sharpless. The results of their work are presented in the catalogue of the Washington Observatory [16]. In this catalogue there are contained in all 68 stars in the region of the sky under discussion, scattered

over a rather large area; several stars within the apparent boundaries of the cluster are not covered by the photometric investigations.

For various reasons 14 of the 68 stars were not measured by us. Therefore selection of cluster members based on the criterion of proper motion of the stars was carried out by us for only 54 stars which had accurate three-color photometry on the UBV system. In the paper [7] the cluster NGC 1502 was investigated along with other clusters. Below some data are presented for the cluster NGC 1502 from this paper:

m - M	R	$E_{(B - V)}$	$(B - V)_T$	S_p
$9^m.7 \pm 0^m.4$	880	$0^m.77$	$-0^m.29$	B O

(here the notations are the same as in Tables 1 and 5); as is evident, the cluster NGC 1502 appears to be very young based on $(B - V)_T$ and the spectral type S_p. Hopmann [4] considers the maximum age of this cluster to be of the order of 5×10^6 years.

According to the paper [7], the value of the insterstellar absorption in the region of the sky occupied by the cluster NGC 1502 varies within the limits $0^m.68$-$0^m.84$. Therefore prior to carrying out the selection of cluster members from background stars, we investigated the distribution of color excesses over regions of the sky, for which the three-color UBV photometric data presented in the catalogue of the Washington Observatory [16] was used.

With the aid of Johnson's nomogram [18] for the quantities B - V and U - B, we found the color excesses for each star. One can apply this nomogram only to stars of the main sequence of spectral class earlier than AO. Meanwhile not all the stars measured by us had spectral data available. Therefore at first we selected stars which were suitable on the two-color diagram for application of Johnson's nomogram and then arranged the individual color excesses obtained in the system of coordinates measured by us over the area of the sky occupied by the cluster. In order to lessen the effect of accidental errors on the determination of the individual color excesses, the region of the sky occupied by the cluster was divided into small sections, and in each section the average value of $E_{(B - V)}$, i.e., $\overline{E}_{(B - V)}$, was taken.

The final results are presented in Table 7 and in Figure 10, where x and y /16 are the average values of the rectangular coordinates of the stars located in the given section of the sky (they are expressed in minutes of arc and referred to the point having equatorial coordinates $\alpha_{1950.0} = 04^h03^m.4$, $\delta_{1950.0} = +62°12'$); $\overline{E}_{(B-V)}$ is the average value of the color excess in the given section, and ϵ is its probable error.

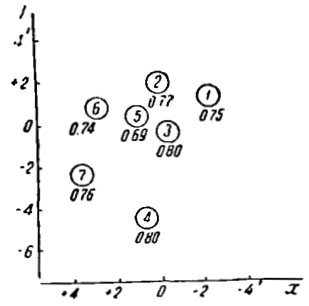

Figure 10. Distribution of the color excesses in the region of the cluster NGC 1502.

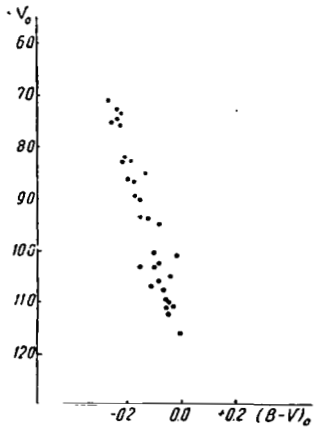

Figure 11.

We calculated the probable error on the basis of the deviations of the individual $E_{(B-V)}$ values from the average value of the color excesses for the stars situated in the corresponding section. In Figure 10 each section

TABLE 7

Section No.	Number of stars	x	y	$\overline{E}_{(B-V)}$	ϵ
1	3	−2.3	+1.5	$0^m.75$	$\pm 0^m.02$
2	4	+0.1	+2.1	0.77	±0.01
3	5	−0.3	−0.4	0.80	±0.01
4	5	+0.7	−4.5	0.80	±0.02
5	5	+1.0	+0.5	0.69	±0.01
6	4	+2.8	+0.8	0.74	±0.02
7	4	+3.8	−2.3	0.76	±0.01

is surrounded by a circle whose center corresponds to the average values of the rectangular coordinates of the stars of each section. The number of the section is inscribed in the circle, and under it, the value of $\overline{E}_{(B - V)}$. As is evident from Figure 10 and Table 7, although the investigated region of the sky is small (of the order of 10'), the distribution of absorbing material situated between the sun and the cluster NGC 1502 is rather nonuniform.

The selection of cluster stars was carried out by the investigators using approximations. At first the cluster members were selected from the color-stellar magnitude diagram. Thereupon the diagram was constructed after correction of the V and B - V values for each star for interstellar reddening and total light absorption. The $[V_0, (B - V)_0]$ diagram for the stars finally selected as members of the cluster under investigation is given in Figure 11. /17

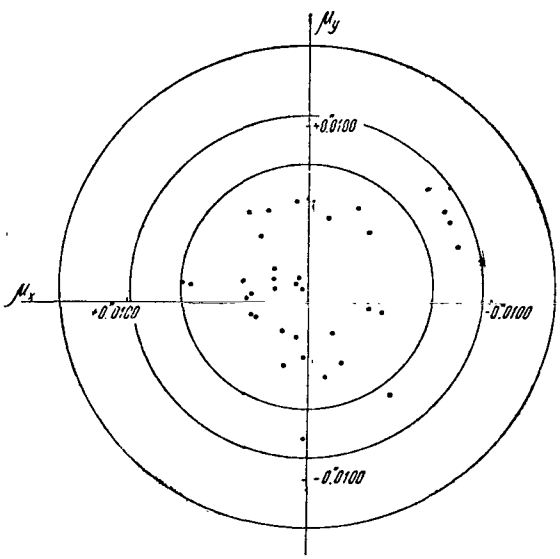

Figure 12.

On the initially constructed $[V_0, (B - V)_0]$ diagram 40 stars were situated along the main sequence. In order to consider them as cluster members with assurance according to the photometric criterion, we carried out an additional selection of cluster members from the background stars on the basis of their individual color excesses. Thereupon the stars 161, 164, 152, and 180 of our catalogue turned out to be background stars; one can assign the remaining 36 stars to cluster membership with assurance on the basis of the photometric criterion.

The final selection of cluster members among the 36 stars was carried out on the basis of their proper motions. As a result, 35 stars turned out to be cluster members. The vector diagram for the cluster members is presented in Figure 12, and a list of them is given in Table 8, in which $No._I$, $No._Z$, and $No._W$ denote the numbers of the stars from the

papers [3],[14], and [16], respectively; m_I is the photographic stellar magnitude in the international system [1]; V_0 and $(B - V)_0$ are the stellar magnitude and the color index corrected for reddening and total light absorption [16]; $E_{(B - V)}$ is the color excess; μ_x and μ_y are the annual proper motion expressed in 0".0001 [3]; and S_p is the spectral type of the star according to Trumpler.

The relative proper motion of the cluster NGC 1502 was obtained as the average of μ_x and μ_y of the individual stars (Table 8); it turned out to be equal to:

$\overline{m}$	$\overline{\mu}_x$	$\overline{\mu}_y$	Number of stars
$12^m.1$	+0".0001	+0".0009	35
	±0".0003	±0".0003	

/18

where $\overline{m}$ is the average stellar magnitude of the cluster members.

TABLE 8

№I	№Z	№W	m_I	V_0	$(B-V)_0$	$E_{(B-V)}$	μ_x	μ_y	S_p
219		3	9.8	7.58	−0.23	+0.66	+0.0005	+0.0014	
161	8	5	10.0	7.24	−0.24	+0.79	− 9	− 41	B5
147	7	6	10.1	7.14	−0.27	+0.84	+ 3	− 31	B3
156	10	7	10.2	7.46	−0.24	+0.78	+ 14	− 36	B3
186		57	14.4	11.62	0.00	+0.71	− 33	+ 40	
171	37	47	13.9	10.76	−0.11	+0.84	− 78	+ 49	
191	33	19	13.4	10.30	−0.10	+0.82	+ 19	+ 19	
158	26	16	12.9	10.31	−0.16	+0.71	− 27	+ 53	B8
152		53	14.2	11.02	−0.05	+0.83	− 40	− 5	
178	13	10	11.2	8.29	−0.19	+0.81	+ 2	− 78	B5
212	44	52	14.0	11.10	−0.03	+0.76	+ 36	+ 13	
217	42	50	14.0	11.11	−0.05	+0.75	+ 30	− 8	
202	46	23	14.2	11.19	−0.05	+0.79	− 33	− 3	
197	20	14	12.1	9.37	−0.15	+0.74	+ 7	+ 58	
164	36	43	13.6	10.52	−0.04	+0.80	− 44	− 52	A0
159	9	27	9.6	6.55	−0.22	+0.85	+ 66	+ 11	B3
149	14	8	10.9	8.33	−0.22	+0.72	+ 19	+ 9	B4
181		41	13.2	10.74	−0.07	+0.67	+ 71	+ 12	
204	17	31	11.2	8.51	−0.13	+0.74	+ 3	+ 9	B8
168		34	11.6	9.00	−0.15	+0.71	− 83	+ 32	
195	25	33	11.4	8.25	−0.21	+0.87	− 65	+ 65	B7
208	6	28	9.7	7.48	−0.26	+0.66	+ 15	− 17	B2
196	11	29	10.2	7.36	−0.23	+0.79	− 11	+ 49	B3
185	23	36	11.9	9.43	−0.13	+0.69	− 74	+ 52	B8
167	32	40	13.2	10.60	−0.09	+0.71	+ 27	+ 38	
182	18	35	11.5	9.25	−0.18	+0.65	+ 22	+ 54	B6
132	28	15	12.8	10.09	−0.02	+0.72	+ 33	+ 52	B9
137	30	38	13.1	10.08	−0.11	+0.82	+ 32	+ 5	B2
165	16	32	11.2	8.66	−0.18	+0.72	+ 19	+ 14	B8
142	15	9	11.1	8.62	−0.20	+0.70	+ 32	− 7	B2
157	19	13	11.9	8.93	−0.17	+0.82	+ 6	+ 11	
194	27	17	13.1	10.25	−0.09	+0.76	+ 34	+ 3	
151	43	49	14.0	10.96	−0.06	+0.80	+ 7	− 20	
172	22	12	11.8	9.11	−0.17	+0.75	− 13	− 17	
133	29	37	12.8	9.79	−0.08	+0.81	− 18	− 34	

Hopmann [4] determined the proper motions of 146 stars to the 13th photographic magnitude in the cluster NGC 1502 and its surroundings. As observational material he used the following: first epoch, five plates obtained at the Washington Observatory in 1906; second epoch, two photographs taken with the normal astrograph at Vienna, and four photographs taken in 1955 with the 10-cm refractor of the McCormick Observatory.

He found the average error of the proper motions of the stars to be of the order of ±0".004 in x and ±0".005 in y. According to Hopmann, 25 stars appeared to be cluster members, of which he considers the cluster membership of 6 stars to be doubtful. For the remaining 19 definite cluster members the following was obtained:

$$\mu_x = +0''.0011, \quad \mu_y = +0''.0100.$$

Cluster NGC 7380. The diffuse star cluster NGC 7380 ($\alpha_{1950.0} = 22^h44^m.9$, $\delta_{1950.0} = +57°52'$) is located in the constellation Cepheus. The probable errors of the proper motions of the stars in this region were found to be the same as in the case of the cluster NGC 1502, i.e., $\varepsilon_x = \pm 0''.0031$, $\varepsilon_y = \pm 0''.0035$. The radii of the concentric circles on the vector diagram of the proper motions are equal, respectively, to: $r_1 = 0''.0069$, $r_2 = 0''.0098$, $r_3 = 0''.0138$. /19

The proper motions of the stars in this region were determined by Li Hen [5]. For this he used one pair of plates with a difference in epoch of 16 years. According to the distribution of the star density in the region of the sky occupied by the cluster, Li Hen estimated the apparent angular size of the cluster NGC 7380 and carried out a selection of cluster members. In order to isolate the cluster from the background stars he applied Ebbighausen's method [6] and took as the value of the radius of the circle in the vector diagram

$$r = \sqrt{|\bar{\mu}_x|^2 + |\bar{\mu}_y|^2},$$

where $\bar{\mu}_x$ and $\bar{\mu}_y$ are the averages of the proper motions of the stars located within the apparent boundaries of the cluster. To the first approximation this is the proper motion of the cluster.

Li Hen did not give a list of cluster members. We present below some data from this paper:

Number of cluster stars	$\bar{\mu}_x$	$\bar{\mu}_y$	r	m	Angular diameter
54	+0".0009	+0".0015	0".0127	$13^m.2$	9'

In the catalogue [16] for the stars in the region of the cluster NGC 7380 are given the results of three-color photometry of 132 stars to the 16th photovisual stellar magnitude, of which we measured 58 stars; the remaining 74 stars were not contained on our photographs. In the paper [7], as was mentioned above, the UBV photometry of 106 diffuse star clusters was investigated. We present some data from this paper for the cluster NGC 7380:

m - M	R	$E_{(B-V)}$	$(B-V)_T$	S_p
$16^m.6 \pm 0^m.3$	2100	$0^m.58$	$-0^m.30$	09

According to $(B - V)_T$ and the spectral type S_p one can assign the cluster NGC 7380 to the category of the very young, with an age close to 10^6 years. According to the paper [7], the value of the interstellar absorption in the area of the sky occupied by this cluster varies within the limits of $0^m.50$ to $0^m.78$. Therefore, prior to carrying out a selection of cluster members from background stars, we investigated, as in the case of NGC 1502, the distribution of color excesses over the sections of the sky occupied by the cluster. The results are presented in Table 9 and in Figure 13, where the notations are the same as in Table 7. Then the stellar magnitudes V and color indices B - V of each star were corrected for the reddening and total light absorption corresponding to the star.

The color-stellar magnitude diagram $[V_0, (B - V)_0]$ based on corrected values of V and B - V for the stars which are definite cluster members is presented in Figure 14. Basing our work on a similar diagram for all stars having UBV photometry and proper motions as well as on the individual color excesses, we carried out the selection of cluster members. Thirty stars were located on /20 the main sequence of this $[V_0, (B - V)_0]$ diagram. According to the color excesses, they also belong to the cluster.

Selection of cluster members by Ebbighausen's method showed that stars 453, 454, 488, 495, and 509 can be taken as background stars, since they are located on the vector diagram outside the circle of radius $r_3 = 2\sqrt{2\sigma}$. The remaining 25 stars can be considered to be definite cluster members. The location of

the cluster members in the vector diagram is shown in Figure 15. A list of these stars is given in Table 10, where the numbers of the stars according to the catalogue [16] are presented in the graph as No.$_W$. The remaining notations are the same as in Table 8.

TABLE 9

Section No.	Number of stars	x'	y'	$\overline{E}_{(B-V)}$	ε
1	2	−9.9	−4.0	$0^m.64$	$\pm 0^m.04$
2	5	−4.2	−1.7	0.59	±0.02
3	4	−1.4	+0.1	0.57	±0.03
4	4	−0.4	+3.0	0.63	±0.02
5	7	+0.4	−3.0	0.60	±0.02
6	7	+2.3	+0.9	0.62	±0.03
7	2	+2.7	−3.3	0.76	∓0.02

Stars 453 and 454, which are located within the apparent boundaries of the cluster, appear to be components of a binary. Based on the photometric data and the spectral class (O6) one can take them to be cluster members. However, the proper motions of the stars deviate significantly from the proper motion of the cluster. Therefore, according to the criterion for selection of cluster members according to the proper motions of the stars,

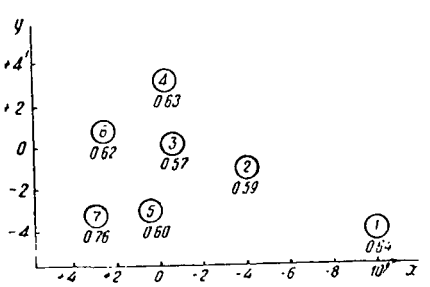

Figure 13. Distribution of color excesses in the region of the cluster NGC 7308 [sic].

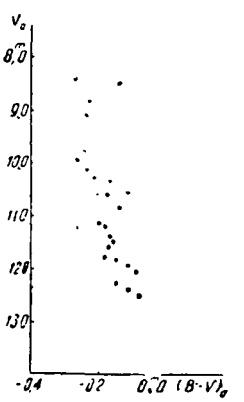

Figure 14.

stars 454 and 453 cannot belong to the cluster. Below we present some data on these stars:

No. I	m	μ_x	μ_y
453	$9^m.3$	+0".0163	-0".0551
454	$7^m.9$	+0".0126	-0".0696

As always, the relative proper motion of the cluster NGC 7380 was found as the average of all the μ_x and μ_y of the individual cluster members, i.e. the stars included in Table 10: /21

$\bar{m}$	$\bar{\mu}_x$	$\bar{\mu}_y$	Number of stars
$13^m.0$	+0".0021	-0".0018	25
	±0.0003	±0.0003	

Absolute proper motions and tangential velocities of the clusters.

The relative proper motions obtained above for the clusters NGC 7788, NGC 7790, NGC 2422, NGC 1502, and NGC 7380 were converted into absolute values by a statistical method. Using the well-known distances and radial velocities (for the clusters NGC 1502 and NGC 7380) of the cluster under discussion we calculated from the equations

$$\mu_x = \frac{x_\odot \sin\alpha - y_\odot \cos\alpha}{kr} + \mu_x',$$

$$\mu_y = \frac{x_\odot \cos\alpha \sin\delta + y_\odot \sin\alpha \sin\delta + z_\odot \cos\delta}{kr} + \mu_y',$$

$$V_r = V_r' + V_0 \cos\lambda$$

the corrections of the absolute proper motions and radial velocities of the clusters for the motion of the sun in space. Here $x_\odot$, $y_\odot$, $z_\odot$ are the projections of the velocity of the sun on the coordinate axes x, y, z, respectively, where the X-axis is directed towards the point of the vernal equinox, the Y-axis lies in the plane of the equator 90 degrees away in the direction of increasing right ascension, and the Z-axis is directed towards the North Pole; α, δ are the equatorial coordinates of the cluster; r is the distance to the cluster in parsecs; k = 4.738; μ_x, μ_y are the peculiar motions of the

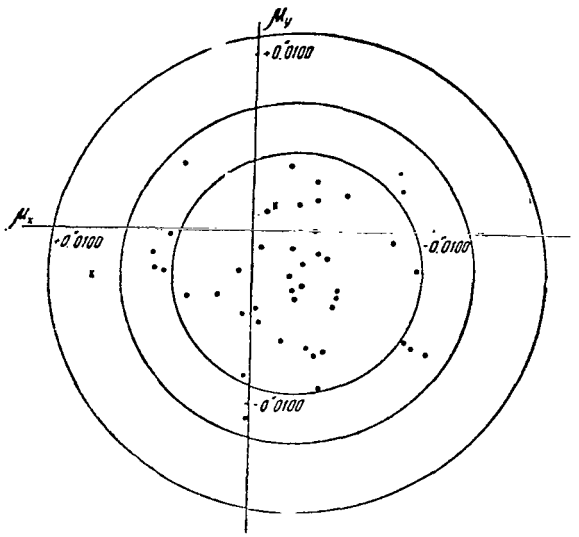

Figure 15.

clusters; V_r is the radial velocity; V_r' is the peculiar radial velocity; $V_0 \cos \lambda$ is the parallactic part of the radial velocity V_r; and λ is the angular distance of the clusters from the apex. /22

Thereupon the standard coordinates of the apex and velocity of the sun were taken (A = 270°, D = +30°, $V_\odot$ = 19.5 km/sec), and the radial velocities of the clusters NGC 1502 and NGC 7380 were taken from the paper [19]. The tangential velocities were calculated from the equation

$$V_t = 4.738\,\mu \cdot r,$$

TABLE 10

№ I	№ W	m I	V_0	$(B-V)_0$	$E_{(B-V)}$	μ_x	μ_y
319	72	$14^m.5$	$12^m.31$	$-0^m.15$	$0^m.62$	−0.0056	−0.0006
450	77	14.8	12.42	−0.10	0.64	+ 62	− 46
525	16	13.7	10.84	−0.13	0.78	+ 31	+ 30
358	68	14.4	11.54	−0.24	0.81	+ 7	− 72
398	38	12.0	10.16	−0.26	0.57	+ 32	− 16
527	32	10.9	8.39	−0.30	0.73	+ 29	+ 17
374	41	12.3	9.97	−0.29	0.63	+ 2	+ 12
474	64	14.2	11.80	−0.15	0.68	+ 64	+ 49
437	63	14.2	11.77	−0.19	0.69	+ 64	− 14
357	25	15.0	13.27	+0.03	0.47	+ 25	− 2
380	15	13.4	11.50	−0.16	0.54	+ 4	− 28
397	67	14.4	11.94	−0.10	0.67	+ 42	+ 43
472	37	12.0	9.79	−0.27	0.65	− 17	− 73
392	12	12.4	10.60	−0.18	0.53	+ 36	− 14
426	40	12.1	10.28	−0.23	0.56	− 12	− 50
409	8	10.8	9.08	−0.26	0.53	+ 1	− 32
493	43	12.3	10.35	−0.17	0.57	+ 51	− 14
526	4	10.4	8.49	−0.14	0.54	+ 44	− 70
492	59	14.1	11.14	−0.14	0.82	− 6	− 62
489	9	10.9	8.85	−0.25	0.61	+ 50	+ 28
480	54	13.8	11.23	−0.19	0.72	− 12	− 4
402	44	12.4	10.59	−0.22	0.54	+ 15	− 49
417	22	14.6	12.07	−0.08	0.67	− 36	− 76
449	23	14.7	12.49	−0.06	0.61	− 30	− 61
442	13	13.2	10.58	−0.10	0.71	+ 19	+ 41

where μ is the total peculiar proper motion of the cluster expressed in seconds of arc. The results obtained are presented in Table 11, where μ_x, μ_y are the components of the absolute annual proper motion of the cluster; μ_{xp}, μ_{yp} are the same corrected for the motion of the sun; μ_p is the total amount of the peculiar proper motion; Q is the position angle of the peculiar motion calculated from north towards east; V_t, V_r, V are the tangential, radial, and space peculiar velocities expressed in kilometers per second.

TABLE 11

Cluster	μ_x	μ_y	μ_{xp}	μ_{yp}	μ_p	Q	R	V_t	V_r	V
NGC 7788	−0.″0015	−0.″0022	−0.″0030	−0.″0018	0.″0035	219°	2410	40		
NGC 7790	−0.0014	−0.0025	−0.0024	−0.0022	0.0033	226	3600	56		
NGC 2422	−0.0064	−0.0008	−0.0034	+0.0017	0.0038	157	480	9		
NGC 1502	+0.0018	−0.0033	+0.0002	+0.0009	0.0009	42	880	4	−16	16
NGC 7380	+0.0005	−0.0041	−0.0011	−0.0041	0.0042	257	2100	42	−24	48

REFERENCES

1. Ishmukhamedov, Kh., Tsirk. TAO, "Fan" Press of the UzSSR, 1967, No. 345.

2. Ishmukhamedov, Kh., Tsirk. TAO, "Fan" Press of the UzSSR, 1967, No. 346.

3. Ishmukhamedov, Kh., Tsirk. TAO, "Fan" Press of the UzSSR, 1967, No. 347.

4. Hopmann, J., and coworker, Mitt d. Univ.-Sternw., Vienna, Vol. 9, 1958, pp. 181-211.

5. Li Hen, Annales Obs. Zo-Ze, Vol. XXIII, 1954.

6. Ebbighausen, H. G., A. J., 1942, No. 1, p. 50.

7. Johnson, H. L., Hoag, A. A., Iriarte, B., Mitchell, R. I., and Hallam, K. L., Lowell Obs. Bull. No. 113, Vol. 5, 1961.

8. Becker, W., "The Galactic Star Clusters, NGC 7788", Memorie della Societa Astronomica Italiana, Vol. 36, f. 3, 1965.

9. Barkhatova, K. A., Sbornik rabot po astronomii Ural'skogo universiteta [Collection of papers on Astronomy of Ural University], No. 1, 1963.

10. Alekseyev , I. Ye., Soobshcheniya GAI im. P.K. Shternberg [Communications of the GAISh (Shternberg Astronomical Observatory)], 1962, No. 124, pp. 32-35.

11. Sandage, A., Ap. J., 128, No. 2, 1958.

12. Kukarkin, B. V., Parenago, P. P., Yefremov, Yu. I., and Kholopov, P. I., Obshchiy katalog peremennykh zvezd [General Catalog of Variable Stars], Vol. 1, AN USSR Press, Moscow, 1958.

13. Kraft, R. R., Ap. J., 128, No. 2, 161, 1958.

14. Zug, R. S., Lick Obs. Bull., No. 454, 1932-1934.

15. Lynga, G., Archiv für Astronomie, Vol. 2, No. 4, 1960.

16. Hoag, A. A., Johnson, H. L., Iriarte, B., Mitchell, R. I., Hallam, K. L., and S. Sharpless, Publ. US Naval Observatory, Second Series, Vol. 17, 7, 1961.th

17. Van Schewick, Publications of the Astronomy Institute of Bonn University, No. 74.

18. Johnson, H. L., Lowell Obs. Bull., No. 90, 1958.

19. Hayford, P., Lick Obs. Bull., No. 448, 1932-1934.

20. Lavdovskiy, V. V., Pulkovo Astronomical Observatory Bull., Vol. 23, Issue 1, 1962, No. 171.

PROPER MOTIONS OF FOUR VARIABLE STARS OF THE U GEMINORUM TYPE AND STARS IN THEIR VICINITY

Sh. Primkulov

ABSTRACT. The proper motions of the four U Geminorum-type stars SS Aur, X Leo, TW Vir, and UZ Ser are derived from 1st epoch plates taken in 1935 by Kozlov with the Tashkent normal astrograph and 2nd epoch plates taken by the author with the same instrument.

In addition the author presents a catalogue of relative proper motions for 1946 stars to the 15th photographic magnitude located near the four U Geminorum stars. The proper motion of the variable star R Leo was also determined.

As a result of his proper motion studies, the author also found some binary and multiple star systems among the background stars investigated.

Variable stars of the U Geminorum type are some of the most interesting /24 objects of the galaxy. The spectra of these stars vary from the early classes B and A at maximum to late classes G and K at minimum and at intervals between outbursts resemble the spectra of new stars, and at the maximum brightness, the spectra of white dwarfs, which is why they are sometimes called quasi-periodic new dwarfs. If the stars of the type U Geminorum can be considered dwarfs, then the distance to them should not be more than several tens of parsecs. The determination of the proper motions of U Geminorum stars is of great interest in finding their absolute stellar magnitudes and the study of their spatial distributions.

In the present paper are presented proper motions of the variables SS Aurigae, X Leonis, TW Virginis, and UZ Serpentis, and also a catalogue of the relative proper motions of 1946 stars to the 15th photographic magnitude in the vicinity of these variables. The photographs of V. I. Kozlov, taken in 1935 with the Tashkent normal astrograph (D = 330 mm, F = 3470 mm), were used as the first epoch for the derivation of the proper motions of the stars. The photographs of the second epoch were obtained by us on the same instrument

using the "through-glass" method. The data on the observational material are presented in Table 1.

All pairs, except the first, were measured on the Repsold instrument of the Astronomical Institute of the Academy of Sciences, Uzbek SSR, and the third pair of the TW Virginis region on the UIM-21, No. 630351, which was adapted for this purpose. All stars acceptable for measurement and lying within a central circle of radius of about 40 mm were measured.

In the region of X Leonis the variable star R Leonis appeared at a distance of 56 mm from the center. Therefore in addition 16 stars around this star were measured for the determination of its proper motion.

From 30 to 60 reference stars, uniformly distributed over the entire field, were selected in each region for deriving the plate constants. Based on the rectangular coordinates x and y and the differences Δx and Δy between the images of the first and second epochs, the equations of condition were formulated as follows:

$$\left.\begin{aligned} ax + by + c + \tau\mu_x &= \Delta x \\ a'x + b'y + c' + \tau\mu_y &= \Delta y \end{aligned}\right\} \qquad (1)$$

without taking into account higher order terms, since the conditions of the observations and also the optical centers of the plates of the two epochs coincide.

Solving the system (1) without the terms $\tau\mu$ by the method of least squares, we found the constants of pairs of plates: a, b, c, a', b', c', and then calculated the relative proper motions of each star. /25

The proper motion of R Leonis was determined from two groups of reference stars: 32 reference stars distributed in the central circle, and 16 stars around R Leonis. The convergence of the values found appeared to be good within the limits of the errors. Therefore the value of the proper motion obtained with the aid of the constants of the central circle are presented in the catalogue.

Simultaneously with the measurement of the difference in coordinates on the conditional scale the diameters of the star images in each pair on the plates of the second epoch were estimated. The transfer from the conditional scale to the standard photographic stellar magnitudes was carried out with

the help of special photometric plates obtained on the same normal astrograph together with the reference areas of the Mount Wilson catalogue [1].

TABLE 1

Region	Pair	Number of the plate	Dates of observations	Difference in epochs, years	Exposure, minutes	Hour angle, minutes	Type of plate
SS Aur	I	95	27.II 1935	28.06	40	120	Ilford
		1542	21.III 1963		30	120	Astro-Agfa
	II	96	27.II 1935	28.06	40	168	Ilford
		1543	21.III 1963		30	168	Astro-Agfa
	III	·90	26.II 1935	29.94	60	165	Ilford
		1954[a]	3.II 1965		45	165	Astro-Agfa
X Leo	I	98	28.II 1935	29.93	15	—92	Ilford
		1952	3.II 1965		15	—92	Astro-Agfa
	II	99	28.II 1935	29.93	15	—71	Ilford
		1953	3.II 1965		15	—71	Astro-Agfa
	III	100	28.II 1935	29.93	15	—50	Ilford
		1954	3.II 1965		15	—50	Astro-Agfa
TW Vir	I	108	30.III 1935	29.92	120	—44	Ilford
		1972	2.III 1965		90	—50	Astro-Agfa
	II	110	31.III 1935	30.09	120	04	Ilford
		2018	3.V 1965		70	15	Astro-Agfa
	III	111	2.IV 1935	29.99	120	—50	Ilford
		1995	30.III 1965		90	—50	Astro-Agfa
UZ Ser	I	137	7.VII 1935	29.00	120	12	Ilford
		1835	6.VII 1964		90	12	Astro-Agfa
	II	142	25.VII 1935	29.93	120	22	Ilford
		2045	29.VI 1965		80	22	Astro-Agfa

The technique of obtaining photometric plates and their reduction are expounded in the paper [2]. The characteristic curves for the various regions, constructed from the diameters of the star images and their international magnitudes, are presented in Figure 1, where the characteristic curve I is for the stars of the standard region and curve II, for the intervening stars in the region under investigation. The field error was not taken into account since previous investigation [3] showed that the effect of the field error of the photographic objective of the normal astrograph is negligible within the limits of a 100 x 100 mm field. The probable errors of the brightness determination of the stars are given below:

Region	ρ_m
SS Aur	±0.31
X Leo	±0.19
TW Vir	±0.18
UZ Ser	±0.22

It is evident from this that the stellar magnitudes obtained by us are sufficiently accurate for the determination of the brightness equation and for other purposes. /26

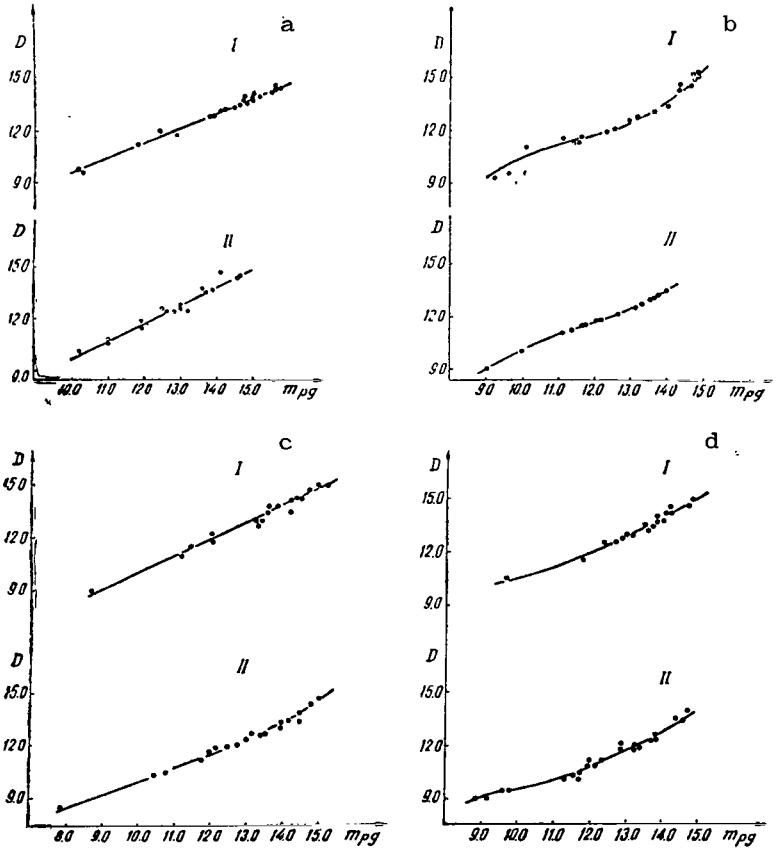

Figure 1. Characteristic curves for brightness determination for the stars in the regions:

a - SS Aur; b - X Leo; c - TW Vir; and d - UZ Ser.

The proper motions of stars can often be distorted by errors in the brightness equation which depends on various factors (the quality of the guiding, variation in the collimation of the objective between observations at the two epochs, and so forth). For the detection of this error we investigated the proper motions of stars for each pair separately by the method expounded in the paper [4].

The values found for the differences P_x to $\bar{\mu}_x$ and P_y to $\bar{\mu}_y$, between pairs of all the regions differ little among themselves; therefore we averaged the values of these differences both in x and in y for the corresponding groups of stars in all pairs in each region, and then constructed the characteristic curve (Figure 2). The numerical values of the corrections taken from these curves are presented in Table 2; these corrections were not included in the proper motions of the stars mentioned above.

The probable errors of the proper motion of each star were calculated /27
from the well-known Peter's equation

$$\rho = \pm 0.8454 \frac{\sqrt{p}}{1+p} \cdot \frac{\Sigma|\Delta|}{n-1}, \qquad (2)$$

where

1	is the weight of the worst pair;
p	is the weight of the pair under investigation;
$\Sigma\|\Delta\|$	is the sum of the absolute values of the differences of the proper motions for the two pairs being investigated; and
n	is the number of stars for which the probable error is calculated.

A. N. Deich [5] showed that if the pairs of plates of the region under investigation are obtained with an identical difference in epochs and have an identical limiting stellar magnitude, then the weight of each pair can be calculated from the reference stars. It is evident from Table 1 that the pairs in all investigated regions satisfy these conditions. Therefore the weights for /28
each pair were determined from the reference stars. Our calculations also showed that all pairs of these regions are practically uniform. On account of this the probable errors of proper motion of the individual star for these four regions were found from the simplified Peter's equation

$$\rho = \pm 0.4227 \frac{\Sigma|\Delta|}{n-1}. \qquad (3)$$

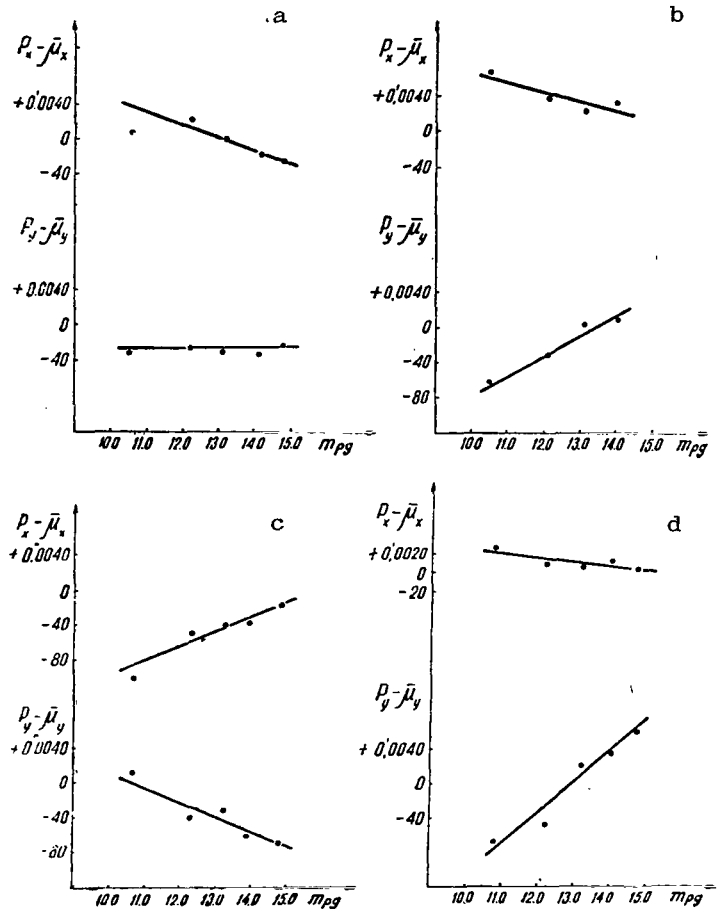

Figure 2. Characteristic curves of the brightness equation for the regions:

a - SS Aur; b - X Leo; c - TW Vir; d - UZ Ser.

We present the results of these calculations:

Region	ρx (0".0001)	ρy (0".0001)
SS Aur	±24	±21
X Leo	±22	±20
TW Vir	±21	±22
UZ Ser	±22	±21

The transfer of the relative proper motions to absolute values was carried out by a statistical method. The errors, taking into account the parallactic shift of the reference stars, are taken from the papers [6 and 7], and the values of the coefficients Q and Q', which take into account the galactic rotation, are taken from Zhukov's Table [8].

Thus we obtained for the variable stars of the U Geminorum type the values of the proper motion (Table 3).

TABLE 2

m_{pg}	*SS* Aur		*X* Leo		*TW* Vir		*UZ* Ser	
	$\Delta\mu_x$	$\Delta\mu_y$	$\Delta\mu_x$	$\Delta\mu_y$	$\Delta\mu_x$	$\Delta\mu_y$	$\Delta\mu_x$	$\Delta\mu_y$
9.5	+60	−2	—	—	—	—	—	—
9.8	56	2	+36	−74	—	—	—	—
10.0	52	1	32	68	—	—	+32	−120
10.2	48	−1	30	62	—	—	−30	112
10.5	44	0	27	56	−84	+60	28	104
10.8	40	0	24	48	78	56	26	96
11.0	36	0	21	42	74	52	22	88
11.2	32	0	18	38	68	46	20	80
11.5	28	0	15	32	62	42	18	72
11.8	24	0	12	26	56	38	16	66
12.0	20	0	10	20	50	34	14	60
12.2	16	0	8	16	44	30	12	54
12.5	12	0	+ 4	− 8	38	26	10	46
12.8	8	0	0	0	32	22	8	38
13.0	+4	0	− 2	+ 6	26	18	6	28
13.2	0	0	4	12	20	14	4	18
13.5	−4	0	8	18	14	10	+ 2	− 8
13.8	8	0	10	24	8	6	0	0
14.0	12	0	12	28	− 2	+ 2	− 2	+ 4
14.2	16	+1	−14	+32	+ 4	− 2	4	12
4.5	20	1	—	—	10	6	6	20
14.8	24	2	—	—	16	10	8	30
15.0	−28	+2	—	—	+22	+14	−10	+40

NOTE. The value of the brightness equation is given to 0".0001.

The proper motions of TW Virginis and X Leonis have been determined by other authors [9], [10]. The results of these determinations are given below:

Star	Δt (in years)	μ (0".0001)	Author
X Leo	10.5	952	Miczaika and Becker
TW Vir	10.1	820	Rosino

TABLE 3

Star	Proper motions			
	Relative		Absolute	
	μ_x	μ_y	μ_x	μ_y
SS Aur	+0".0032	−0".0206	+0".0029	−0".0279
X Leo	− 241	+ 37	− 343	− 27
TW Vir	+ 299	− 153	+ 194	− 184
UZ Ser	+ 20	− 135	+ 22	− 163

TABLE 4

Number of the stars	m_{pg}	X	Y	μ_x (0".001)	μ_y (0".001)	r
			Region SS Aur			
39	14.^{m}2	−39'.4	−25'.6	+22	+ 8	0'.1
40	13.6	−39.4	−25.7	+18	+ 4	
65	12.3	−35.5	−26.0	+15	+13	3.0
83	14.0	−32.8	−25.0	+17	+14	
145	13.5	−25.9	− 0.8	+ 1	+14	1.2
147	12.9	−25.7	− 1.8	+ 1	+14	
171	14.2	−23.6	−12.9	+14	+11	2.8
185	14.1	−22.3	−15.2	+12	+10	
810	11.9	+31.7	+ 9.6	−16	− 8	4.2
834	12.3	+35.4	+ 7.6	−18	− 7	
13*	13.8	+ 3.0	−21.4	−11	−54	4.1
14*	8.6	+ 5.5	−18.2	− 7	−47	
21*	11.4	+25.4	+11.4	−15	−35	5.7
22*	10.2	+30.4	+ 8.7	−15	−39	
			Region X Leo			
51	13.6	−10.0	+ 9.6	−27	+ 8	3.4
53	13.6	− 9.6	+13.0	−29	+12	
2*	9.0	−55.0	−30.4	−64	+30	1.0
3*	10.2	−54.9	−30.3	−68	+24	
			Region TW Vir			
13	12.3	−23.0	+12.2	−39	+ 6	9.0
5*	13.5	−23.2	+ 3.2	−43	+ 2	
19	12.9	−17.1	+21.8	+13	−20	8.7
30	13.5	−11.0	+15.6	+14	−20	6.4
36	13.4	− 7.4	+20.9	+12	−19	
51	11.8	+ 0.1	+18.6	−18	+22	0.7
52	13.4	+ 0.1	+17.9	−20	+18	5.5
65	13.6	+ 3.8	+22.7	−19	+26	
85	15.2	+18.2	+19.6	− 3	+22	2.1
86	15.1	+18.8	+21.6	− 1	+21	
			Region UZ Ser			
167	15.0	−16.9	+12.8	−21	− 4	0.3
175	15.0	−16.6	+12.8	−23	− 8	
214	14.8	−13.2	+13.7	+ 2	+28	0.1
215	14.6	−13.2	+13.8	+ 4	+24	
216	15.0	−13.0	0.0	−18	− 3	0.2
221	14.8	−13.0	− 0.1	−22	− 3	
375	15.0	− 0.3	− 9.9	−18	− 8	2.1
396	14.2	+ 1.6	−10.3	−18	− 2	
716	15.0	+24.6	− 7.0	+25	+ 3	0.3
718	15.0	+24.7	− 7.3	+24	0	

In addition to the equatorial coordinates of the variable stars their proper motions obtained from plates of the Heidelberg Observatory with a difference in epochs of about 10 years are also presented in the paper [9]. It is obvious from Table 2 of this paper that the positions of the stars for which the authors calculated proper motions are determined rather roughly. /30

Mannino and Rosino [10], reducing the very same material, independently of each other arrived at identical results. This observational material was obtained with a reflector (D = 600 mm, F = 2100 mm) with a difference in epochs of 9.7 years. Such a difference in epochs at a scale of 98"/mm is not sufficient for the determination of reliable proper motions of stars.

Incidentally, we investigated the proper motions of background stars for detecting stars physically connected with each other. The investigation was carried out with the method presented in the paper [2]. As a result, some binary and multiple systems were found in these four regions of the sky, and data on them are presented in Table 4.

The relative proper motions of the stars in the vicinity of the variables SS Aurigae, X Leonis, TW Virginis, and UZ Serpentis are given in the catalogue presented below. In the first column are given the numbers of the stars (the numbers of the reference stars are denoted by asterisks). The stars in each region are numbered according to increase in the coordinate X. In the second column the photographic stellar magnitude on the international scale is given. In the third and fourth columns the rectangular coordinates X and Y are given. In each region the optical center of the plate is taken as the origin of the rectangular coordinates or the variable star, if it is located close to the optical center. In the last two columns the relative proper motions of the stars in thousandths of seconds of arc are given. The stars with large proper motions are numbered separately and are presented at the end of each region.

REFERENCES

1. Mount Wilson. Catalogue of Photographic Magnitudes in Selected Areas 1-139, Washington, 1930.

2. Primkulov, Sh., Tsirkulyar TAO [Circular of the Tashkent Astronomical Observatory (TAO), Tashkent, "Fan" Press, 1966, No. 334.

3. Primkulov, Sh., Tsirkulyar TAO [Circular of the Tashkent Astronomical Observatory (TAO)], Tashkent, AN UzSSR Press, 1963, No. 321.

4. Fatchikhin, N. V., Izvestiya GAO [Proceedings of the Main Astronomical Observatory (GAO)], No. 148, Vol. 19, Issue 1, Leningrad, 1952, 11.

5. Deich, A. N., Perepelkin, Ye. Ya., Trudy GAO [Proceedings of the GAO)], Series 2, Vol. 45, Leningrad, 1935, 1.

6. Binnendijk, L., Bulletin of the Astronomical Institutes of the Netherlands, Vol. 10, No. 362, 1943.

7. Parenago, P. P., AZh, Vol. 23, Issue 2, Moscow, 1946, 65.

8. Zhukov, L. M., AZh, Vol. 43, Issue 5, Moscow, 1966, 1107.

9. Miczaika, G. R., Becker, U., Veröffentlichungen der Badischen Landesstern-warte zu Heidelberg [Publications of the Regional Observatory of Bavaria at Heidelberg], Vol. 15, No. 8, Königstuhl, 1948.

10. Mannino, G, Rosino, L., Contributi dell'astronomico dell'universita di Padova in Asiago [Contributions of the Astronomical University of Padova in Asiago], No. 14, Padova, 1950.

CATALOGUE

Region *SS* Aur

$\alpha_{1950} = 06^h09^m.3$ $\quad \delta_{1950} = +47°36'$

No. of the star	m_{pg}	X	Y	μ_x	μ_y	No. of the star	m_{pg}	X	Y	μ_x	μ_y
1	13.4	−49.5	+ 3.1	0	+ 4	51*	13.1	−38.5	+ 3.8	+ 6	+ 4
2	14.1	−48.6	+ 1.5	+14	+ 10	52	13.6	−38.5	+ 3.8	+ 6	+ 6
3	13.5	−48.4	− 2.2	+15	+ 5	53*	13.1	−38.4	+18.8	+ 9	+ 14
4	12.8	−48.0	− 9.2	+ 1	+ 3	54	12.9	−37.5	+23.2	0	+ 8
5	13.2	−47.2	+ 4.3	+10	+ 11	55	12.2	−37.3	−14.9	− 5	+ 4
6	13.8	−46.5	− 2.8	+ 5	− 5	56	9.6	−37.0	+ 4.5	+10	+ 7
7	13.3	−46.5	−12.8	+13	− 24	57	14.1	−36.8	+13.0	+ 8	− 2
8	12.8	−46.2	+ 4.7	+15	− 5	58	14.0	−36.6	+13.8	+16	− 3
9	12.5	−46.1	+10.9	− 7	+ 7	59	13.0	−36.5	+ 6.3	− 8	− 7
10	13.8	−45.7	−10.8	+24	− 23	60	14.1	−36.4	+ 0.9	+10	− 1
11	13.2	−45.6	− 2.9	+ 5	+ 12	61	13.8	−36.3	+ 5.7	− 3	+ 9
12	13.8	−45.3	− 9.8	+ 3	+ 6	62	13.3	−36.0	−12.9	+19	− 16
13	12.2	−45.2	− 1.6	− 3	+ 2	63	13.3	−35.9	−12.3	+16	+ 3
14	13.7	−44.9	+ 8.9	− 3	+ 7	64	14.2	−35.9	−16.6	+ 4	+ 7
15*	12.7	−44.9	− 6.0	+ 3	+ 5	65	12.3	−35.5	−26.0	+15	+ 13
16	13.3	−44.8	−15.8	+ 3	+ 7	66	12.6	−35.5	+10.8	0	− 2
17	11.0	−44.5	− 9.2	+17	− 14	67	14.3	−35.3	− 1.8	+ 8	+ 6
18	14.3	−44.6	−17.6	+ 8	− 8	68	10.2	−34.9	−11.6	+ 3	+ 2
19	12.0	−43.5	+15.2	+ 8	+ 3	69	14.5	−34.6	− 4.2	+ 1	− 3
20	14.5	−44.3	− 4.1	+ 6	+ 7	70	12.5	−34.5	+ 9.2	+ 1	+ 6
21	14.5	−43.3	− 5.8	+ 8	+ 12	71	13.1	−34.5	+20.8	+ 2	+ 5
22	13.8	−43.1	+10.0	+21	+ 7	72	13.0	−34.5	−32.6	+ 4	+ 4
23	13.4	−42.7	− 4.7	+21	+ 10	73	13.2	−34.3	−21.7	+ 6	+ 4
24	14.0	−42.7	−11.6	+16	+ 0	74	13.9	−33.7	−10.6	+ 1	+ 3
25	13.8	−42.5	−19.8	+ 6	+ 3	75	14.5	−33.5	+ 5.3	− 2	+ 1
26	13.1	−42.5	− 6.2	+ 9	− 2	76	13.7	−33.5	+22.0	+ 7	+ 6
27	11.6	−42.4	+16.0	+ 4	− 7	77	13.8	−33.4	+18.8	+ 7	+ 11
28	14.5	−42.3	− 6.6	+ 5	+ 2	78*	13.1	−33.4	−15.4	− 6	− 3
29	11.6	−42.0	−25.8	− 7	+ 1	79*	13.1	−33.1	−26.1	− 7	+ 3
30	13.6	−41.8	+11.8	+ 6	+ 7	80	13.5	−33.1	−29.0	+15	+ 5
31	12.7	−41.4	− 0.7	+ 6	+ 5	81	13.2	−32.8	+ 1.5	− 2	− 13
32	13.1	−40.6	+19.8	−10	+ 6	82	14.2	−32.8	−18.6	+ 7	+ 15
33	12.2	−40.5	− 8.6	− 2	0	83	14.0	−32.8	−25.0	+17	+ 14
34	12.7	−40.4	−17.6	+ 3	+ 9	84*	13.6	−32.7	+10.4	+ 8	+ 7
35	13.0	−40.1	−26.0	0	+ 7	85	12.5	−32.7	+22.4	− 9	− 3
36	14.2	−39.8	−25.6	+14	+ 2	86	13.1	−32.7	−26.6	+ 7	+ 9
37	14.3	−39.7	+ 4.9	+11	+ 4	87	11.9	−32.5	+ 9.7	− 8	− 5
38	13.1	−39.6	−24.4	+ 8	+ 8	88	14.4	−32.4	−32.4	+ 8	+ 13
39	14.2	−39.4	−25.6	+22	+ 8	89	14.1	−32.3	+19.8	+10	+ 10
40	13.6	−39.4	−25.7	+18	+ 4	90	14.5	−32.3	−22.8	+ 2	+ 9
41	12.0	−39.3	− 8.1	0	− 23	91	13.1	−32.2	−33.2	+ 6	+ 1
42	14.1	−39.1	− 3.4	− 0	− 28	92	12.8	−32.1	0	+13	+ 4
43	13.2	−39.1	+18.6	+ 5	− 4	93	13.8	−32.0	−31.0	0	+ 12
44	12.4	−39.0	+12.8	−17	− 15	94	11.2	−31.9	−31.8	− 5	+ 1
45	12.0	−38.9	+25.5	+13	+ 16	95	12.6	−31.7	−29.6	+11	− 4
46	12.9	−38.9	−27.7	+12	+ 9	96	13.8	−31.7	−11.2	+ 4	− 12
47	13.4	−38.8	+ 6.3	+ 6	0	97	13.1	−31.6	+17.8	+ 7	+ 9
48	14.2	−38.6	+ 4.9	+ 8	+ 8	98	14.3	−31.6	+17.5	+ 7	+ 10
49	13.3	−38.6	+16.3	+ 8	+ 8	99	13.4	−31.1	+27.7	− 3	+ 12
50	13.8	−38.6	+26.0	+ 8	+ 13	100	14.2	−31.1	+16.5	+ 5	− 28

Continuation of the CATALOGUE

No. of the star	m_{pg}	X	Y	μ_x	μ_y	No. of the star	m_{pg}	X	Y	μ_x	μ_y
		′	′					′	′		
101	9.6	−30.5	−33.8	−17	− 18	153	13.6	−25.4	−29.0	+ 6	− 5
102	13.3	−30.4	+ 1.3	+ 6	+ 5	154	11.3	−25.4	−12.6	+ 7	− 17
103	10.7	−30.3	−22.8	− 2	− 12	155	14.4	−25.4	−22.9	+ 6	+ 6
104	12.6	−30.2	+29.8	+ 8	+ 3						
105	14.4	−30.2	+13.4	+20	+ 14	156	12.2	−25.1	−18.1	+12	− 5
						157	13.5	−25.1	−35.4	+ 5	+ 2
106	14.8	−30.1	− 2.1	+ 1	− 1	158	13.0	−25.0	−26.2	+19	− 12
107	12.9	−30.0	−15.4	−16	− 9	159*	14.1	−25.0	+16.4	− 4	+ 6
108	14.5	−29.8	−37.1	+ 4	+ 6	160	12.0	−24.9	−30.8	+ 4	+ 7
109	12.9	−29.7	−35.9	+ 5	+ 6						
110	14.6	−29.7	−18.3	− 2	− 2	161	13.5	−24.7	−33.6	+ 5	+ 4
						162	14.8	−24.5	+11.5	+13	+ 5
111*	13.7	−29.7	− 3.9	+ 1	+ 6	163	14.5	−24.5	+ 2.4	+ 5	+ 6
112	14.4	−29.5	+ 2.4	+14	+ 5	164	14.5	−24.4	+ 6.2	− 9	+ 2
113	12.3	−29.2	+10.0	+ 5	− 2	165	14.2	−23.9	−12.6	+12	+ 2
114	14.3	−29.2	+17.4	+ 6	+ 12						
115	14.3	−29.1	+31 4	+13	+ 4	166*	13.0	−23.9	+32.4	− 2	− 6
						167	13.5	−23.8	−18.8	+ 5	+ 5
116	14.0	−29.0	−10.5	+ 5	+ 2	168	13.8	−23.7	−27.0	+ 4	+ 3
117	14.3	−28 9	+ 3.8	− 2	− 11	169	14.3	−23.7	+ 4.5	+12	− 10
118	14.4	−28.8	+ 8.4	+ 6	+ 4	170	14.7	−23.7	−19.9	+ 1	+ 5
119	14.4	−28.7	−34.5	+10	+ 4						
120	12.8	−28.6	−35.5	− 5	+ 3	171	14.2	−23.6	−12.9	+14	+ 11
						172	12.8	−23.3	−28.2	+ 4	+ 2
121	14.1	−28.5	+30.9	+14	− 1	173	14.8	−23.1	−25.5	+10	+ 8
122	14.4	−28.4	−29.0	+ 9	− 2	174	11.9	−23.0	+17.0	+ 6	− 1
123	13.8	−28.3	+22.7	− 1	+ 3	175	12.2	−23.0	+15.8	− 6	+ 5
124	9.6	−28.3	+ 3.0	+11	+ 19						
125	14.1	−28.3	−20.6	+ 3	− 2	176	15.0	−22.7	−41.6	+ 5	+ 9
						177	14.1	−22.7	−23.1	+ 5	− 1
126	12.0	−28.2	−18.1	− 5	− 6	178	11.0	−22.6	−29.8	+ 2	+ 2
127	14.6	−28.1	−22.2	+ 2	+ 3	179	14.1	−22.5	−33.6	+ 9	− 4
128	13.8	−27.9	−36.6	− 3	+ 6	180	14.3	−22.3	+15.4	− 2	0
129	14.6	−27.7	+12.4	0	− 1						
130	14.5	−27.7	−11.6	+10	+ 11	181	14.5	−22.2	+16.0	+ 2	+ 12
						182	14.2	−22.3	−25.6	+15	+ 10
131	12.0	−27.5	−23.6	− 2	+ 1	183	14.5	−22.1	− 4.8	− 4	+ 8
132	13.5	−27.4	+10.7	+ 6	+ 9	184	12.2	−22.1	−12.4	+ 7	− 16
133	12.3	−27.3	− 2.3	+ 5	− 4	185	14.1	−22.3	−15.2	+12	+ 10
134	14.5	−27.3	+17.5	0	+ 8						
135	14.3	−27.0	− 1.4	+ 4	− 6	186	14.5	−22.3	+26.3	+ 6	+ 4
						187	13.3	−21.8	−41.4	+ 5	+ 4
136	13.5	−26.8	+21.8	+ 1	− 5	188	14.4	−21.7	+23.3	− 4	+ 5
137	14.1	−26.7	−10.1	+ 6	− 6	189	13.8	−21.6	−10.2	− 1	+ 1
138	14.1	−26.7	−13.5	+ 7	+ 6	190	12.6	−21.5	− 5.1	+ 3	+ 5
139*	13.3	−26.5	−13.4	− 3	+ 1						
140	14.5	−26.5	+17.0	− 1	+ 4	191	14.2	−21.5	+13.1	+ 7	− 6
						192	13.9	−21.4	− 5.1	+ 3	+ 19
141	13.1	−26 5	+28.7	+ 4	+ 7	193	14.8	−21.3	−28.1	0	+ 2
142	13.0	−26.2	−19.6	− 3	− 1	194	13.0	−21.3	−32.8	+12	− 5
143	14.0	−26.3	+ 7.9	+ 6	+ 2	195*	12.6	−21.0	−24.8	+ 7	− 1
144	13.8	−26 0	−34.6	− 6	0						
145	13.5	−25.9	− 0.8	+ 1	+ 14	196	14.9	−20.7	−29.6	+ 1	+ 4
						197	13.0	−20.7	−33.2	+ 7	− 1
146	13.8	−25.7	+ 3.0	+ 3	+ 4	198	13.8	−20.6	−34.6	+ 7	+ 15
147	12.9	−25.7	− 1.8	+ 1	+ 14	199	14.4	−20.6	+ 9.5	− 6	+ 3
148	11.4	−25.7	−25.5	0	+ 4	200	13.7	−20.5	−30.4	0	+ 3
149	11.5	−25.7	+33.4	+ 6	− 6						
150	10.3	−25.6	+ 8.9	+12	− 7	201	12.9	−20.5	+ 3.6	− 3	+ 7
						202	12.5	−20.4	+ 0.1	− 1	+ 2
151	13.6	−25.5	+34.3	+ 6	+ 1	203	13.7	−20.3	−15.6	+ 8	+ 12
152	9.3	−25.5	+ 1.1	+10	− 7	204	14.5	−20.3	−13.6	+10	+ 4
						205	14.0	−20.3	−35.4	+12	+ 2

Continuation of the CATALOGUE

No. of the star	m_{pg}	X	Y	μ_x	μ_y	No. of the star	m_{pg}	X	Y	μ_x	μ_y
		′	′					′	′		
206	13.1	—19.9	— 3.1	+ 4	— 3	258	14.5	—15.5	+ 8.8	+ 4	+ 7
207	9.9	—19.7	— 5.1	0	— 24	259	13.6	—15.5	+ 0.8	0	+ 1
208	12.6	—19.7	—14.4	0	— 9	260*	13.5	—15.5	+39.9	+ 1	+ 3
209	14.2	—19.6	—13.6	+ 1	+ 11						
210	12.9	—19.5	— 9.6	+ 5	+ 6	261	13.1	—15.4	—20.2	+ 5	+ 9
						262	13.0	—15.3	— 4.9	— 3	— 1
211*	12.9	—19.3	—10.8	— 6	+ 11	263	13.5	—15.2	—12.9	+19	— 4
212	13.8	—19.3	+ 7.3	+12	+ 6	264	13.7	—15.2	+26.8	— 9	+ 1
213	10.9	—19.3	—43.5	0	— 4	265	13.0	—14.9	—38.8	— 4	— 10
214	13.8	—19.1	—24.5	+10	+ 4						
215	13.1	—19.1	+11.7	— 4	+ 7	266	14.6	—14.8	—16.8	— 8	+ 3
						267	13.3	—14.7	+16.5	— 7	+ 2
216	12.9	—19.1	— 7.3	+ 3	+ 2	268	13.3	—14.7	+24.3	+ 8	+ 2
217	13.6	—18.9	— 6.2	0	+ 1	269	14.1	—14.3	+28.2	+ 3	+ 2
218	12.8	—18.7	—10.4	— 5	+ 1	270	13.8	—14.5	+23.8	— 5	+ 1
219	14.2	—18.6	—13.1	+ 6	— 1						
220	14.6	—18.6	—16.0	+ 6	+ 3	271	13.1	—14.5	+ 4.2	+ 2	+ 4
						272	14.0	—14.5	— 0.7	— 3	— 10
221	13.1	—18.5	+ 4.4	— 4	+ 3	273	13.8	—14.5	—23.9	+11	— 2
222	11.0	—18.5	—28.6	— 6	— 13	274	13.8	—14.4	+ 1.0	+ 4	+ 7
223	12.3	—18.4	—34.0	— 4	— 17	275	12.5	—14.4	+ 3.4	— 1	— 7
224	13.6	—18.0	+ 3.1	+17	— 12						
225	13.2	—18.0	—19.6	+ 2	+ 7	276	13.8	—14.3	+ 6.7	+ 2	+ 2
						277	14.2	—14.3	— 0.3	+ 2	— 4
226	14.6	—18.0	—19.6	+16	+ 5	278	13.7	—14.1	— 9.8	— 1	— 13
227*	13.1	—17.9	+11.1	—14	— 8	279	13.0	—14.1	+34.0	+ 5	— 3
228*	13.4	—17.9	+15.8	+ 3	+ 3	280	13.8	—14.0	—24.3	— 5	0
229	13.2	—17.7	—41.8	+ 2	+ 7						
230	13.9	—17.7	— 6.2	+13	— 13	281	13.6	—13.9	+41.4	+ 4	+ 15
						282	12.9	—13.9	+40.3	— 4	+ 11
231	12.4	—17.7	+40.4	+ 2	+ 17	283	12.8	—13.7	—42.6	+ 5	— 3
232	13.8	—17.6	+22.4	+ 2	— 2	284	13.0	—13.7	—26.8	+ 9	+ 3
233	14.6	—17.6	+23.4	+ 6	0	285	13.1	—13.6	—41.0	— 1	— 12
234*	13.0	—17.6	—43.6	— 1	+ 5						
235	14.4	—17.5	—37.8	— 1	— 11	286	12.3	—13.6	—34.4	+ 6	— 7
						287	13.6	—13.6	+21.9	+ 5	+ 5
236	12.9	—17.5	—29.6	+ 2	+ 9	288	13.5	—13.3	+16.0	+ 6	+ 7
237	13.9	—17.5	—26.0	+ 5	+ 9	289	14.7	—13.0	—10.1	0	0
238	14.6	—17.4	—22.2	— 2	— 3	290	13.7	—12.7	+34.8	— 1	+ 5
239	13.6	—17.3	— 8.8	0	+ 1						
240	13.8	—17.3	— 0.8	+ 4	+ 9	291	13.1	—12.7	—11.2	— 7	0
						292	12.6	—12.6	+ 0.1	— 2	+ 5
241	13.6	—17.2	—26.2	+10	+ 10	293	14.1	—12.6	—25.9	+19	— 9
242*	12.8	—17.1	—33.3	—12	— 18	294	14.5	—12.5	—41.6	+17	+ 11
243	11.4	—17.0	+33.4	— 6	— 3	295	14.1	—12.5	—33.3	+ 9	+ 8
244	13.8	—16.8	+15.5	+ 1	+ 3						
245	13.1	—16.7	—33.2	+ 4	+ 2	296	13.1	—12.3	—43.8	+ 5	0
						297	14.3	—12.3	+13.4	— 6	0
246	13.7	—16.7	—17.3	+ 5	— 8	298	13.2	—12.3	—26.8	+ 1	0
247	12.8	—16.7	—23.5	—12	— 18	299	12.7	—12.3	—25.9	— 1	+ 1
248	14.3	—16.4	—22.4	+19	— 2	300	12.6	—12.2	+23.8	+ 6	— 5
249	14.4	—16.4	—28.4	+ 8	+ 3						
250	14.5	—16.3	— 4.1	— 3	+ 9	301	12.8	—11.8	—40 0	+ 8	— 6
						302*	12.8	—11.8	+ 3.6	0	+ 4
251	13.9	—16.1	+30.2	0	+ 4	303	14.5	—11.8	— 3.2	— 3	+ 14
252	14.8	—15.9	—38.8	+16	+ 5	304	12.3	—11.8	—23.4	+ 4	0
253	12.7	—15.8	+ 2.4	—10	0	305*	13.7	—11.7	—18.2	+ 9	+ 7
254	12.9	—15.8	— 2.0	+ 3	+ 4						
255	14.0	—15.7	—23.6	0	+ 7	306	14.1	—11.7	+20.6	+10	+ 4
						307	14.5	—11.6	—33.6	+ 6	+ 2
256	12.2	—15.7	—43.1	0	+ 12	308	14.1	—11.5	—29.8	+ 6	+ 3
257	13.8	—15.5	+ 4.9	+ 5	0	309	14.1	—11.5	—30.0	+10	+ 4
						310	14.1	—11.4	—19.1	+ 2	— 2

Continuation of the CATALOGUE

No. of the star	m_{pg}	X	Y	μ_x	μ_y
311	10.9	—10.8	+36.0	+11	— 8
312	14.0	—10.7	+ 5.4	— 3	+ 11
313	11.4	—10.7	+24.1	+ 2	— 12
314	14.6	—10.6	—15.0	— 6	+ 1
315	14.3	—10.6	—25.4	+13	+ 6
316	13.7	—10.5	— 9.5	+ 1	+ 3
317	13.8	—10.5	+16.4	— 1	0
318	14.5	—10.5	—41.6	+ 5	+ 9
319	13.8	—10.4	— 8.6	+ 7	— 1
320	14.3	—10.4	+ 4.3	— 8	— 2
321	13.8	—10.4	—33.8	+ 7	+ 8
322	14.6	—10.4	—34.4	+ 5	— 3
323	13.8	—10.3	—22.6	— 2	+ 4
324	11.1	—10.2	—31.6	+ 4	— 17
325	12.3	—10.2	+16.4	—10	+ 3
326	12.8	—10.2	+14.0	+ 6	+ 6
327	14.0	—10.1	+24.1	— 1	+ 10
328	13.5	— 9.9	—40.6	— 7	+ 10
329	13.7	— 9.7	—22.5	—17	+ 19
330	13.8	— 9.7	—34.8	+ 1	+ 2
231	13.1	— 9.6	+20.6	+ 8	— 6
332	13.0	— 9.5	+42.4	0	+ 7
333	13.6	— 9.5	+32.3	+ 8	+ 5
334	12.4	— 9.4	—29.6	+ 7	+ 8
335	12.5	— 9.3	— 4.1	— 7	+ 7
336	14.0	— 9.3	—37.9	— 4	— 5
337	12.2	— 9.1	+ 7.9	+ 1	— 4
338	14.6	— 9.0	—40.6	— 3	— 4
339	12.0	— 9.0	+33.5	— 2	+ 9
340	13.7	— 8.9	+10.6	+ 7	+ 9
341	12.9	— 8.7	+37.3	+ 3	— 3
342	12.8	— 8.7	—38.0	+ 5	0
343	12.4	— 8.7	—36.6	+ 5	+ 1
344	12.2	— 8.7	— 2.6	— 2	— 13
345	13.8	— 8.7	—21.2	— 4	+ 3
346	12.9	— 8.6	+ 6.8	— 1	— 1
347	13.8	— 8.6	+17.4	— 7	+ 5
348	13.8	— 8.6	+13.7	+14	+ 9
349	14.3	— 8.5	— 8.8	— 5	+ 5
350	14.3	— 8.5	—13.6	— 5	— 4
351	13.0	— 8.5	—34.2	+ 8	+ 9
352*	12.5	— 8.4	+27.4	+ 1	+ 4
353	11.7	— 8.3	+17.4	+31	+ 8
354	12.7	— 8.1	—10.3	—16	— 11
355*	12.5	— 8.0	— 9.3	—15	+ 1
356	13.8	— 7.9	— 8.7	+ 5	— 2
357*	12.2	— 7.8	—44.4	— 3	0
358	13.2	— 7.7	— 3.7	0	+ 4
359	12.2	— 7.7	—11.9	+ 2	+ 8
360	11.2	— 7.7	+36.3	— 2	— 2
361	13.7	— 7.6	+40.2	+ 2	+ 6
362	14.6	— 7.3	—15.4	— 4	+ 13
363	12.8	— 7.5	—47.6	— 6	+ 12
364*	13.7	— 7.4	+41.7	— 5	— 4
365	13.4	— 7.4	—13.0	— 1	+ 1
366	14.2	— 7.4	— 8.1	— 8	+ 2
367	12.7	— 7.4	+ 1.8	+12	+ 4
368	14.3	— 7.3	—44.7	+ 1	+ 2
369	14.6	— 7.3	—15.4	+10	+ 4
370	13.8	— 7.2	+22.4	0	— 1
371	13.8	— 7.1	+ 1.6	+ 3	— 4
372	11.0	— 7.1	+41.3	— 6	— 3
373	14.2	— 7.0	+29.2	+ 7	+ 8
374	14.8	— 6.9	—34.4	+10	— 7
375	11.8	— 6.9	+ 5.4	— 4	+ 6
376	12.8	— 6.7	— 2.1	— 3	+ 1
377*	12.7	— 6.7	— 3.2	+ 4	— 11
378	13.9	— 6.7	—13.2	0	+ 6
379	14.6	— 6.7	+39.5	+ 3	+ 3
380	14.2	— 6.5	—14.8	+ 1	+ 1
381	14.7	— 6.5	—33.8	+15	+ 4
382	14.6	— 6.5	—44.5	— 4	0
383	14.1	— 6.3	—21.8	+ 2	+ 4
384	12.9	— 6.2	—19.7	— 1	0
385	13.7	— 6.2	—18.7	+ 2	+ 2
386	13.7	— 6.1	+ 1.7	+ 1	+ 2
387	14.5	— 6.1	+21.9	+ 9	+ 1
388	13.5	— 6.1	—40.6	+ 1	— 1
389	13.2	— 6.1	—43.0	+ 6	+ 4
390	13.4	— 5.9	+27.7	— 3	— 4
391*	13.2	— 5.8	+10.0	+10	— 5
392	13.1	— 5.8	—42.5	+ 3	+ 1
393	13.6	— 5.7	—42.5	+ 8	+ 6
394	13.0	— 5.6	+38.2	+10	+ 5
395	14.5	— 5.5	—47.6	+12	+ 6
396	14.3	— 5.5	—30.7	— 1	— 6
397	11.7	— 5.5	+ 1.1	+ 2	0
398	10.2	— 5.4	+39.9	— 8	+ 8
399	14.2	— 5.3	— 1.3	— 5	+ 7
400	13.9	— 5.3	+11.4	+ 2	— 4
401	14.0	— 5.3	—28.6	—10	0
402	14.0	— 5.0	+15.8	+ 6	+ 5
403	13.4	— 4.7	+ 4.5	— 2	— 2
404	13.8	— 4.6	+ 2.7	+ 2	— 1
405	13.9	— 4.6	+ 2.0	— 1	+ 7
406	14.2	— 4.5	+ 9.8	— 7	+ 2
407	13.0	— 4.4	+26.2	+ 4	— 15
408	12.2	— 4.3	—30.6	—10	— 9
409	13.4	— 4.3	—16.9	— 1	+ 1
410	12.6	— 4.1	—17.6	— 3	— 7
411*	13.0	— 4.1	—25.3	+ 3	+ 3
412*	13.6	— 4.1	+15.0	+ 1	— 2
413	14.4	— 4.1	— 2.2	—13	+ 3
414	13.1	— 4.0	+37.0	+ 6	+ 3
415	14.3	— 3.9	+ 5.4	— 3	+ 7

Continuation of the CATALOGUE

No. of the star	m_{pg}	X	Y	μ_x	μ_y
416	11.5	−3.9	−35.4	+ 4	− 5
417	12.0	− 3.8	− 3.0	+ 7	+ 1
418	14.2	− 3.7	−40.9	+ 5	+ 2
419	14.3	− 3.6	+17 0	+ 6	+ 3
420	13.2	− 3.6	+ 0.9	− 5	+ 8
421	14.8	− 3.6	+ 3.7	+ 6	− 18
422	12.7	− 3.6	+35.4	− 3	− 1
423	14.2	− 3.5	−43.4	+13	+ 14
424	13.4	− 3.4	− 0.7	+14	− 12
425	14.5	− 3.3	+26.7	+ 1	+ 3
426	13.2	− 3.2	+ 8.0	− 4	− 4
427	14.5	− 3.1	+11.6	+ 2	+ 2
428	14.2	− 3.1	+28.4	−14	+ 4
429	14.8	− 3,1	+ 3.8	+ 4	+ 7
430	13.7	− 2.9	−22.1	+10	+ 4
431	14.4	− 2.9	+ 2.3	+ 5	− 4
432	7.6	− 2.7	−10.0	+10	+ 15
433	11.8	− 2.6	+40.4	− 5	− 4
434*	12.9	− 2.5	−17.6	− 1	− 7
435	14.9	− 2.5	−33.7	+ 4	− 7
436	13.5	− 2.4	− 4.4	− 5	− 3
437	14.6	− 2.3	+19.8	+ 2	+ 4
438	12.8	− 2.3	− 1.4	− 1	+ 5
439*	12.2	− 2.3	+38.4	0	− 9
440	13.0	− 2.3	−13.5	− 1	+ 7
441	14.5	− 2.2	+ 6.1	−12	− 4
442	14.4	− 2.1	− 8.4	+ 2	+ 5
443	14.5	− 2.0	− 4.0	+10	− 2
444	14.6	− 2.0	+11.5	− 4	0
445	14.0	− 1.7	−12.3	− 3	+ 5
446	14.8	− 1.6	+26.7	+10	− 3
447	14.4	− 1.5	−19.7	+ 1	+ 5
448	14.6	− 1.5	+16.2	+ 2	+ 5
449*	13.0	− 1.5	−33.7	+13	− 1
450	11.8	− 1.5	− 4.8	− 8	− 1
451	14.1	− 1.4	+21.7	+ 2	+ 6
452	12.2	− 1.4	− 3.8	− 7	+ 4
453	13.7	− 1.3	+40.5	+12	+ 3
454	12.5	− 1.2	+32.5	− 2	+ 8
455	14.3	− 1.1	− 4.6	− 3	− 4
456	14.4	− 1.1	+20.8	− 2	+ 2
457	14.1	− 0.9	−41.9	− 2	+ 1
458	13.9	− 0.7	+38.0	+ 4	− 3
459	10.2	− 0.6	+22.2	+ 9	− 3
460	13.0	− 0.5	+11.8	+ 3	− 3
461	11.7	− 0.4	+14.6	+ 5	+ 13
462	13.7	− 0.3	− 6.8	− 3	+ 4
463	14.0	− 0.3	−12.1	+ 3	+ 6
464	13.0	− 0.2	+39.5	+ 2	+ 3
465*	13.5	− 0.2	+31.9	0	+ 5
466	13.0	− 0.1	+ 4.8	− 9	+ 8
467	12.7	0	+14.0	−10	+ 12
468	11.8	0	+28.4	− 2	0
469	12.7	+ 0.1	− 8.2	− 1	− 29
470	14.1	+ 0.1	+34.8	− 4	− 4
471	14.1	+ 0.1	+36.2	+15	− 8
472	14.1	+ 0.1	+ 6.2	− 5	+ 4
473*	12.5	+ 0.3	+ 3.5	− 1	+ 1
474	12.6	+ 0.3	+16.6	− 2	0
475	14.0	+ 0.3	−10.3	− 3	+ 9
476	11.9	+ 0.4	−22.0	− 1	− 4
477	13.2	+ 0.4	+31.1	+ 6	+ 4
478	13.0	+ 0.4	−40.4	+ 2	0
479	11.8	+ 0.6	+19.3	+ 9	− 4
480	13.0	+ 0.6	+ 4.3	+ 1	+ 2
481	14.5	+ 0.7	−25.0	− 1	+ 7
482*	13.4	+ 0.9	+17.2	0	0
483	13.6	+ 1.0	+16.7	− 1	+ 6
484	14.3	+ 1.0	− 6.8	− 3	+ 7
485	13.0	+ 1.0	−40.7	0	− 5
486	11.5	+ 1.1	− 3 6	− 7	− 8
487	14.1	+ 1.3	−29.6	− 1	+ 5
488	14.5	+ 1.5	− 1.6	+ 7	− 10
489	14.1	+ 1.5	+29.6	− 6	− 13
490	13.6	+ 1.5	+ 7.6	+ 5	+ 7
491	13.5	+ 1.7	−46.8	+ 2	+ 8
492	11.7	+ 1.8	+ 1.1	−12	− 3
493	12.2	+ 1.9	−28.7	0	− 6
494	14.2	+ 1.9	+18.8	− 4	+ 1
495	13.7	+ 2.0	+23.6	+ 2	+ 3
496	14.3	+ 2 0	+ 0.7	− 2	+ 4
497	12.9	+ 2.0	−22.4	+ 3	+ 2
498	14.4	+ 2.1	−24.5	− 4	+ 3
499	13.4	+ 2.2	+23.6	+ 6	− 1
500	14.1	+ 2.3	−38.3	+ 2	+ 4
501	13.7	+ 2.3	+39.4	+ 2	− 14
502	13.8	+ 2.6	+21.9	+ 6	− 5
503	14.2	+ 2.6	+36.2	+ 3	− 4
504	14.3	+ 2.8	−27.8	− 5	+ 8
505*	13.8	+ 2.9	+ 7.7	+ 3	− 2
506	14.4	+ 2.9	+13.4	− 8	+ 12
507	14.4	+ 3.0	+13.2	−15	+ 14
508	13.2	+ 3.4	−25.0	− 2	+ 2
509	13.2	+ 3.4	−25.2	− 6	+ 3
510	13.0	+ 3.4	−18.9	−16	+ 7
511	14.1	+ 3.5	+10.0	+ 2	0
512	13.0	+ 3.5	+27.7	− 2	+ 5
513	12.6	+ 3.5	+31.4	− 8	− 1
514	11.9	+ 3.6	−28.1	− 4	− 2
515	13.9	+ 3.8	−14.2	+ 3	+ 6
516	13.1	+ 4.2	− 4.6	− 6	+ 3
517	12.7	+ 4.4	− 9.6	− 4	− 24
518	13.0	+ 4.5	−27.6	−14	− 10
519	13.0	+ 4.7	−39.4	+ 2	0
520	14.1	+ 4.7	+13.8	− 1	− 3

Continuation of the CATALOGUE

No. of the star	m_{pg}	X	Y	μ_x	μ_y
521	12.2	+ 4.7	− 4.6	− 6	+ 2
522	13.8	+ 4.7	+35.8	+26	− 21
523	13.3	+ 4.8	+37.4	− 1	+ 3
524	13.4	+ 4.8	+ 1.8	+ 9	0
525	12.5	+ 4.9	−43.4	+ 8	− 15
526	13.0	+ 4.9	−39.2	− 6	− 3
527	12.9	+ 5.0	−17.1	0	+ 6
528	13.1	+ 5.0	− 3.1	+ 7	+ 5
529	12.9	+ 5.1	−31.6	+ 1	+ 1
530*	13.8	+ 5.1	− 3.2	− 3	− 1
531	14.3	+ 5.3	+21.0	0	+ 7
532	12.4	+ 5.3	+27.1	− 5	− 1
533	11.2	+ 5.3	+11.4	+ 1	− 10
534	14.4	+ 5.4	−17.4	− 4	+ 1
535	14.3	+ 5.5	+ 1.1	−11	− 4
536	14.1	+ 5.6	+26.8	− 5	− 2
537	12.5	+ 5.7	−38.8	0	− 8
538	13.4	+ 5.7	−36.5	+ 9	− 18
539	14.3	+ 5.9	− 3.5	− 3	+ 13
540	14.4	+ 6.2	+ 9.4	+ 2	− 5
541	12.7	+ 6.3	−33.4	+ 2	− 5
542	12.2	+ 6.5	−24.6	+ 3	− 19
543	14.5	+ 6.5	−15.8	0	+ 4
544	14.5	+ 6.5	−17.6	+ 5	+ 3
545	13.1	+ 6.6	−42.0	+ 5	− 1
546	12.5	+ 6.6	−38.3	+13	− 2
547	13.8	+ 6.6	−12.3	− 6	+ 2
548	14.3	+ 6.7	− 0.1	+ 5	+ 9
549	14.3	+ 6.8	+16.2	− 1	+ 1
550	14.6	+ 6.9	+28.4	− 5	+ 2
551	13.6	+ 7.0	− 3.3	0	+ 3
552	13.4	+ 7.3	−16.6	+ 1	+ 5
553	13.6	+ 7.5	+35.4	+ 5	+ 3
554*	13.8	+ 7.6	+12.4	+ 3	+ 2
555	13.0	+ 7.6	+23.4	+ 2	− 1
556*	13.7	+ 7.7	−27.5	− 5	+ 16
557	11.3	+ 8.1	+27.7	+ 3	+ 11
558	13.8	+ 8.3	+ 4.8	−14	+ 6
559	11.0	+ 8.3	−12.9	+11	− 16
560*	13.4	+ 8.4	−17.3	+ 2	+ 3
561	13.7	+ 8.4	−21.0	+ 1	+ 1
562	12.0	+ 8.4	+ 5.9	−14	− 17
563	14.1	+ 8.4	+33.2	+ 4	+ 4
564	12.9	+ 8.5	+38.5	− 6	0
565	13.9	+ 8.5	+24.5	0	0
566	14.3	+ 8.3	+26.0	+ 3	− 5
567	14.0	+ 8.6	+ 1.9	− 2	+ 3
568	12.2	+ 8.7	−26.6	+11	− 6
569	14.2	+ 8.7	+26.0	+ 2	+ 1
570	12.5	+ 8.8	+ 9.8	− 8	− 2
571	14.1	+ 8.8	+16.5	− 1	− 3
572	14.5	+ 8.9	−16.1	− 3	+ 10
573	11.4	+ 9.0	− 1.6	+ 2	− 8
574	13.8	+ 9.1	− 7.6	− 4	+ 3
575	14.4	+ 9.3	+ 8.2	+ 2	− 1
576	14.5	+ 9.3	+26.5	+ 1	− 9
577	14.6	+ 9.4	+25.7	+ 1	− 2
578	14.5	+ 9.4	+26.7	+ 8	− 25
579	14.8	+10.0	−43.0	+ 9	+ 4
580*	13.4	+10.2	−43.2	+ 1	+ 1
581	13.3	+10.3	−42.6	+10	+ 2
582	13.1	+10.3	−28.8	+ 3	− 2
583*	13.1	+10.3	− 8.6	− 1	− 3
584	14.5	+10.4	− 4.6	+ 2	+ 10
585	14.7	+10.4	−37.8	− 4	+ 2
586	14.8	+10.5	−36.4	− 2	+ 7
587	13.8	+10.6	+14.8	+ 5	0
588	14.3	+10.6	+ 6.6	+ 1	0
589	13.1	+10.9	−30.8	0	− 2
590	13.0	+11.3	−40.6	− 3	− 1
591	14.5	+11.3	−38.4	+ 5	− 2
592	14.5	+11.4	−12.8	− 6	+ 2
593*	14.0	+11.4	+ 4.6	+ 5	+ 1
594	13.6	+11.5	+14.4	− 6	+ 2
595	13.0	+11.6	+29.1	+ 5	− 1
596	14.3	+11.6	− 8.6	− 9	− 3
597	14.6	+11.7	+ 8.8	+ 8	− 4
598	12.3	+11.8	−26.2	− 4	+ 3
599	12.7	+11.9	−38.2	+ 3	− 10
600	12.5	+11.9	+23.6	− 2	− 5
601	13.1	+11.9	− 1.1	+ 1	− 11
602	12.9	+11.9	− 1.6	− 5	+ 3
603	13.0	+12.1	−19.4	+11	− 5
604	14.0	+12.1	−41.6	+ 6	− 4
605	14.2	+12.3	+ 7.3	+ 2	− 3
606	12.2	+12.3	+ 1.2	−15	+ 3
607	12.4	+12.4	− 2.0	−11	+ 8
608	14.6	+12.4	−13.2	+15	− 5
609	14.8	+12.4	−12.5	+11	− 8
610	13.0	+12.4	+28.7	+ 2	− 5
611	11.8	+12.4	−33.6	+ 4	− 6
612	14.3	+12.5	−43.5	− 1	− 8
613	13.1	+12.6	+29.5	− 8	− 1
614*	12.2	+12.6	+12.8	+ 5	− 7
615	14.8	+12.6	−15.6	− 5	− 18
616	14.2	+12.7	−22.6	+ 4	− 5
617*	13.6	+12.7	+31.9	+ 1	+ 2
618	13.8	+12.8	−21.9	+ 4	0
619	14.2	+12.8	−13.6	− 1	− 5
620	14.6	+12.8	− 3.5	− 6	− 2
621	13.1	+13.0	+26.6	− 1	+ 6
622	14.1	+13.0	+34.8	0	+ 3
623	13.8	+13.1	+32.4	+ 3	+ 12
624	13.1	+13.3	+11.1	+ 5	+ 2
625	14.0	+13.4	−20.6	+ 13	+ 19

Continuation of the CATALOGUE

No. of the star	m_{pg}	X	Y	μ_x	μ_y
626	11.9	+13.4	− 8.2	− 6	+ 4
627	12.6	+13.4	−41.8	− 5	+ 2
628*	13.8	+13.5	+39.0	+ 3	+ 14
629	14.8	+13.5	−27.7	+14	+ 11
630	12.5	+13.7	−25.6	+ 9	+ 9
631	13.2	+13.7	− 5.7	− 2	0
632	12.5	+13.8	+20.8	−13	− 1
633	13.4	+14.1	− 4.6	−12	+ 13
634	14.2	+14.2	+18.7	+ 4	+ 2
635*	13.8	+14.2	+23.7	− 5	+ 1
636	13.8	+14.5	−35 9	+ 4	0
637	12.7	+14.5	−29.0	− 5	− 6
638	13.4	+14.5	−25.1	− 8	− 1
639	14.4	+14.6	+16.4	+ 4	+ 2
640	11.3	+14.7	+19.7	+ 1	− 7
641	13.9	+14.7	−33.7	− 8	+ 3
642	13.2	+14.7	−35.6	0	− 10
643	14.0	+14.7	−37.6	+ 2	− 1
644	14.1	+14.7	+30.7	− 4	− 1
645	15.0	+14.8	+24.4	− 2	+ 4
646	14.2	+14.9	+24.6	− 7	− 6
647	13.4	+15.0	+ 7.5	+ 4	− 3
648	13.5	+15.3	− 0.9	− 5	+ 6
649	13.9	+15.4	−21.0	− 1	+ 3
650	12.5	+15.4	−16.2	− 4	− 8
651	13.7	+15.4	+18.1	−10	− 2
652	14.4	+15.5	−26.5	+ 8	− 3
653	12.2	+15.5	−35.6	+ 4	− 4
654	13.4	+15.6	−37.6	+ 1	+ 5
655	12.9	+15.6	− 8.4	0	+ 6
656	14.1	+15.7	+11.3	− 6	0
657	13.0	+15.7	−14.4	+ 3	+ 1
658	14.2	+16.0	+ 7.8	+ 1	+ 7
659	12.9	+16.2	+13.4	− 5	− 18
660	13.1	+16.5	+ 4.6	− 6	− 2
661	13.1	+16.9	+12 2	− 6	+ 2
662	12.5	+17.1	+22 9	− 9	0
663*	13.5	+17.4	−13.6	+ 6	+ 6
664	14.2	+17.5	+23.4	+ 4	− 5
665	14.0	+17.5	−33.2	− 5	+ 2
666	13.6	+17.6	+29.9	+ 3	− 8
667	13.2	+17.6	−17.4	+ 1	− 1
668	12.5	+17.7	−16.6	+ 1	− 4
669	13.7	+17.7	+21.2	− 3	− 1
670	13.1	+17.8	+11.8	− 2	+ 5
671	14.5	+17.9	−17.6	− 4	+ 2
672	13.8	+17.9	− 2.1	− 4	− 4
673	12.9	+18.2	−30.4	− 7	− 6
674	11.9	+18.3	+13.1	− 2	− 19
675*	13.1	+18.3	− 4.4	− 5	− 2
676	12.6	+18.3	−17.6	+ 9	− 10
677	12 5	+18.4	− 2.4	− 4	+ 18
678	13.8	+18.5	−32.7	+ 6	+ 7
679	13.4	+18.5	+ 2.3	0	− 4
680*	13.4	+18.6	+ 3.0	− 1	− 2
681	12.6	+18.6	−34.6	+ 1	+ 2
682	13.4	+18.6	+19.3	+ 7	− 4
683	13.0	+18.7	−27.2	− 3	− 2
684	14.1	+18.7	−30.0	0	− 5
685	14.2	+18.7	−13.2	− 6	+ 1
686	10.4	+18.8	−20.9	− 6	− 17
687	14.5	+18.8	−16.2	+ 6	+ 7
688	12.7	+19.1	−11.8	−19	− 3
689	13.4	+19.3	− 6.0	−12	+ 7
690	12.8	+19.3	+10.4	− 1	− 2
691*	13.2	+19.3	−35.5	+ 2	+ 6
692	13.2	+19.4	+21.0	+ 1	+ 1
693	13.1	+19.5	−37.9	+ 2	− 1
694	14.0	+19.5	−19.9	+18	− 2
695	13.2	+19.5	−19.9	+13	− 5
696	12.6	+19.6	+30.0	− 2	− 3
697	14.1	+19.6	−31.0	− 5	− 3
698	14.1	+19.7	−31.0	− 8	− 6
699	12.1	+19.7	− 5.8	−10	− 21
700	13.9	+19.8	−14.1	+ 7	− 5
701	12.6	+19.9	+29.8	+ 7	− 16
702	14.0	+19.9	−20.6	− 1	+ 3
703	12.7	+19.9	+11.4	−10	− 8
704	13.1	+20.0	−27.0	0	+ 6
705	14.5	+20.2	+21.3	+ 2	+ 4
706	13.0	+20.3	+22.6	− 8	+ 3
707*	13.3	+20.3	−23.6	0	− 5
708	13.5	+20.3	−18.1	−11	− 5
709	14.8	+20.4	− 3.5	− 7	+ 4
710	14.3	+20.5	− 7.6	− 2	− 18
711	12.7	+20.5	+29.6	− 3	− 6
712	12.5	+20.6	−26.2	+20	− 3
713	14.1	+20.6	−30.9	+ 3	+ 1
714	12.9	+20.7	+20.7	− 3	+ 2
715	12.5	+21.0	+ 5.6	+ 3	− 11
716	13.8	+21.1	+11.8	−29	− 3
717	13.0	+21.1	−16.6	− 4	− 21
718	12.2	+21.2	−26.2	−14	+ 2
719	12.9	+21.3	−22.4	− 5	− 1
720*	12.9	+21.3	+18.1	− 2	0
721	13.2	+21.3	+17.7	− 1	0
722	14.7	+21.3	− 5.9	+11	− 8
723	13.3	+21.4	+ 7.8	+ 8	+ 3
724	14.1	+21.5	+28.2	+ 5	− 9
725	14.0	+21.5	+25.5	− 4	+ 1
726	12.4	+21.5	−31.0	− 3	0
727	13.8	+21.7	+ 9.5	− 2	+ 7
728	14.4	+21.8	+ 4.6	− 2	+ 6
729	12.7	+22.2	−34.6	− 4	− 3
730*	13.4	+22.2	+27.9	− 4	− 3

Continuation of the CATALOGUE

No. of the star	m_{pg}	X	Y	μ_x	μ_y
731	13.1	+22.3	−21.4	+ 1	+ 17
732*	13.4	+22.4	+18.7	+ 2	— 2
733	13.4	+22.5	+ 5.7	— 4	+ 4
734	13.9	+22.6	+ 5.8	+ 3	+ 1
735*	13.4	+22.6	— 9.0	+ 4	— 2
736	13.5	+22.6	+26.4	+ 4	0
737	14.5	+22.7	−10.5	— 3	+ 1
738	14.5	+22.7	+ 3.2	0	— 3
739	13.7	+22.9	−26.1	— 3	— 3
740	12.8	+23.1	+ 1.3	— 8	+ 5
741	12.6	+23.1	+ 7.1	+ 5	+ 6
742	14.1	+23.3	−29.5	+ 2	0
743	13.9	+23.5	+ 9.8	−10	— 12
744	13.8	+23.6	+ 9.2	+ 5	— 8
745	12.9	+23.6	+15.2	+ 2	+ 8
746	12.3	+23.7	+30.0	+ 2	— 2
747	12.3	+23.8	— 6.6	— 3	+ 6
748	12.9	+23.9	+31.6	— 3	+ 4
749	13.3	+24.0	−32.6	+ 7	+ 4
750	14.3	+24.1	+25.7	— 4	— 1
751	14.1	+24.2	+24.4	+ 1	— 3
752	13.0	+24.3	−33.4	— 7	+ 1
753	14.5	+24.2	— 0.1	— 2	+ 8
754	13 0	+24.5	−24.1	+ 3	— 7
755	14.9	+24.6	−26.8	+ 8	— 4
756	13.8	+24.6	−29.3	+ 2	0
757	12.5	+24.7	−18.3	−11	+ 4
758	10.3	+25.2	−17.8	−11	— 6
759	13.1	+25.5	+10.8	−14	— 3
760	12.8	+25.3	−33.6	+ 2	— 6
761	12.0	+25.6	+30.4	— 5	— 9
762	13.2	+25.9	+ 5.7	−11	0
763	13.4	+26.0	— 2.3	— 3	+ 2
764	12.8	+26.2	−15.2	−14	— 25
765	12.5	+26.3	+29.4	— 4	+ 7
766	13.1	+26.3	−25.6	— 4	+ 2
767	14.5	+26.3	— 8.6	— 6	+ 5
768	14.3	+26.5	−31.6	+ 9	+ 8
769*	13.0	+26.5	−31.4	— 1	0
770	14.1	+26.6	+14.6	+ 2	+ 5
771	13.8	+26.6	— 7.4	+ 3	— 2
772	12.9	+26.8	+29.2	0	— 2
773	14.3	+26.9	−24.7	— 3	— 2
774	11.7	+26.9	+ 6.7	— 3	— 23
775	13.1	+26.9	−16.3	— 2	— 3
776	13.9	+27.3	+ 5.3	−12	— 2
777	14.1	+27.3	— 2.7	— 3	+ 5
778	14.5	+27.6	−25.6	+ 6	— 2
779	14.1	+27.9	−19.6	+ 5	0
780*	12.4	+28.0	+ 7.4	— 6	— 1
781	11.9	+28.1	−20.1	— 5	— 8
782	14.3	+28.2	+16.4	+ 1	+ 4
783	9.2	+28.2	−10.8	−21	— 27
784	14.1	+28.3	+20.8	— 5	+ 4
785	14.3	+28.3	−25.0	+ 5	+ 5
786	13.4	+28.3	+26.7	+ 3	+ 11
787	12.6	+29.2	+10.4	— 3	— 11
788	14.5	+29.2	−26.2	+ 7	0
789	13.0	+29.3	+ 0.6	— 2	— 1
790	14.3	+29.3	−16.3	+ 4	+ 3
791	12.9	+29.4	+16.9	— 1	+ 5
792	13.0	+29.6	+14.4	— 1	— 20
793	14.1	+29.6	−19.3	+ 2	+ 1
794	12.9	+29.7	−16.2	— 6	— 10
795	14.3	+29.7	+18.1	+ 8	— 6
796	13.6	+29.9	−24.9	— 2	— 3
797	12.9	+30.0	−15.8	— 6	+ 4
798*	13.8	+30.3	−19.9	+ 6	— 4
799	13.3	+30.6	−28.0	— 6	— 5
800	12.0	+30.7	−27.0	−11	— 4
801	12.6	+30.7	— 5.6	— 4	— 7
802	14.0	+30.9	+23.1	+ 2	+ 3
803	11.4	+31.0	+19.8	— 9	+ 1
804	14.2	+31.1	−25.6	+10	0
805	12.3	+31.1	— 3.9	−19	— 14
806	14.1	+31.3	+11.7	— 5	+ 5
807	10.8	+31.4	−14.2	— 1	0
808	14.5	+31.5	+ 1.2	— 1	+ 6
809	13.8	+31.6	+ 7.4	0	— 1
810	11.9	+31.7	+ 9.6	−16	— 8
811	14.0	+31.7	— 3.3	+ 7	— 3
812	14.3	+32.1	−13.2	0	— 2
813	14.2	+32.2	−15.6	— 8	+ 6
814	13.0	+32.3	−17.6	+ 3	— 7
815*	13.6	+32.3	— 6.6	— 3	+ 1
816	14.5	+32.3	— 4.8	0	+ 4
817	11.9	+32.3	+ 4.8	−14	— 16
818	13.8	+32.5	+16.3	— 6	— 6
819	12.9	+32.6	+19.9	— 1	+ 4
820	9.1	+32.7	−10.9	— 1	— 7
821	13.2	+32.8	+21.4	— 7	+ 5
822*	13.2	+33.3	+15.2	— 1	— 5
823	13.8	+33.4	— 7.6	−13	+ 4
824	13.9	+34.0	−15.8	+ 5	+ 3
825	14.5	+34.1	−20.9	+12	— 6
826	14.6	+34.3	— 4.7	— 4	+ 7
827	13.8	+34.3	+18.5	+ 5	+ 1
828	12.4	+34.6	+ 9.9	−10	— 7
829	13.1	+34.6	— 4.6	+ 2	— 1
830	13.5	+34.7	+10.8	— 5	— 11
831	13.8	+34.9	+18.2	— 3	+ 4
832	12.7	+35.0	— 8.3	— 4	+ 4
833	14.2	+35.1	— 4.3	−10	— 1
834	12.3	+35.4	+ 7.6	−18	— 7
835*	13.0	+35.5	— 1.2	— 3	+ 7

Continuation of the CATALOGUE

No. of the star	m_{pg}	X	Y	μ_x	μ_y	No. of the star	m_{pg}	X	Y	μ_x	μ_y
836	14.2	+35.5	−13.2	+ 5	+ 4	841	13.5	+37.0	+ 4.0	− 8	+ 2
837	12.8	+35.7	−18.3	− 9	− 7	842	11.2	+37.0	+ 8.8	− 4	+ 22
838	13.1	+35.8	−12.4	+ 4	− 2	843	12.3	+38.5	+ 0.9	− 2	− 9
839	12.2	+36.1	− 3.6	0	+ 2	844	13.8	+38.7	− 3.9	+16	+ 4
840	13.6	+36.5	−18.8	−12	− 5						

Stars with large proper motions

1	13.9	−36.5	+ 8.4	+ 9	− 54	13	13.8	+ 3.0	−21.4	−11	− 54
2	11.9	−33.4	− 1.3	+10	− 41	14	8.6	+ 5.5	−18.2	− 7	− 47
3	12.7	−33.2	− 3.8	+10	− 59	15	12.2	+ 6.8	+21.9	−12	− 41
4	12.3	−32.9	−31.2	+88	− 37						
5	6.8	−16.3	+19.4	−37	− 25	16	12.2	+ 7.1	+28.0	−90	−153
						17	13.3	+ 9.7	−24.2	+43	− 56
6	11.1	− 3.6	− 2.3	+25	− 52	18	12.3	+15.1	− 7.4	+49	− 88
7	13.6	− 2.0	+37.2	−35	− 27	19	12.6	+18.8	− 7.6	+91	− 31
8	13.0	− 1.2	−34.6	+11	−115	20	14.2	+21.8	−31.5	+26	− 27
9	12.7	− 0.5	−23.2	+26	− 25						
10	12.2	− 0.4	+24.4	+28	− 28	21	11.4	+25.4	+11.4	−15	− 35
						22	10.2	+30.4	+ 8.7	−15	− 39
11	12.0	+ 0.3	+23.7	− 2	− 51	23	10.6	+39.7	−31.3	+48	−504
12	11.6	+ 1.6	−29.9	+80	− 97						

Region X Leo

$\alpha_{1950} = 09^h48^m.4$ $\quad \delta = +12°07'$

1	13.8	−51.3	− 9.3	0	+ 10	31*	13.4	−20.8	− 5.4	+14	+ 3
2	13.9	−51.2	− 8.0	+ 9	+ 21	32	11.8	−20.1	−28.9	+ 1	− 4
3	12.1	−45.4	+15.5	− 9	+ 14	33	13.5	−19.8	+11.0	+ 5	− 20
4*	12.7	−44.6	− 9.2	−12	+ 12	34	14.0	−19.6	−13.6	− 3	+ 8
5*	12.7	−43.8	+ 9.3	− 6	+ 5	35	14.0	−18.8	−14.5	−14	+ 11
6	13.0	−43.0	− 9.1	+ 6	+ 16	36*	13.0	−18.0	−21.1	− 3	+ 16
7	12.5	−42.0	−12.6	− 3	+ 13	37*	12.9	−17.1	+29.2	+ 4	+ 10
8	11.0	−41.8	− 6.9	−14	− 16	38	13.4	−16.7	−28.0	−15	+ 12
9	11.5	−40.0	+ 5.8	+ 6	+ 13	39	12.4	−16.2	+35.6	+29	− 10
10	13.8	−36.5	−31.6	−20	+ 11	40	13.0	−16.1	−32.5	+12	− 6
11	13.6	−36.2	− 9.2	− 1	+ 13	41*	12.7	−14.4	+17.4	+ 9	− 6
12	13.8	−35.4	− 0.7	+25	+ 18	42	12.2	−13.4	−38.0	−32	− 15
13	13.5	−34.4	−22.2	− 9	+ 11	43	14.0	−13.0	+18.5	−18	+ 6
14	12.4	−34.0	−27.0	− 6	+ 31	44	13.4	−12.4	−28.6	−19	+ 9
15*	12.7	−32.0	−32.0	+ 5	+ 3	45*	12.7	−12.3	+33.5	−17	− 15
16*	12.7	−31.3	−17.2	−10	+ 3	46	13.9	−12.3	+37.6	− 5	+ 3
17	13.9	−30.7	+24.0	−12	+ 17	47	13.8	−11.8	− 3.8	− 2	+ 8
18	14.0	−29.8	− 8.8	+ 6	+ 5	48	12.9	−11.5	−12.2	−23	− 12
19	14.0	−29.1	−32.1	−16	− 23	49*	12.9	−10.6	−21.6	+ 5	+ 24
20	13.4	−28.0	+ 6.9	− 3	+ 16	50	13.2	−10.1	+28.2	− 6	+ 17
21*	12.7	−27.0	+12.5	+ 7	+ 12	51	13.6	−10.0	+ 9.6	−27	+ 8
22	13.8	−25.3	+ 3.2	0	− 5	52	13.4	− 9.9	−43.6	−31	+ 3
23*	12.1	−24.7	+35.1	+ 8	+ 2	53	13.6	− 9.6	+13.0	−29	+ 12
24	13.8	−24.5	+38.2	− 6	+ 15	54	14.0	− 9.1	+ 8.4	+31	− 1
25	14.0	−24.2	− 5.0	+ 5	+ 13	55	13.8	− 8.0	+ 4.5	−12	+ 11
26	11.8	−24.0	+30.5	+17	− 1	56	14.0	− 7.4	−11.4	−19	+ 23
27	14.0	−23.3	− 44.	0	+ 15	57	14.0	− 6.2	−27.2	− 3	+ 5
28	13.2	−22.2	+30.8	+ 4	+ 13	58*	12.9	− 5.9	−33.2	+ 1	+ 5
29	14.0	−21.4	+30.9	−33	+ 7	59	13.8	− 5.2	−18.0	−16	+ 14
30	10.0	−21.2	+13.3	−29	− 9	60	12.7	− 5.2	+44.4	− 9	− 5

Continuation of the CATALOGUE

No. of the star	m_{pg}	X	Y	μ_x	μ_y	No. of the star	m_{pg}	X	Y	μ_x	μ_y
		′	′					′	′		
61*	12.4	— 4.8	—10.8	+15	— 25	79*	13.4	+16.4	+22.8	— 3	+ 6
62	12.1	— 3.0	—38.4	—20	— 15	80	13.8	+17.0	+17.6	—10	— 9
63	13.8	— 1.6	—30.9	+12	— 13						
64	13.9	— 1.6	+16.3	—25	+ 1	81	13.6	+17.4	+29.1	+19	+ 4
65	13.4	— 0.2	—10.0	—16	— 3	82*	12.3	+18.1	+11.8	—20	+ 15
						83	12.2	+20.8	+13.2	— 2	+ 25
66*	12.7	+ 0.2	+19.5	— 2	— 29	84*	12.7	+22.2	— 5.1	—10	— 5
67*	12.4	+ 1.2	—37.2	— 5	+ 10	85	12.4	+23.0	—35.8	— 7	— 0
68*	12.1	+ 3.7	— 9.0	+12	— 1						
69*	13.2	+ 6.5	+32.3	0	+ 1	86	13.5	+23.0	+10.9	+ 4	+ 2
70*	13.6	+ 8.0	—18.9	—10	— 2	87*	11.8	+23.4	+30.1	+ 2	— 2
						88*	13.4	+27.2	—26 0	— 7	+ 1
71*	13.2	+ 8.8	+32.9	— 1	+ 20	89	13.5	+29.7	—24.9	—11	+ 3
72	12.9	+ 9.0	+36.7	—29	— 7	90*	11.8	+31.0	+17.1	— 1	— 1
73*	12.7	+10.0	+11.4	+23	— 8						
74*	13.5	+10.2	+ 1.7	+ 6	— 7	91	14.0	+31.2	+ 7.3	—10	0
75	13.8	+12.8	— 1.6	—19	— 6	92	13.4	+32.3	+22 2	— 6	— 2
						93	14.0	+32.6	+ 7.9	— 9	+ 22
76	13.5	+14.9	—20.2	—18	— 1	94	13.6	+33.0	— 9.4	—31	+ 1
77*	12.7	+15.4	—37.0	+ 5	+ 2	95	13.4	+35.3	— 8.2	—34	+ 3
78	13.9	+16.3	—10.0	+ 6	— 4						
						96	10.2	+38.3	—13.2	+16	+ 1

Reference stars around the variable X Leonis

1	12.1	—67.2	—34.4	— 3	— 12	8	13.5	—44.1	—34.2	+ 2	— 1
2	13.4	—60.0	—19.5	—11	+ 5	9	12.7	—43.7	—33.5	+14	— 14
3	13.8	—58.0	—27.2	— 8	+ 21	10	12.9	—42.6	—39.0	— 9	+ 10
4	12.1	—57.2	—19.4	—14	+ 20						
5	12.7	—56.8	—30.6	+ 3	+ 18	11	11.0	—39.8	—35.2	+34	— 5
						12	12.9	—38.0	—34.6	—17	+ 12
6	10.2	—56.0	—27.6	—12	— 8	13	13.2	—36.3	—31.9	—11	+ 12
7	13.6	—46.2	—32.8	+ 6	+ 5	RZeo	11.5	—51.6	—27.5	+16	— 35

Stars with large proper motions

1	13.2	—61.1	—21.0	—80	— 52	14	12.9	— 9.5	+33.8	0	+ 45
2	9.0	—55.0	—30.4	—64	+ 30	15*	13.4	— 3.0	— 2.3	+14	— 40
3	10.2	—54.9	—30.8	—68	+ 24						
4	13.8	—39.0	0	+13	— 47	16	13.8	+ 5.0	+20.2	—35	— 6
5	14.0	—34.0	—31.2	+37	— 72	17	13.2	+ 7.0	+27.3	+37	+ 11
						18	13.2	+ 7.2	+16.8	—33	+ 24
6	9.0	—30.0	+13.3	—120	+ 40	19	11.5	+12.6	+38.2	—35	+ 36
7	14.1	—26.2	+25.0	—30	— 87	20	12.9	+14.9	+30.8	+57	— 37
8	11.8	—18.8	+35.8	—60	+ 22						
9	9.0	—18.0	—46.9	—319	— 53	21	12.1	+15.8	—28.2	—78	+ 14
10	11.8	—16.5	—22.2	—46	— 27	22	11.0	+16.8	+20.7	—61	+ 41
						23	11.8	+23.2	—35.0	—17	— 47
11	13.2	—13.6	+33.2	—22	+ 30	24	12.3	+28.4	+26.1	+21	— 29
12	12.9	—13.2	+ 1.8	—27	+ 33	25	10.0	+35.4	—13.8	+79	— 89
13*	11.8	—12.3	+13.6	—20	— 33						
						26	14.0	+48.0	+ 4.0	—93	— 35

Region TW Vir

$\alpha_{1950} = 11^h42^m.1$ $\quad \delta_{1950} = -04°05'$

1*	12.9	—31.1	—10.4	— 4	— 10	8	12.4	—26.4	+19.6	+11	+ 1
2	13.4	—29.4	— 9.0	+ 9	+ 1	9	12.8	—25.2	—22.4	—28	— 9
3	12.6	—28.3	+ 5.2	— 7	+ 4	10	14.5	—24.6	+ 1.0	—16	+ 12
4	12.9	—28 3	0	— 2	— 6						
5*	13.4	—28.3	+ 6.1	+15	+ 9	11*	14.8	—24.5	+ 1.1	+ 3	— 3
						12*	13.9	—23.6	+10.7	—16	+ 8
6*	13.7	—28.0	+20.0	+ 2	— 11	13	12.3	—23 0	+12.2	—39	+ 6
7	13.1	—27.7	— 8.0	0	— 2	14	13.3	—22.2	+21.6	+ 3	+ 10

Continuation of the CATALOGUE

No. of the star	m_{pg}	X	Y	μ_x	μ_y
15	13.3	−21.0	+ 6.9	− 6	+ 15
16*	14.5	−20.2	+28.3	+ 4	+ 2
17	10.5	−18.9	− 5.0	−13	+ 19
18	10.9	−18.2	+ 0.3	+21	+ 21
19	12.9	−17.1	+21.8	+13	− 20
20*	14.1	−16.2	+21.7	− 1	− 6
21*	14.6	−15.5	− 2.2	− 4	+ 2
22	13.1	−15.1	+16.6	+20	− 3
23*	14.6	−14.8	−25.3	−10	− 11
24	13.1	−14.2	−32.3	− 1	+ 8
25*	13.1	−13.5	−33.6	+17	+ 6
26*	14.2	−13.3	+12.0	− 2	− 5
27	14.1	−12.3	− 4.0	−20	− 19
28	12.4	−12.0	− 6.0	− 2	+ 4
29*	13.8	−11.2	+ 7.0	+16	+ 1
30	13.5	−11.0	+15.6	+14	− 20
31	12.9	−10.3	−20.9	− 8	+ 6
32	15.1	− 9.4	+ 1.1	−20	+ 18
33	13.9	− 9.0	+15.3	+ 6	− 2
34*	13.4	− 8.2	−20.3	−12	+ 13
35	12.3	− 7.7	−33.2	−13	− 8
36	13.4	− 7.4	+20.9	+12	− 19
37	14.2	− 7.2	−21.0	−34	+ 9
38	14.0	− 7.1	+11.5	− 6	+ 11
39*	14.9	− 6.4	−10.4	+ 2	+ 3
40	12.4	− 4.8	+37.6	+ 2	+ 10
41	13.4	− 4.4	−31.6	−24	− 5
42	13.3	− 4.1	−25.4	−12	− 21
43	12.6	− 3.6	+10.6	− 8	+ 9
44*	14.6	− 3.2	+28.6	− 9	− 7
45	12.4	− 3.1	+37.9	−14	+ 18
46*	14.5	− 2.6	−29.2	+ 2	− 9
47*	14.8	− 2.2	−22.4	−22	+ 4
48	13.2	− 0.9	+ 8.6	+ 5	− 11
49	14.4	− 0.2	+ 5.6	− 2	+ 19
50	11.4	− 0.2	+20.9	−13	− 21
51	11.8	+ 0.1	+18.6	−18	+ 22
52	13.4	+ 0.1	+17.9	−20	+ 18
53*	14.0	+ 0.3	+32.7	− 7	− 15
54*	14.6	+ 0.6	−32.9	− 8	+ 7
55	15.0	+ 0.9	−28.4	− 3	+ 6
56	15.0	+ 1.1	−28.5	−18	+ 15
57	15.1	+ 1.2	+12.2	+ 4	− 4
58	13.3	+ 1.7	−19.4	+ 1	+ 13
59	10.3	+ 2.0	− 5.0	+14	− 30
60	13.7	+ 2.0	+38.6	− 8	+ 9
61	14.6	+ 2.9	+ 7.5	−18	0
62	15.0	+ 3.0	+ 0.6	−10	− 15
63	13.5	+ 3.4	+13.9	+10	+ 7
64*	14.1	+ 3.6	+ 7.6	+ 5	− 4
65*	13.6	+ 3.8	+22.7	−19	+ 26
66	15.2	+ 4.3	+24.3	+11	− 11
67	12.6	+ 5.4	+13.6	+10	− 19
68	11.5	+ 5.7	+35.6	− 7	+ 10
69	13.4	+ 6.0	+ 9.0	−25	+ 1
70	14.0	+ 6.1	+23.5	− 8	+ 11
71	12.4	+ 7.8	+33.5	− 8	+ 1
72	11.9	+ 9.1	−26.8	− 5	− 4
73	15.2	+ 9.9	+25.6	−17	− 16
74*	13.8	+10.8	−30.6	+13	− 4
75*	14.1	+10.8	− 0.8	+ 3	+ 3
76*	14.0	+10.9	+12.7	+10	+ 8
77	13.0	+11.2	−23.6	−21	+ 7
78*	14.2	+11.9	−12.4	−11	− 6
79	12.4	+12.1	−28.6	−14	− 3
80	13.4	+13.1	+ 0.1	−23	+ 11
81	12.4	+13.4	+ 3.1	+10	− 14
82*	14.6	+15.4	+27.0	− 1	− 2
83*	13.9	+15.8	+ 7.7	+ 5	− 20
84	13.0	+15.9	− 2.6	+11	− 14
85	15.2	+18.2	+19.6	− 3	+ 22
86	15.1	+18.8	+21.6	− 1	+ 21
87	14.6	+18.9	−25.2	−11	+ 5
88	14.8	+19.1	+21.2	+19	+ 3
89*	14.1	+19.2	−21.1	− 4	+ 3
90*	14.6	+19.4	+21.8	+16	+ 14
91	13.6	+19.6	+22.6	+ 7	+ 12
92*	12.9	+20.2	+14.4	− 1	+ 2
93	11.8	+20.9	+ 9.8	−26	+ 18
94	12.6	+22.2	+17.6	+ 3	− 12
95*	13.7	+25.0	− 1.8	+ 4	+ 2
96	11.8	+26.7	+ 5.6	+19	− 23
97	13.5	+27.5	− 3.0	+16	0
98	13.4	+28.5	− 3.7	+26	0
99	13.2	+28.6	+ 9.0	+12	− 3
100	13.5	+28.9	+10.3	−22	+ 1
101	12.3	+29.4	+ 8.2	+12	+ 7
102*	13.8	+29.8	+ 1.1	+ 5	− 4
103	11.5	+30.6	−17.4	− 2	+ 8
104	9.6	+30.8	−11.3	−19	− 19
105	14.9	+34.9	−20.6	−23	+ 23
106	14.5	+36.0	− 1.4	−22	+ 4
107	13.9	+38.4	−24.4	+23	− 21

Stars with large proper motions

1	13.8	−48.3	− 0.2	−62	+ 35
2	10.8	−39.2	+24.2	−70	− 33
3	12.6	−38.0	+21.2	−119	+ 44
4	13.9	−35.2	+25.5	−36	− 6
5	13.5	−23.2	+ 3.2	−43	+ 2

Continuation of the CATALOGUE

No. of the star	m_{pg}	X	Y	μ_x	μ_y
6	13.5	−19.0	− 6.7	−74	− 11
7	10.1	−18.2	+33.9	+14	− 35
8	12.9	−12.4	− 4.0	+19	−102
9	11.4	−10.2	+24.5	−69	+ 25
10	11.9	− 9.0	+13.6	+52	− 20
11	10.5	− 4.9	−43.0	−43	− 2
12	14.5	− 4.8	− 5.3	−38	0
13	14.5	− 3.2	−18.7	−44	+ 2
14	14.9	− 2.1	+32.6	+75	− 2
15	11.0	− 1.8	+ 6.9	+26	− 30
16	11.8	− 1.6	+ 1.7	−40	+ 26
17	7.9	0.0	0.0	−15	− 42
18	15.0	+ 3.7	−11.0	−35	+ 36
19	12.6	+12.8	+ 9.6	+24	− 54
20	11.8	+14.4	+ 7.9	−52	+ 51
21	13.2	+17.6	+28.6	−45	+ 21
22	12.8	+20.0	+46.1	− 8	− 62
23	12.9	+22.1	−21.5	−42	+ 4
24	12.4	+22.7	+ 5.7	−18	− 43
25	12.5	+23.1	− 8.7	−38	+ 12
26	10.3	+29.9	+46.6	+24	− 27
27	14.2	+32.0	+45.8	+ 1	+ 42
28	13.7	+36.4	+15.2	−186	−133

Region *UZ* Ser

$\alpha_{1950} = 18^h09^m.2$ $\quad \delta_{1950} = -14°56'$

No. of the star	m_{pg}	X	Y	μ_x	μ_y
1	13.0	−36.6	− 2.2	+ 17	+ 5
2	13.0	−36.4	− 1.8	+12	+ 7
3*	14.0	−36.4	− 0.8	+13	− 6
4	12.4	−36.2	− 3.4	+ 1	+ 30
5	12.2	−35.3	+ 4.9	+14	+ 7
6	14.5	−35.1	+ 1.7	+21	+ 8
7	14.5	−35.0	+ 1.0	+ 6	+ 6
8*	13.9	−34.8	− 8.2	+14	− 2
9	13.8	−34.2	− 4.3	+24	+ 19
10	13.1	−34.4	+12.6	+ 5	− 2
11	14.1	−33.9	+ 5.8	+ 6	+ 2
12	13.6	−33.8	+ 2.3	+14	− 8
13	13.5	−33.5	− 5.9	−14	− 28
14	13.2	−33.3	+ 8.3	− 6	+ 2
15	12.2	−33.1	+10.8	+ 5	+ 4
16	9.5	−33.0	+ 3.5	−13	− 2
17	13.6	−33.0	+ 3.0	+ 3	− 13
18	14.0	−32.9	− 7.2	− 4	− 7
19	14.5	−32.5	+ 6.1	− 9	− 8
20*	13.9	−32.5	+ 6.0	− 6	− 9
21	13.9	−32.2	−11.5	− 4	− 32
22	14.3	−32.1	− 2.8	− 8	+ 6
23	12.7	−32.0	−11.0	0	− 2
24	14.5	−32.0	−25.1	−16	+ 1
25	13.4	−31.9	−25.2	−12	− 2
26	12.8	−31.9	−15.3	−16	− 2
27	13.5	−31.8	+ 2.8	− 4	− 7
28	13.0	−31.8	− 0.7	− 8	− 1
29	12.8	−31.6	+14.1	−10	− 14
30	14.6	−31.6	+ 4.5	+ 5	0
31	13.9	−31.6	− 7.5	+ 3	+ 6
32	13.0	−31.1	−13.9	−12	− 4
33	13.5	−31.1	+ 1.2	+ 6	+ 8
34	12.4	−30.9	−16.6	+ 5	+ 6
35	13.6	−30.8	−11.7	+ 2	− 10
36	14.7	−30.8	+ 2.8	+ 2	− 5
37	12.2	−30.6	−16.3	−11	− 3
38*	13.9	−30.6	+16.1	− 2	+ 1
39	14.0	−30.6	+11.1	+11	+ 7
40	14.1	−30.5	+13.0	− 1	− 8
41	14.8	−30.4	+ 1.5	+26	− 2
42	14.0	−30.2	+11.3	− 1	− 6
43	12.5	−30.1	+ 8.0	+17	− 4
44	13.2	−30.1	+ 6.9	+12	+ 4
45	13.6	−30.1	+ 1.7	− 1	− 11
46	11.8	−30.1	+ 1.6	− 2	0
47	14.0	−29.9	− 8.0	+18	− 4
48	12.3	−29.7	+ 3.8	+ 4	− 8
49	13.9	−29.7	−20.8	−14	− 6
50	13.8	−29.6	− 3.6	− 3	− 2
51	13.9	−29.5	− 7.2	+ 6	− 4
52	14.6	−29.4	− 1.1	−19	− 19
53	13.2	−29.4	− 2.1	+18	− 10
54	14.9	−29.3	− 1.4	− 6	− 8
55	10.9	−29.2	−19.3	− 4	+ 4
56	14.0	−29.2	−19.8	− 3	+ 10
57	13.5	−29.1	+16.2	− 4	− 10
58	13.3	−28.9	+ 4.5	− 1	+ 6
59	14.1	−28.8	−11.0	+ 9	− 8
60	12.5	−28.8	−24.5	+ 1	+ 22
61	14.4	−28.7	−24.6	+18	+ 26
62	12.5	−28.5	+16.2	− 4	+ 5
63	14.5	−28.2	− 1.8	0	0
64	13.2	−28.0	+21.2	+ 8	+ 8
65	13.3	−27.9	+15.0	+ 6	− 6
66	14.6	−27.6	− 0.5	0	+ 2
67	13.3	−27.2	−23.0	+ 6	+ 7
68	13.5	−27.1	+13.6	− 2	+ 1
69	12.0	−27.0	+ 5.5	+ 2	+ 6
70	13.9	−26.9	−10.9	−12	0
71	14.6	−26.9	+ 5.8	− 2	+ 10
72	14.5	−26.8	+ 7.6	− 7	− 3

Continuation of the CATALOGUE

No. of the star	m_{pg}	X	Y	μ_x	μ_y
73	10.7	−26.7	−22.8	−12	+ 3
74	14.0	−26.7	+16.8	0	− 6
75	13.5	−26.5	+ 4.0	− 8	+ 14
76*	13.4	−26.4	−17.2	− 8	0
77	13.4	−26.3	−17.6	− 6	+ 5
78	13.0	−26.3	+17.6	+ 2	− 10
79	13.3	−26.3	+11.4	+ 4	+ 8
80	13.1	−26.2	− 0.7	0	+ 2
81	13.3	−26.0	−18.8	− 2	− 8
82	12.4	−26.0	+24.0	+10	− 2
83	13.6	−26.0	− 2.8	+ 6	+ 16
84	14.2	−25.9	−14.2	−18	− 3
85	12.0	−25.7	−10.6	− 2	+ 8
86*	13.6	−25.6	−24.0	+ 8	+ 17
87*	13.6	−25.6	+ 1.9	− 2	+ 5
88	14.2	−25.5	+18.5	− 2	+ 2
89	12.3	−25.4	− 3.7	−12	− 3
90	14.6	−25.3	−17.6	−11	− 6
91	14.2	−25.3	−11.7	−30	− 4
92*	14.0	−25.3	−11.8	− 2	− 8
93	14.3	−25.3	−20.9	−28	− 25
94	14.1	−25.2	−22.8	− 6	− 8
95*	13.8	−25.2	+20.3	− 5	− 6
96	13.5	−25.0	−20.2	+ 4	0
97	12.6	−24.9	+ 7.0	+ 2	+ 12
98	14.4	−24.7	+ 9.4	− 6	0
99	13.2	−24.6	+24.2	+ 1	− 2
100	12.7	−24.6	−11.0	− 2	− 14
101	13.9	−24.4	+20.2	− 6	− 20
102*	13.9	−24.3	+12.0	− 4	+ 1
103	14.2	−24.0	− 3.9	− 8	+ 2
104	12.4	−24.0	−18.4	+ 1	− 14
105	12.7	−23.9	+22.6	+28	− 11
106	14.6	−23.8	− 9.2	+ 4	− 8
107	13.2	−23.8	+18.4	0	− 6
108	13.7	−23.5	− 6.5	−18	− 4
109	14.6	−23.4	− 8.8	0	+ 1
110	13.8	−23.2	− 1.8	−27	+ 2
111	14.7	−23.1	− 9.7	+ 2	+ 2
112	12.8	−22.9	− 7.9	− 2	0
113	14.7	−22.9	−18.4	− 6	− 4
114	15.0	−22.9	− 4.0	− 6	− 4
115	13.1	−22.7	+26.4	+10	+ 10
116	13.6	−22.7	−20.8	− 4	+ 6
117	13.3	−22.6	−10.9	+ 4	+ 10
118	13.2	−22.6	+ 2.8	+ 2	+ 7
119	13.2	−22.5	−27.4	− 3	− 4
120	14.8	−22.4	+ 7.2	−13	− 11
121	12.7	−22.2	− 4.1	− 2	+ 1
122	13.9	−22.1	+25.6	+ 9	+ 10
123	11.2	−22.0	− 2.3	− 8	+ 16
124	14.0	−21.8	+ 3.3	+10	+ 6
125	14.7	−21.8	− 3.8	+ 6	− 12
126	11.8	−21.8	− 1.4	+ 4	+ 4
127	14.9	−21.6	+16.3	− 7	+ 13
128	13.0	−21.6	+11.2	− 2	− 4
129	14.5	−21.2	−12.2	+14	+ 2
130	14.6	−21.2	−19.9	+30	+ 6
131	13.5	−21.2	−24.3	−16	+ 2
132	13.4	−21.2	−27.8	− 2	− 8
133	14.0	−21.0	−17.9	− 6	+ 2
134	12.7	−21.0	−27.2	− 4	+ 2
135	14.5	−21.0	− 2.8	− 3	+ 6
136	13.9	−21.0	− 6.6	−12	− 6
137*	13.9	−21.0	− 4.6	− 3	+ 1
138*	13.6	−20.9	−19.8	+12	+ 1
139	14.9	−20.9	− 1.6	+ 7	− 14
140	13.6	−20.8	− 5.4	−11	− 9
141	13.5	−20.7	−17.2	− 8	0
142	11.4	−20.7	− 7.8	+10	+ 8
143	13.6	−20.6	+26.2	+ 8	+ 2
144	14.6	−20.6	+ 9.4	+ 2	+ 13
145	12.8	−20.4	+ 6.3	− 6	+ 4
146*	13.6	−20.4	+ 6.0	+ 4	+ 5
147	14.0	−20.3	− 0.8	− 2	− 12
148	13.6	−20.2	+19.4	+ 7	− 14
149	13.6	−20.2	+15.1	− 4	0
150	13.0	−20.1	− 8.6	− 2	− 2
151	12.7	−19.9	−19.5	+ 5	+ 4
152	13.6	−19.9	− 2.4	− 2	+ 10
153	13.8	−19.9	− 7.9	− 5	− 4
154	13.1	−19.8	+ 7.0	+ 6	+ 14
155	12.8	−19.5	−14.2	−11	− 8
156	13.0	−19.4	−27.6	+ 6	− 8
157	13.6	−19.0	−14.4	− 8	− 12
158	14.0	−18.7	−17.4	+ 8	+ 2
159	13.5	−18.5	−15.5	0	+ 8
160	13.5	−18.3	−12.0	− 2	− 8
161	13.2	−18.2	− 7.8	0	+ 10
162	14.8	−17.7	− 0.8	+ 1	+ 6
163	13.4	−17.6	+ 1.0	− 6	+ 10
164	13.1	−17.2	−17.1	+ 5	+ 12
165	13.4	−17.1	−18.8	− 7	+ 9
166	12.8	−17.1	−29.8	−12	− 2
167	15.0	−16.9	+12.8	−21	− 4
168*	14.0	−16.8	−27.7	− 6	− 1
169	14.4	−16.7	+ 8.9	+ 6	− 26
170	13.9	−16.7	− 1.3	+ 9	− 4
171	13.3	−16.7	+26.6	+ 6	− 20
172	15.0	−16.7	+22.7	− 4	− 4
173	13.6	−16.6	+ 2.2	− 4	− 2
174	13.0	−16.6	−19.8	+ 2	+ 10
175	15.0	−16.6	+12.8	−23	− 8
176	14.0	−16.5	+12.0	−15	0
177	13.5	−16.3	−13.9	+10	− 15

Continuation of the CATALOGUE

No. of the star	m_{pg}	X	Y	μ_x	μ_y
178	14.5	−16.2	+11.0	−16	− 11
179	13.3	−16.1	+29.2	+ 2	− 4
180	13.4	−16.0	+ 2.2	− 6	+ 2
181	13.6	−16.0	− 4.8	+ 2	+ 2
182	13.3	−16.0	− 4.6	+ 6	+ 4
183	13.3	−16.0	−19.7	−17	+ 5
184*	14.0	−16.0	+19.4	+ 1	+ 2
185	13.4	−15.8	−11.5	− 9	0
186	14.4	−15.6	+ 8.1	− 8	− 10
187	13.8	−15.2	−11.5	+ 4	+ 7
188*	14.0	−15.2	−21.2	− 6	+ 2
189	14.8	−15.1	−18.0	+ 4	+ 6
190	12.8	−15.0	+32.2	− 2	− 4
191	12.4	−14.8	−20.8	− 7	− 12
192	13.5	−14.8	−29.8	+ 3	0
193*	13.6	−14.7	+27.3	+ 3	− 2
194	10.2	−14.7	+12.6	−24	− 16
195	15.0	−14.6	−20.8	+ 4	+ 11
196	13.5	−14.6	+ 5.6	+12	+ 6
197*	13.6	−14.5	−32.8	−10	+ 1
198	13.5	−14.4	+32.2	+10	− 2
199	14.3	−14.1	−17.3	− 4	− 2
200	14.7	−14.0	−17.9	− 1	− 6
201	13.6	−14.0	+ 2.2	−12	+ 2
202	14.0	−14.0	− 9.0	− 6	− 10
203	14.9	−13.9	+18.5	+10	− 5
204	14.8	−13.9	+ 0.4	0	− 6
205	13.1	−13.8	− 3.0	+ 2	− 8
206	14.6	−13.8	− 6.3	− 6	+ 9
207	13.1	−13.6	+33.4	− 2	+ 7
208	13.0	−13.6	+15.1	− 4	− 8
209	14.6	−13.5	−12.8	− 8	+ 7
210	14.8	−13.5	+ 1.5	−14	+ 4
211	15.0	−13.4	+11.6	0	− 1
212	14.1	−13.3	− 9.4	0	+ 2
213	13.3	−13.2	−21.1	− 3	− 6
214	14.8	−13.2	+13.7	+ 2	+ 28
215	14.6	−13.2	+13.8	+ 4	+ 24
216	15.0	−13.2	0	−18	− 3
217	14.2	−13.1	−32.7	− 2	− 18
218	14.1	−13.1	+19.6	− 8	− 1
219	13.5	−13.1	− 9.6	+ 1	0
220	13.0	−13.0	+32.6	− 2	− 14
221	14.8	−13.0	− 0.1	−22	− 3
222	15.0	−13.0	− 8.8	+ 3	0
223	13.4	−12.9	−20.2	+ 5	− 4
224*	14.1	−12.9	+12.2	− 4	− 2
225	13.6	−12.8	+ 3.4	− 8	0
226	13.4	−12.7	−11.3	+ 2	+ 2
227	12.8	−12.4	+ 1.2	−10	+ 4
228	12.0	−12.3	+15.2	+ 4	+ 3
229	14.9	−12.2	−19.5	− 4	− 10
230	15.1	−12.2	+15.3	+ 6	+ 6
231	14.4	−12.2	−12.1	0	− 16
232	13.6	−12.0	−24.6	− 8	− 11
233	13.7	−11.8	+ 4.3	0	+ 2
234	13.3	−11.8	− 0.1	−10	− 14
235	14.0	−11.8	+25.3	− 8	+ 6
236	13.4	−11.7	+27.8	+ 3	− 3
237	14.8	−11.6	+11.6	+ 6	+ 4
238	15.0	−11.6	−15.4	+ 7	− 18
239	15.0	−11.6	−15.5	− 7	+ 5
240	14.1	−11.6	+31.3	− 2	− 4
241	14.6	−11.4	+ 5.5	+12	+ 22
242	13.9	−11.4	−21.3	−18	− 6
243	13.1	−11.4	−21.5	+ 9	− 15
244	14.4	−11.2	−31.7	− 8	− 13
245*	13.5	−11.2	+ 6.2	− 4	− 7
246	14.6	−11.2	−12.2	− 6	− 9
247	13.5	−11.0	−30.2	−11	− 10
248	12.2	−11.0	−13.2	− 2	+ 4
249	13.1	−11.0	−15.6	+ 4	+ 1
250	13.1	−10.9	+32.4	+11	− 12
251	15.0	−10.7	−20.4	− 5	+ 6
252	14.7	−10.7	+12.5	− 3	− 8
253	10.0	−10.6	+31.2	+ 2	+ 6
254	14.6	−10.5	+10.5	+ 6	− 4
255	14.6	−10.2	+ 3.2	+ 1	− 2
256	12.2	−10.2	+15.8	+ 1	+ 2
257	13.1	−10.2	+13.7	0	− 4
258	13.5	−10.0	−18.6	+ 4	+ 10
259	13.4	−10.0	33.2	+ 6	− 5
260	13.6	− 9.9	−10.7	− 6	− 4
261*	13.8	− 9.9	+ 0.8	+11	+ 3
262	13.2	− 9.8	−17.8	+ 6	+ 1
263	14.2	− 9.8	+29.8	−16	− 24
264	14.3	− 9.8	+27.6	− 4	+ 2
265	12.2	− 9.6	+34.1	+ 7	0
266	14.8	− 9.6	+ 0.6	− 2	0
267	13.5	− 9.5	−26.7	+12	− 6
268	14.6	− 9.5	+16.4	+12	0
269	13.0	− 9.2	−18.6	+14	− 5
270	14.8	− 9.2	− 0.7	− 2	0
271	14.6	− 9.1	+33.0	+10	− 15
272	14.6	− 9.1	+ 2.2	+ 3	− 7
273	14.5	− 9.0	+26.4	−12	− 3
274	13.2	− 8.9	−20.6	−28	− 18
275*	13.7	− 8.9	−24.0	+ 2	+ 2
276	13.6	− 8.9	+25.3	−10	− 7
277	14.9	− 8.4	+33.4	+12	− 3
278	14.8	− 8.3	− 0.9	+ 4	+ 3
279	12.2	− 7.9	− 6.9	− 4	+ 7
280	14.0	− 7.8	+34.2	+ 2	− 8
281	14.6	− 7.8	− 8.3	+20	+ 6
282	14.7	− 7.7	+27.6	+17	− 2
283	13.3	− 7.6	− 1.1	0	+ 8

Continuation of the CATALOGUE

No. of the star	m_{pg}	X	Y	μ_x	μ_y
284	14.4	— 7.3	+18.4	+ 3	— 7
285*	13.5	— 7.2	—29.3	+ 2	+ 2
286	13.8	— 7.1	—25.8	— 6	— 4
287	12.2	— 7.0	—31.4	+10	— 7
288*	13.3	— 7.0	— 7.9	— 2	+ 1
289	13.0	— 6.9	+21.5	— 4	+ 8
290	12.8	— 6.8	+26.8	— 6	+ 6
291	14.0	— 6.8	+ 4.1	+13	— 12
292	13.5	— 6.5	—13.1	— 2	— 5
293	13.1	— 6.3	+24.3	+ 2	+ 4
294	14.6	— 6.2	—21.5	+ 6	+ 8
295	13.4	— 6.2	+27.4	+ 5	0
296	12.0	— 6.2	+23.1	+10	+ 9
297	13.1	— 6.2	—11.6	— 3	+ 3
298	14.6	— 6.0	+26.2	— 2	+ 13
299	10.5	— 6.0	—29.6	— 7	+ 3
300*	14.0	— 6.0	+20.2	— 3	+ 5
301	12.7	— 5.9	—15.7	+ 8	— 14
302	14.2	— 5.8	— 8.7	— 4	— 4
303	14.9	— 5.8	—13.8	+ 8	— 5
304	14.9	— 5.8	—17.7	+ 3	— 5
305*	13.9	— 5.7	+28.6	+ 1	+ 4
306	13.8	— 5.6	—25.4	—10	+ 1
307	12.8	— 5.4	+ 3.5	—19	+ 9
308	13.4	— 5.2	+15.6	+ 4	+ 12
309	14.4	— 5.2	—16.9	— 4	+ 3
310*	13.8	— 5.1	—16.6	— 7	— 6
311	14.0	— 5.0	—15.4	— 8	— 8
312	15.0	— 4.8	+ 3.4	— 8	+ 2
313	13.8	— 4.8	+22.6	— 6	— 2
314	13.5	— 4.6	—20.6	+ 4	+ 4
315	13.0	— 4.6	—23.5	— 4	— 8
316	13.3	— 4.6	+ 5.1	— 5	— 4
317	14.0	— 4.4	+26.8	— 2	+ 4
318	14.9	— 4.3	—14.8	— 7	+ 5
319	13.5	— 4.3	+26.9	0	— 2
320	11.9	— 4.2	+30.1	+ 8	— 4
321	14.4	— 4.2	+19.3	+10	— 16
322	13.4	— 4.1	—34.3	+ 7	— 10
323	12.2	— 4.1	—31.8	+ 3	+ 2
324	13.6	— 4.1	+29.5	— 1	+ 5
325*	14.0	— 4.1	+11.2	— 4	+ 4
326	14.0	— 4.0	— 8.8	—24	— 15
327	9.0	— 4.0	—16.2	— 3	+ 4
328	13.4	— 3.8	+ 5.2	— 2	— 1
329	13.3	— 3.7	+ 8.0	+12	0
330	14.5	— 3.6	+ 3.1	—17	— 3
331	14.6	— 3.5	+26.8	+14	+ 2
332	14.8	— 3.2	—28.7	+ 8	+ 2
333	14.6	— 3.1	+11.3	—18	— 8
334	13.4	— 3.0	—34.4	+ 5	+ 4
335	14.9	— 3.0	— 8.6	— 4	0
336	13.9	— 2.9	—13.4	—14	+ 2
337*	13.8	— 2.9	+ 3.2	+ 1	— 6
338	13.1	— 2.8	—15.4	— 2	0
339	12.0	— 2.8	—28.1	+ 4	+ 6
340	14.6	— 2.7	— 7.7	+ 6	— 8
341	14.7	— 2.7	— 6.5	— 7	— 6
342	14.5	— 2.6	—12.9	+ 4	— 4
343	12.2	— 2.6	+ 6.2	+ 2	+ 12
344	12.5	— 2.4	—16.4	+ 6	— 2
345	13.8	— 2.4	— 3.4	0	— 6
346	15.0	— 2.2	+28.2	+ 8	— 1
347	14.7	— 2.2	+19.8	— 8	+ 8
348	15.1	— 2.1	— 7.4	— 4	— 6
349	15.0	— 1.9	— 6.9	— 8	+ 6
350	13.0	— 1.8	—34.0	+ 4	— 1
351	10.8	— 1.8	— 9.4	+ 1	+ 5
352	14.8	— 1.7	—25.4	+13	— 3
353	14.6	— 1.7	+28.4	— 4	0
354	12.0	— 1.7	+ 7.6	+ 4	+ 4
355	14.0	— 1.7	— 9.6	+ 7	+ 5
356	12.8	— 1.6	—33.2	+ 2	— 15
357	13.9	— 1.5	+24.8	+ 5	+ 5
358	14.0	— 1.5	—11.9	0	— 8
359	14.7	— 1.4	— 7.1	+ 6	+ 3
360	14.9	— 1.4	— 5.5	— 2	+ 22
361	13.8	— 1.2	—32.0	—10	0
362	13.9	— 1.2	—12.6	—12	+ 4
363	14.9	— 1.1	— 6.8	—11	+ 4
364	13.0	— 1.0	— 6.5	— 6	+ 12
365	14.4	— 1.0	— 3.0	— 8	— 5
366	13.6	— 1.0	—13.8	— 6	+ 2
367	14.6	— 0.9	—33.8	+18	— 23
368	14.8	— 0.8	+14.2	— 2	0
369	12.8	— 0.8	+ 9.6	— 6	+ 12
370	14.2	— 0.8	— 3.0	+ 8	+ 8
371	14.6	— 0.8	—11.7	—11	— 5
372	13.9	— 0.7	+26.2	+14	0
373	14.0	— 0.4	+26.3	0	— 12
374	13.8	— 0.4	— 9.5	— 1	+ 6
375	15.0	— 0.3	— 9.9	—18	— 8
376	15.0	— 0.3	+10.5	+11	+ 8
377	13.4	— 0.1	— 8.3	— 8	0
378	11.2	0	0	—15	+ 16
379	14.6	0	— 1.7	—14	+ 10
380	14.5	0	—23.1	— 4	+ 11
381	10.2	+ 0.1	+10.8	— 8	+ 10
382	14.0	+ 0.3	— 2.6	— 2	+ 3
383	14.0	+ 0.3	—14.8	— 2	+ 8
384	13.4	+ 0.5	+ 7.2	+ 3	— 10
385	10.9	+ 0.7	+ 6.4	0	— 4
386*	14.0	+ 0.7	— 5.5	— 6	— 3
387	12.2	+ 0.8	+10.8	+21	+ 8

Continuation of the CATALOGUE

No. of the star	m_{pg}	X	Y	μ_x	μ_y
388	14.7	+ 1.0	— 8.0	— 6	— 4
389	14.6	+ 1.1	+22.6	+ 4	— 6
390	15.0	+ 1.1	— 4.7	+ 2	— 8
391	14.0	+ 1.1	—10.8	0	— 3
392*	14.0	+ 1.2	+26.1	+ 2	0
393	11.6	+ 1.3	+27.2	+ 8	+ 6
394	14.8	+ 1.3	— 9.9	0	+ 1
395	14.6	+ 1.6	0	+ 6	+ 2
396	14.2	+ 1.6	—10.3	—18	— 2
397	11.4	+ 1.7	—21.2	0	+ 11
398	13.2	+ 1.8	—29.6	— 5	+ 2
399	14.9	+ 1.9	+14.1	0	— 2
400	14.6	+ 2.0	+27.4	+11	— 4
401	14.0	+ 2.0	+ 3.0	+ 1	— 14
402	11.4	+ 2.0	+ 1.2	+ 8	+ 3
403	13 5	+ 2.4	— 8.9	+ 2	+ 1
404	14.0	+ 2.5	0	— 8	+ 10
405	13.6	+ 2.5	—28.0	+14	+ 3
406	13.3	+ 2.7	+20.1	—12	0
407	13.4	+ 2.7	—19.4	+10	+ 2
408	13.6	+ 2.7	—31.8	+ 7	— 2
409	12.6	+ 2.7	—34.8	+ 1	— 2
410	13.4	+ 2.8	—34.8	—13	— 14
411	13.0	+ 3.0	— 6.2	+ 1	— 6
412	12.3	+ 3.2	—16.1	+ 4	— 1
413	14.4	+ 3.3	— 7.9	— 9	— 3
414	14.5	+ 3.4	—26.4	—12	— 3
415	13.6	+ 3.4	—29.9	+16	— 1
416	13.3	+ 3.4	—28.0	+ 2	+ 11
417	13.1	+ 3.5	— 5.7	+ 8	0
418	13.5	+ 3.6	+34.2	+ 3	— 6
419	13.3	+ 3.8	+ 7.7	0	— 7
420	12.7	+ 3.8	—15.7	—10	— 8
421	13.5	+ 3.9	+25.3	— 5	— 14
422	15.0	+ 4.0	+14.8	— 8	— 1
423	14.8	+ 4.0	—14.6	0	— 5
424	13.0	+ 4.1	+11.4	— 2	+ 2
425	12.2	+ 4.1	+10.8	—10	+ 1
426	12.3	+ 4.1	+ 0.4	+ 8	+ 2
427*	13.7	+ 4.2	—20.4	+ 7	+ 7
428*	13.8	+ 4.2	+ 5.8	+10	+ 4
429	14.6	+ 4.3	+11.4	0	— 20
430	13.4	+ 4.6	—23.6	+ 6	— 4
431	14.8	+ 4.8	— 9.8	— 5	— 3
432	13.5	+ 4.9	+32.0	— 2	— 12
433*	14.3	+ 5.0	+16.5	— 6	0
434	14.6	+ 5.0	—10 3	+ 5	+ 1
435	14.4	+ 5.0	+ 3.2	+ 1	— 10
436	14.7	+ 5.2	+22.5	—10	— 9
437	14.4	+ 5.2	+16.0	— 9	— 6
438	12.7	+ 5.2	+10 1	— 4	— 10
439	13.4	+ 5.2	— 9.5	— 1	— 5
440	14.2	+ 5.3	+19.9	0	+ 14
441	13.4	+ 5.4	—28.1	+ 9	+ 4
442	14.9	+ 5.4	—33.0	+ 4	— 2
443	13.5	+ 5.5	—25.9	—13	— 1
444	13.0	+ 5.7	+30.0	— 6	+ 14
445	14.0	+ 5.7	— 5.6	+10	— 2
446	14.6	+ 5.8	—30.7	+10	— 18
447	13.2	+ 5.9	+ 0.2	— 1	+ 3
448	14.0	+ 5.9	— 6.8	+ 6	+ 2
449	13.6	+ 5.9	—27.2	—10	— 6
450	14.4	+ 5.9	—28.6	— 9	+ 8
451	14.3	+ 6.0	+24.3	+ 6	+ 5
452	14.5	+ 6.0	—21.4	+ 4	— 8
453	14.6	+ 6.0	—24.0	+ 3	+ 2
454	13.5	+ 6.0	—32.8	+ 9	+ 5
455	10.7	+ 6.0	—14.8	—22	— 2
456	13.2	+ 6.1	— 3.8	—12	+ 7
457	13.2	+ 6.2	+ 7.9	—10	+ 10
458	13.9	+ 6.2	+ 3.6	0	— 4
459*	13.5	+ 6.2	—15.5	—12	— 6
460	11.6	+ 6.3	—28.6	0	— 6
461	13.9	+ 6.4	+ 2.7	—11	— 12
462	14.6	+ 6.5	+14.0	+ 2	— 18
463	13.2	+ 6.6	— 6.2	+ 5	— 8
464	12.7	+ 6.6	—27.4	— 2	— 2
465	14.6	+ 6.9	—20.6	— 6	0
466	11.9	+ 6.9	—28.0	+ 8	+ 6
467	13.1	+ 6.9	—25.8	+ 3	+ 4
468	13.6	+ 6.9	—15.7	—12	— 4
469	14.2	+ 6.9	—14.6	+ 4	+ 4
470	13.1	+ 7.0	—31.7	+ 9	— 3
471	14.4	+ 7.1	+10.1	0	+ 3
472	13.8	+ 7.1	—25.8	— 6	0
473	14.5	+ 7.1	—13.8	— 5	— 21
474	13.3	+ 7.2	— 5.8	— 2	+ 2
475	11.6	+ 7.2	—12.4	— 2	+ 4
476	11.6	+ 7.3	+19.8	+ 8	— 4
477	13.9	+ 7.3	—27.4	— 4	— 9
478	14.7	+ 7.3	—19.8	— 3	+ 3
479	14.4	+ 7.3	—22.8	+18	+ 19
480	14.3	+ 7.3	—21.0	+ 9	— 4
481	13.0	+ 7.4	—36.1	+ 6	— 18
482	13.6	+ 7.4	—20.4	+ 5	— 16
483*	13.6	+ 7.6	+25.3	+ 1	— 2
484	12.8	+ 7.6	+ 5.2	+ 6	+ 24
485	13.5	+ 7.6	—36.0	+ 4	0
486	12.8	+ 7.7	—17.0	— 8	— 8
487	13.8	+ 7.8	+26.2	+ 7	0
488	13.7	+ 8.0	—28.1	— 8	+ 7
489	13.6	+ 8.0	—26.5	— 4	+ 1
490	12.8	+ 8.0	— 8.9	0	— 12
491	14.2	+ 8.0	—14.4	—11	— 12
492	14 4	+ 8.0	—15.8	+11	— 12
493	14.0	+ 8.2	—26.3	0	— 2

Continuation of the CATALOGUE

No. of the star	m_{pg}	X	Y	μ_x	μ_y
491	12.6	+ 8.2	+ 2.4	+ 8	+ 9
495	13.1	+ 8.2	—12.8	— 7	— 12
496	13.5	+ 8.2	—20.8	+11	— 24
497	14.9	+ 8.3	+12.2	+ 4	+ 6
498	14.0	+ 8.4	+23.8	— 1	+ 7
499	12.0	+ 8.6	—24.8	0	+ 5
500*	13.5	+ 8.8	— 6.5	— 3	+ 14
501	14.7	+ 8.8	—17.1	— 5	+ 2
502	13.8	+ 8.8	—29.5	+12	+ 2
503	14.0	+ 8.9	+24.2	+ 2	0
504	14.6	+ 8.9	—14.8	— 5	— 8
505	14.7	+ 8.9	—18.8	—10	+ 5
506	14.0	+ 9.0	— 9.8	— 2	— 1
507	+14.0	+ 9.0	+16.8	+ 4	0
508	14.2	+ 9.0	—17.5	+ 6	— 14
509	13.1	+ 9.0	—16.7	+ 6	+ 8
510	15.0	+ 9.1	+ 0.4	+10	— 5
511	14.0	+ 9.1	— 1.8	—14	0
512	13.0	+ 9.2	+25.3	+ 4	0
513	15.0	+ 9.3	+ 0.8	+ 6	+ 15
514	14.7	+ 9.3	+ 6.0	+ 2	— 4
515	13.3	+ 9.5	—35.2	+ 2	— 3
516	13.6	+ 9.6	+25.2	— 4	— 14
517	14.4	+ 9.8	—27.0	—12	— 21
518*	13.9	+ 9.8	+12.2	— 7	0
519	14.1	+ 9.9	— 7.4	—14	— 8
520	13.7	+10.0	—12.4	— 8	+ 8
521	11.2	+10.0	—16.4	+ 6	+ 2
522*	13.6	+10.0	—27.8	— 2	— 18
523	14.4	+10.0	+17.8	+ 2	— 12
524	13.5	+10.1	+24.2	+ 6	— 6
525	14.7	+10.2	—27.8	+12	0
526	13.6	+10.3	+27.1	+ 6	+ 6
527	13.2	+10.3	+ 7.4	— 1	+ 11
528	13.6	+10.4	—16.9	+ 2	+ 6
529	14.4	+10.5	—31.8	—10	— 8
530	13.2	+10.7	+ 7.8	—16	+ 8
531	13.8	+10.8	+30.4	+ 6	+ 1
532	14.3	+11.0	—12.9	+23	0
533	13.2	+11.0	—31.8	+ 6	— 10
534	13.0	+11.2	+29.8	— 2	— 2
535	12.4	+11.4	+ 8.2	— 4	+ 6
536	14.0	+11.4	—31.6	—12	— 31
537	13.9	+11.7	— 7.0	— 6	+ 6
538	14.0	+11.8	—27.8	+ 7	— 6
539	14.6	+11.8	—15.8	+ 8	— 22
540	13.5	+11.9	+ 4.7	+ 4	+ 10
541	13.4	+12.0	+22.6	+ 5	— 4
542	14.5	+12.0	+15.2	—11	— 2
543*	14.0	+12.2	+ 3.4	+ 1	+ 4
544	14.2	+12.2	— 7.8	+ 6	0
545	13.1	+12.3	—18.2	— 5	— 10
546	13,2	+12.4	—10.2	+13	+ 3
547	14.4	+12.4	—28.3	+ 1	+ 2
548	13.1	+12.7	—18.4	+ 8	0
549	14.3	+12.8	—14.8	— 5	— 7
550	14.2	+12.8	—25.1	+ 4	— 13
551	13.6	+12.9	—22.8	+ 8	+ 8
552	14.3	+13.0	+18.0	— 2	— 10
553	12.7	+13.0	+10.4	+ 2	+ 5
554	13.9	+13.0	— 9.6	0	0
555	13.6	+13.5	—19.6	— 3	+ 6
556	13.9	+13.5	—19.0	—12	— 5
557	13.1	+13.7	—29.8	+ 6	— 26
558	13.4	+14.0	+26.8	+15	+ 18
559	14.0	+14.0	+12.2	+ 8	+ 12
560	13.0	+14.0	—22.7	— 8	— 2
561*	13.6	+14.0	—21.2	+ 2	— 3
562	14.7	+14.0	—31.9	—14	— 4
563	13.5	+14.2	— 3.7	— 2	+ 2
564	13.9	+14.2	—17.8	+14	— 10
565*	13.6	+14.2	—10.8	— 2	— 4
566	14.0	+14.3	—32.0	0	0
567	15.0	+14.4	+ 0.2	+ 8	+ 2
568	13.8	+14.4	—25.5	+ 3	+ 2
569	14.0	+14.6	+17.6	— 6	+ 2
570	13.5	+14.6	+ 1.8	0	— 4
571	14.0	+14.6	—10.1	— 4	— 6
572	13.2	+14.6	—20.2	— 1	— 8
573	14.5	+14.6	—30.7	+ 5	— 6
574	11.2	+14.8	+ 6.6	—10	+ 14
575	10.9	+14.9	—21.8	—11	— 2
576	14.2	+15.0	—22.9	+ 2	— 12
577	12.4	+15.1	+28.0	— 2	+ 4
578	14.0	+15.2	+29.0	+ 1	— 2
579	13.1	+15.2	—14.4	+17	+ 8
580	14.5	+15.2	— 7.0	+ 6	— 4
581	14.9	+15.3	+14.2	— 8	— 7
582	15.0	+15.5	+30.8	+20	+ 11
583*	13.4	+15.5	+20.2	+ 2	0
584	14.7	+15.5	+14.2	+11	+ 4
585	14.1	+15.5	—24.8	+18	— 4
586	14.0	+15.7	+17.4	+ 1	+ 10
587	14.2	+15.8	+26.6	0	0
588	13.0	+15.8	—12.1	0	— 14
589*	13.9	+15.9	— 4.0	+ 4	+ 2
590	14.2	+15.9	—25.2	+11	— 14
591	13.0	+16.0	—23.5	0	+ 10
592	13.3	+16.0	+18.2	— 9	+ 6
593	11.2	+16.0	—30.3	+16	+ 12
594	13.0	+16.2	— 7.4	—16	+ 8
595	14.6	+16.3	—15.7	0	— 4
596	13.1	+16.4	—14.6	— 6	— 6
597	13.4	+16.4	— 7.8	— 2	— 8

Continuation of the CATALOGUE

No. of the star	m_{pg}	X	Y	μ_x	μ_x
598	13.6	+16.4	—10.8	— 2	+ 3
599	14.8	+16.4	—23.5	— 6	+ 4
600	14.6	+16.5	—29.8	+ 2	— 10
601	12.7	+16.6	+25.6	+ 5	+ 7
602	14.9	+16.6	+11.1	—10	— 12
603	14.2	+16.7	+ 4.7	+10	— 2
604	14.7	+16.7	—19.8	—21	— 3
605	12.8	+16.8	+26.2	+18	— 2
606	14.2	+16.8	+ 6.2	+10	— 7
607	14.5	+16.9	—11.8	+ 4	— 2
608	14.6	+17.0	— 0.8	0	+ 2
609	14.8	+17.0	—23.2	+ 4	+ 6
610	13.5	+17.0	—22.8	+ 8	0
611	14.1	+17.1	—25.8	+ 7	+ 4
612	14.0	+17.1	—27.2	+ 4	+ 10
613	12.0	+17.1	—24.5	— 4	+ 8
614	13.1	+17.1	—17.8	—15	+ 6
615	13.9	+17.2	—24.4	+11	+ 6
616	13.3	+17.3	—31.1	+ 6	+ 7
617	13.1	+17.3	—30.2	0	+ 4
618	14.0	+17.4	—25.5	— 4	— 11
619	14.6	+17.5	— 1.8	— 8	— 12
620	14.2	+17.7	—10.9	— 5	— 14
621	13.4	+17.8	— 8.8	+ 8	+ 2
622	12.6	+17.8	+ 2.2	— 2	— 4
623	14.6	+17.9	+19.4	+18	— 10
624	13.0	+17.9	+ 4.3	— 4	— 8
625	14.0	+17.9	+ 2.2	— 3	— 12
626	13.3	+18.0	+23.2	—10	— 16
627	13.1	+18.0	+13.8	+ 9	— 11
628	14.0	+18.0	+ 4.0	—14	— 1
629	14.0	+18.0	+ 7.0	—12	+ 8
630	13.5	+18.0	— 4.8	— 2	— 8
631	14.0	+18.0	—26.7	+ 4	— 2
632	13.2	+18.1	—11.4	— 8	— 7
633	13.9	+18.2	+10.2	+10	— 14
634	14.2	+18.2	+ 3.8	+ 3	— 5
635	13.2	+18.2	— 5.8	+10	— 2
636	14.6	+18.3	+25.6	0	— 8
637	14.0	+18.5	+ 5.2	— 2	— 10
638	13.2	+18.6	—10.8	+16	— 14
639	13.4	+18.6	—15.5	—11	— 17
640	12.3	+18.7	+ 6.8	— 6	+ 5
641	13.2	+18.8	+11.7	+ 2	— 8
642	12.7	+18.8	— 7.1	+ 6	— 10
643	12.8	+19.0	+21.0	+ 4	+ 12
644	11.9	+19.2	+19.4	— 8	+ 8
645	13.1	+19.2	—14.7	— 7	— 7
646	14.6	+19.2	—25.2	+12	— 4
647	14.6	+19.3	—11.9	—19	— 5
648	13.1	+19.3	+27.8	+ 7	+ 2
649*	13.8	+19.7	—16.8	+ 5	+ 6
650	13.0	+19.8	+11.5	+10	— 6
651	13.2	+19.8	—14.8	—14	+ 3
652	13.7	+19.8	—11.4	— 4	— 6
653	14.6	+19.8	—26.7	0	+ 2
654	14.9	+19.9	— 4.6	+10	+ 14
655	13.0	+19.9	—17.8	— 2	0
656	12.6	+20.0	+18.1	+ 6	— 6
657	14.2	+20.0	— 5.2	+ 4	— 8
658	14.9	+20.0	—27.7	+10	— 4
659	13.9	+20.1	— 9.5	+ 3	+ 4
660	12.0	+20.2	—19.6	—12	0
661	12.8	+20.2	—25.6	+ 4	— 24
662	14.5	+20.4	+16.5	+11	— 2
663	13.6	+20.4	—12.7	— 3	— 3
664	13.7	+20.5	+11.8	+15	+ 12
665*	13.4	+20.5	+ 1.2	+ 3	— 1
666	13.7	+20.5	— 7.8	— 3	0
667	14.8	+20.6	+ 0.4	0	— 4
668	13.7	+20.6	— 3.8	— 5	— 12
669	13.5	+20.6	— 2.7	— 8	— 6
670	14.9	+20.7	— 2.6	— 3	— 17
671	13.3	+20.8	+23.5	+18	+ 2
672	13.1	+20.8	+19.8	+ 8	— 3
673	13.9	+21.1	+ 8.4	+14	— 4
674	13.1	+21.2	+17.6	0	— 4
675	14.7	+21.3	+ 3.2	— 2	— 5
676	13.2	+21.3	—15.0	— 3	— 1
677	135	+21.4	—17.7	0	— 2
678	12.2	+21.6	+24.7	+ 2	+ 4
679	14.3	+21.8	— 9.8	+ 1	— 6
680	13.9	+21.8	—28.9	+ 2	+ 6
681	13.2	+21.9	—12.1	+18	+ 6
682	12.6	+22.0	+26.2	+ 3	— 24
683	14.7	+22.0	+ 3.6	— 2	+ 8
684	15.0	+22.0	+ 0.4	+ 5	— 2
685	14.5	+22.0	— 7.8	+ 2	— 3
686	13.3	+22.0	—26.8	0	— 2
687	14.8	+22.0	— 23.7	+ 2	— 10
688	12.4	+22.1	+18.5	— 8	— 4
689	14.5	+22.1	— 5.2	+ 6	+ 10
690	14.6	+22.2	— 8.0	+12	— 4
691	14.0	+22.2	+ 1.5	+ 1	— 7
692	13.4	+22.3	+26.6	+10	— 4
693	14.9	+22.3	+18.9	— 5	+ 1
694	14.6	+22.3	+ 5.0	— 8	+ 8
695	12.0	+22.3	—21.1	— 2	+ 2
696	13.4	+22.3	— 7.3	0	— 6
697	13.8	+22.5	+ 7.2	— 6	+ 9
698	14.6	+22.7	+19.4	— 2	+ 3
699	13.8	+22.7	—12.0	+ 2	+ 4
700	14.2	+22.7	—23.5	+ 8	0
701	15.0	+22.8	+10.8	— 2	— 6
702	13.3	+22.8	—23.9	+ 3	— 2
703	14.6	+22.9	— 8.7	— 2	+ 2

Continuation of the CATALOGUE

No. of the star	m_{pg}	X	Y	μ_x	μ_y	No. of the star	m_{pg}	X	Y	μ_x	μ_y
		′	′					′	′		
704	14.0	+23.0	+ 3.8	+16	— 2	751	14.6	+27.7	+ 6.4	+ 6	— 4
705*	13.8	+23.2	+13.8	— 4	— 2	752	13.8	+27.8	+ 7.9	— 2	— 10
						753	13.5	+28.3	— 4.8	+ 6	— 2
706	13.3	+23.3	—27.4	—14	— 8	754	14.3	+28.3	— 5.4	— 6	— 4
707	14.1	+23.4	— 1.0	— 2	— 4	755	14.5	+28.4	—17.8	— 8	+ 5
708	14.6	+23.5	—11.4	— 8	— 2						
709	14.4	+23.8	+15.9	— 4	+ 1	756*	13.6	+28.5	— 7.6	+ 5	+ 4
710	11.4	+23.9	—27.4	— 6	+ 6	757	14.6	+28.8	— 9.3	+ 4	+ 1
						758	13.6	+28.9	+14.1	+ 2	0
711	11.4	+24.0	+16.1	+ 8	— 4	759	14.9	+29.0	+ 4.9	+12	— 2
712	13.8	+24.0	+ 0.7	— 6	0	760	13.6	+29.2	—20.5	— 8	— 2
713	14.6	+24.1	—22.6	+ 3	— 9						
714	14.8	+24.2	—25.7	+19	+ 10	761	12.2	+29.3	— 6.2	— 4	+ 5
715	11.3	+24.3	+14.2	+ 6	+ 1	762	13.2	+29.5	—10.8	— 5	— 6
						763	14.3	+29.7	—17.8	+20	— 4
716	15.0	+24.6	— 7.0	+25	+ 3	764	13.1	+29.9	— 5.0	+ 7	— 4
717	14.2	+24.6	— 9.8	+ 6	0	765	14.6	+30.0	—16.9	— 4	— 1
718	15.0	+24.7	— 7.3	+24	0						
719	14.8	+24.7	— 4.7	+14	— 2	766	11.4	+30.1	+16.5	+ 3	+ 3
720	14.0	+24.8	— 8.0	+ 6	0	767	14.8	+30.1	+ 6.3	+ 5	— 10
						768	13.4	+30.2	+ 5.2	0	+ 16
721	13.6	+24 9	—21.1	— 4	— 24	769	11.4	+30.2	— 8.8	+ 2	+ 9
722	15.0	+25.1	+ 5.9	+ 7	+ 3	770	14.0	+30.5	+ 7.8	0	0
723	14.6	+25.2	—10.4	— 8	+ 9	771*	13.8	+30.7	+ 7.7	+16	— 6
724	14.9	+25.3	—10.8	+ 2	— 9	772	14.6	+30.7	— 7.0	— 6	— 4
725	14.7	+25.3	—10.2	+ 1	+ 14	773	12.7	+30.8	—12.0	0	0
						774	11.7	+31.0	—14.7	+ 6	+ 3
726	14.1	+25.3	—17.0	+12	+ 6	775	12.7	+31.3	— 4.2	+ 1	0
727	15.0	+25.4	—10.8	+11	— 2	776	13.2	+31.4	— 8.8	+ 6	— 4
728	15.0	+25.7	— 4.7	— 1	+ 6	777	13.3	+31.7	+ 7.5	— 6	— 14
729	13.1	+25.8	—17.8	—22	— 30	778	14.4	+31.8	+ 2.6	— 8	— 2
730	13.1	+25.9	— 0.6	+ 2	— 10	779	13.9	+31.8	—15.1	+ 3	+ 2
						780	14.5	+32.0	— 3.5	—13	+ 19
731	14.6	+26.0	+ 2.2	+ 5	— 2	781	14.0	+32.1	—13.2	+12	— 3
732	14.7	+26.0	+ 1.9	+ 8	+ 1	782	12.8	+32.2	—10.9	+ 3	+ 2
733	14.7	+26.0	—13.8	— 6	+ 9	783	13.9	+32.3	+ 6.8	+12	+ 13
734	14.3	+26.1	+ 4.0	— 4	+ 6	784	14.3	+32.3	— 0.7	+13	+ 8
735	15.0	+26.4	— 4.9	+ 7	+ 9	785	14.6	+32.7	+ 7.9	— 3	+ 2
736	14.0	+26.4	—11.7	+ 6	+ 4	786	13.1	+32.7	—10.1	— 3	— 10
737	13.4	+26.6	+15.4	+ 6	0	787	14.8	+33.0	— 3.6	— 6	— 2
738	14.9	+26.6	+ 1.9	0	+ 2	788	13.3	+33.0	— 7.0	0	+ 2
739	13.3	+26.8	+15.6	— 4	0	789	13.3	+33.2	+ 1.3	+10	+ 8
740	14.0	+26.8	+10.1	+ 21	— 14	790	11.1	+33.3	—10.2	+26	— 2
741	14.7	+26 8	—21.2	— 1	— 7	791	12.3	+34.0	— 9.5	—12	+ 6
742	14.3	+26.9	+21.1	— 7	0	792	14.0	+34.8	+ 1.4	+ 2	+ 2
743	13.5	+26.9	+14.3	+ 2	— 2	793	14.4	+34.8	+ 0.8	+ 3	+ 2
744	14.6	+26.9	+ 5.6	— 2	+ 7	794	14.3	+34.9	+ 2.2	+12	0
745	13.8	+27.0	+ 1.9	0	— 4	795	14.5	+34.9	— 8.6	— 4	+ 14
746	12.5	+27.1	— 3.2	+ 4	+ 9	796	14.1	+34.9	— 3.7	+ 6	+ 4
747	14.2	+27.3	+ 5.4	+ 9	— 3	797	12.8	+35.0	— 4.5	+ 6	+ 4
748	14.9	+27.4	+ 9.2	+13	+ 6	798	13.9	+40.4	— 6.4	+29	0
749	13.1	+27.6	+ 4.3	+ 4	— 14	799	14.6	+40.7	— 5.8	+ 8	0
750	14.6	+27.6	+19.3	+24	— 10	800	12.3	+42.0	+ 3.8	— 6	+ 20

Stars with large proper motions

1	13.9	—32.8	+ 5.4	—16	— 46	6	14.5	0	+ 6.2	0	— 39
2	12.7	—23.4	+17.4	+19	— 62	7	8.8	+14.1	—15.7	+14	+ 54
3	12.2	—15.7	+29.5	+90	— 42	8	14.2	+24.3	—25.4	+31	— 16
4	14.6	—10.5	+ 2.6	+12	— 36	9	13.5	+24.8	—18.8	—19	— 40
5	14.5	— 7.4	+26.0	— 6	—118						

PHOTOELECTRIC METHOD OF RECORDING STAR TRANSITS AND ITS APPLICATION AT THE ASTRONOMICAL INSTITUTE OF THE ACADEMY OF SCIENCES OF THE UZBEK SSR

T. Nuraliyev

ABSTRACT. A photoelectric transit instrument employing a constant-current photoelectric adapter was developed by the author at the Astronomical Institute of the Uzbek SSR in Tashkent. A quartz clock was used to provide time signals. The transit instrument was used to record star transits by means of the photoelectric method. The photoelectric unit employs two photomultiplier tubes arranged to operate in phase opposition. The photoelectric amplifier used includes a constant-current circuit.

A crucial factor in the photoelectric set-up is the delay unit. The amount of the delay in the system is determined mainly by the value of the time constant of the electrometer tube input.

The photoelectric transit instrument was used at Pulkovo to determine 55-time corrections in 1965. The average difference between the photoelectric transit data and etalon time was found to be $+0^{s}.022$. The author suggests that this difference should be considered as a correction to the longitude of the Pulkovo Observatory.

The author also found the temperature dependence of the instrument's azimuth. An increase in temperature produces a decrease in the azimuth. In addition the correction to the accepted longitude of the Astronomical Institute in Tashkent was determined to be $+0^{s}.021$.

Finally, the longitude difference between Pulkovo and Tashkent was determined and found to be $2^{h}35^{m}51^{s}.903 \pm 0^{s}.004$, which results in a longitude for Tashkent which agrees to within $0^{s}.001$ with the earlier value obtained by Shcheglov, thus indicating the absence of systematic errors in observations made with the photoelectric transit instrument as well as the stability of the longitude of the Astronomical Institute.

The photoelectric method is widely used in laboratories at the present time for recording star transits with the complete exclusion of the observer's personal error and a lessening of his effect on the instrument [1,2]. /50

In order to study the photoelectric method, a transit instrument, APM-10, No. 560004, constructed at the Leningrad State Optico-Mechanical Factory was used in the Time Division of the Astronomical Institute of the Uzbek SSR Academy of Sciences. The instrument was acquired by the Tashkent Astronomical Observatory in 1957 for carrying out investigations in the program of the International Geophysical Year and the year of the International Geophysical Cooperation. Observations were carried out on this instrument until the second half of 1963 by the visual method with a contact micrometer, and since November 1964, by the photoelectric method with a photoelectric adapter in the constant-current mode. The conditional designation of this instrument in the newsletter "Etalon Time" until its adaptation to photoelectric work was "Transit Instrument-3"; now it is designated "Transit Instrument 1-F".

A transit instrument of this type is suitably described in the paper [3]. The basic data of the instrument are: diameter of the objective, 100 mm; focal distance, 1000 mm; magnification, 100 times; and the value of a division of the level, $0^{s}.064$.

B. V. Yasevich [4] and E. V. Suvorova investigated the level by the method of A. S. Vasil'yev [5] on the Herbst testing machine; E. V. Suvorova [6] investigated the pivot by the contact method with the aid of an interferometer of the T. T. Uverskiy system, Type IKPV. The deviation of the actual figure of the working section of the pivot from the ideal did not exceed 0.3micron; correspondingly we obtained errors in the inclination of ±0.003, and in the azimuth, ±0.005.

The fundamental time during the period of observation was supplied by a quartz clock of the firm "Rhode and Schwartz". The signals entering the recording device were marked, i.e., the sixtieth second was not marked on the tape of the recorder. This simplified expansion of the tape at the time of reduction of the results of the observations, particularly in its marking. The record of the transit and the marks of the second pulses are made on the usual telegraph tape by the motion of the recorder's pen at the instants of the appearance and disappearance of a star in the gaps of the mirror grating and the pulses from the clock. The output of the photoelectric unit and the pulse from the clock are supplied to one and the same pen of the recorder.

Thus a record of the instants of the transit of stars was produced with the aid of a writing recorder, and the tape was set in motion by means of a motor. The motor is supplied from a 220-volt source. /51

The APM-10, No. 560004, transit instrument is mounted in a wooden pavilion which has the following internal dimensions: the length from east to west is 5.3 m; the width from north to south is 3.2 m; and the height of the walls is 2.8 m.

The height of the floor above the surface of the ground is 0.4 m. The pier on which the instrument is mounted has the dimensions 104 x 70 cm, and its height above the surface of the ground is 1.5 m. The pavilion was slid apart, forming a slit of width 2-2.5 m. The roof of the pavilion is made of the usual iron without additional thermal insulation. It is located on a small rise in the depressed part of the park of the Astronomical Institute of the Uzbek SSR Academy of Sciences, 20 m to the northeast from the Akkurgan irrigation ditch and surrounded by trees.

The longitude of the pier on which the APM-10 transit instrument is mounted, relative to that of the pier of the first transit instrument is equal to

$$\Delta\lambda = +0^{s}.337;$$

and since the longitude of the first transit instrument obtained by V. P. Shcheglov [7] is $\lambda_1 = 4^{h}37^{m}10^{s}.470$, then the longitude of the photoelectric transit instrument is

$$\lambda_{1\text{-}F} = 4^{h}37^{m}10^{s}.807.$$

Photoelectric adapter. The photoelectric adapter for converting the instrument to photoelectric recording of stellar transits was constructed by the author of this paper in the Time Division of the Main Astronomical Observatory of the USSR Academy of Sciences in Pulkovo and consists of the following units: a phototube, a photoelectric amplifier, the power supply unit, and the delay unit. The main circuit diagram of the photoelectric set-up used by us is given in Figure 1.

A list of the details of the diagram is presented below:

Detail	Resistance, capacitance, and tube type	Detail	Resistance, capacitance, and tube type
T_1	1E1P	R_{39}	120 kΩ
T_2,T_2 [sic]	12Zh1L	R_{40}	240 kΩ
T_4,T_5	2Zh27L	$R_{41,42,43}$	5.6 kΩ
T_6	2P1P	R_{44}	82 kΩ
R_1 to R_{17}	1.3 MΩ	$R_{45,46}$	36 kΩ
R_{18}	100 MΩ	R_{47}	100 kΩ
R_{19}	65 Ω	C_1	300 pf
R_{20}	33 Ω	$C_{2,3,4,5}$	100 pf
$R_{21,22,24}$	3.9 MΩ	$C_{6,7,8,9}$	30 μf x 300
$R_{23,26}$	1.0 MΩ	$C_{10,11}$	10 μf x 450
$R_{25,27,28}$	8.2 MΩ	$C_{12,13}$	0.25 μf
R_{29}	28 Ω	$T_{7,8}$	SG-2
R_{30}	14 Ω	T_9	SG-4
$R_{31,32,33}$	12 Ω	T_{10}	SG-3
R_{34}	1.8 kΩ	D_{1-12}	D7Zh
R_{35}	7.5 kΩ	P_1	2.2 MΩ
R_{36}	15 kΩ	$P_{2,3}$	10 kΩ
R_{37}	30 kΩ	$P_{4,5}$	47 kΩ
R_{38}	60 kΩ		

The photostage, assembled with the use of two photomultipliers of the SEU-20 type and a special electrometer tube of the 1E1P type is denoted by a dotted line (Figure 1). The total number of leads of a SEU-20 tube, including the cathode and the collector, is 10. To increase the insulation of the 10th dynode (the collector) its mount was drilled from a plastic tube base and covered with a thin layer of ceresin [5].

The 1E1P electrometer tube is fed from a 20-volt battery of constant current with an 8-volt tap, and the photomultipliers, from BAS-80 dry batteries with a total voltage of around 1000 volts. The voltage dividers for supplying the emitters of the photomultipliers consist of the resistors R_2-R_{18}.

/52

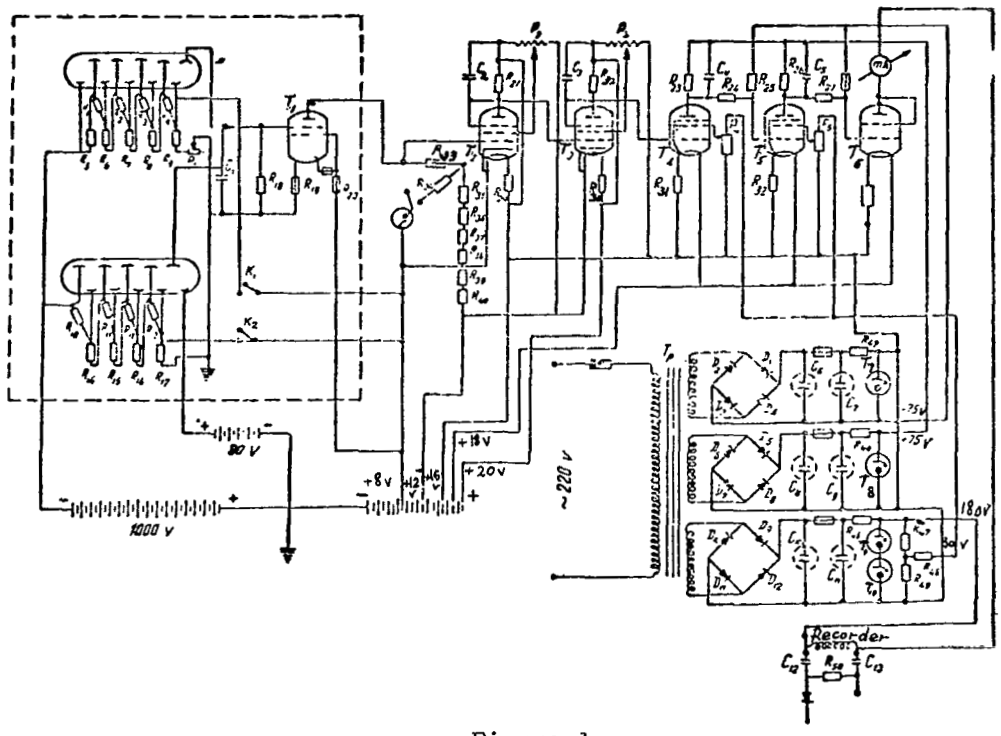

Figure 1.

With the aid of the rheostat R_{19} the voltage supply of one of the photomultipliers is regulated for equalizing their sensitivity. In Figure 1, K_1 and K_2 are the switches of the voltage supply for the separate control of the photomultipliers; R_1 is the load resistance in the photomultiplier circuit and simultaneously the output resistance of the amplifier; R_1 and C_1 form a high frequency filter with $R_1C_1 \approx 0.16$ s. /53

Inside the photocell two lenses are mounted which project the aperture of the objective on the cathode of the photomultiplier. They should be mounted so that the image of the objective on the cathode of the photomultipliers is practically unshifted in case of a shift of the image of the star with respect to the openings of the sighting array (Fabry set-up) [1,2]. In this case the nonuniformity of the SEU cathode has almost no effect on the amount of photocurrent.

The photomultipliers inside the cell can be adjusted for correct placement of the cathode relative to the sighting array. The mounting of the

photo-adapter [1] is accomplished with the aid of a special connecting flange attached to the horizontal axis of the transit instrument from the side of the tube pivot, whose position is rigidly fixed relative to the sighting array.

The photo-adapter is connected to the remainder of the circuit by a 6-strand cable in a shielded cover. In addition, the leads from the anode of T_1, which supplies the photomultipliers, each have independent shielding which prevents current leakage between these leads. To protect the photomultipliers from light and from the electrical shielding of the photo-adapter circuit, they are covered with an impermeable case made of sheet steel.

The mirror sighting array [1-3,8], which consists of a glass plate with an aluminum layer, is mounted at an angle of 45° at a distance of approximately 1.0 mm beyond the focal plane of the instrument's objective. This aluminum layer is removed in strips of about 0.1 mm so that between them mirror strips of the same width remain.

The light from the image of a star falling on the transparent strip strikes the photomultiplier mounted beyond the array [9]. The light from the image falling on the mirror strip is reflected to the side at an angle of 90 degrees and falls on the other photomultiplier mounted sideways from the array. The photomultipliers operate in opposed phases. The position of the photomultipliers is shown in Figure 2. It was stated above that the photo-adapter is mounted on the tube end of the horizontal axis. In connection with this, the tube is turned around the optical axis by 180° in order that the light rays fall on the photomultipliers.

The amplification of the photo-adapter is sufficiently large, but even so cannot give the current strength sufficient to operate the recorder, which is better than the usual chronograph as regards sensitivity, and has a low inertia. Therefore, amplification of the signals is necessary at the output of the photo-adapter [1,3,10,11]. At the present time two amplification circuits are being used: a constant current circuit and a variable current circuit [3,10].

N. N. Pavlov found the best solution of the problem with the constant current circuit. Our photoelectric adapter is also built on the basis of a constant current amplifier. To this end, a five-tube photoelectric amplifier /54

is placed behind the photo-adapter. The construction of a good amplifier with a large amplification coefficient is not a simple problem. Usually, the following requirements are placed on such amplifiers: low level of intrinsic noise, stability of operation, the absence of drift of the operation point and generation, suitable regulation of the operating condition, low and constant delay, and simplicity of operation.

By lowering the voltage of the filament and the anode one can significantly lower the noise of the tube in the low frequency region [1-3]. The Type 12Zh1L tube appeared to be suitable in this respect. One can lessen the drift of the operating point by switching on the amplifier 1 or 1.5 hours before observing. All the contacts in it should be soldered or well tightened. To prevent generation of the amplifier in all the anode circuits of the tubes, blocking capacitors are included. The effect of these capacitors on the response time of our photoelectric adapter is equal to $0^{s}.001$.

Suitable regulation of a constant current amplifier is accomplished by the fact that a significant change of the condition of the first tube cuts off the tubes of all succeeding stages, creating on their control grids large negative or positive voltages. In ordinary variable current amplifiers [3,12], the condition of the tubes of the first stages has practically no effect on the succeeding tubes, since the grid of each tube is protected from a constant component of the anode voltage by an isolation condenser.

In our apparatus, the first two tubes of the amplifier, along with the tubes of the photo-adapter, are supplied from storage batteries with a total voltage of 20 volts and a capacity of 128 amp-hours. The anode circuits of the last three tubes are supplied from a rectifier, and the filament circuits from a storage battery.

The first two tubes in the amplifier, T_2, T_3, are Type 12Zh1L. The next two, T_4, T_5, are Type 2Zh27L, and the last tube, T_6, is a Type 2P1P. The signals from the two photomultipliers in the circuit proposed by N. N. Pavlov [9] are fed to the third (control) grid of T_1. In this circuit, the phase opposition is supplied by the fact that the signal is taken from the last emitter in the FEU_1 photomultiplier position to the side from the sighting array, and from the collector, as usual, in the FEU_2 positioned behind the

sighting array.

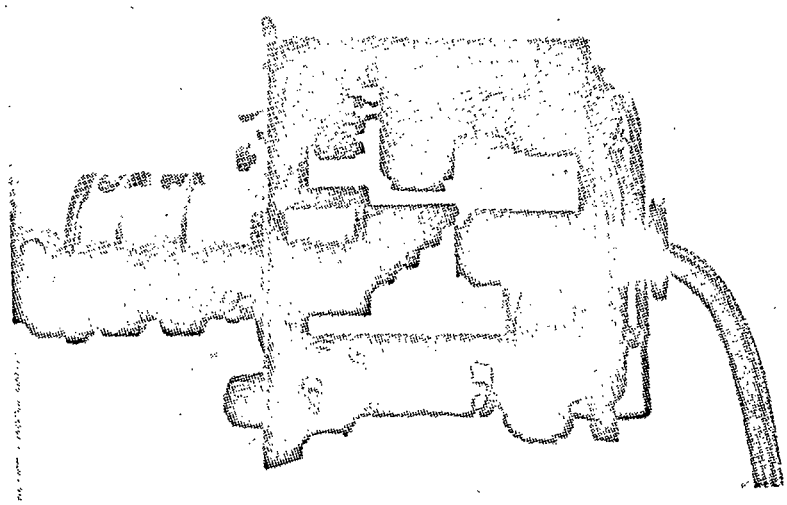

Figure 2. Photo-adapter with the top removed.

In the given amplifier, a change in the condition of the tubes is achieved /55 with the aid of the potentiometers P_2, P_3, P_4, and P_5 which permit changing the voltage on their screen grids. For the correct choice of amplifier conditions, the potentiometers of the first two stages have a base value, since with their

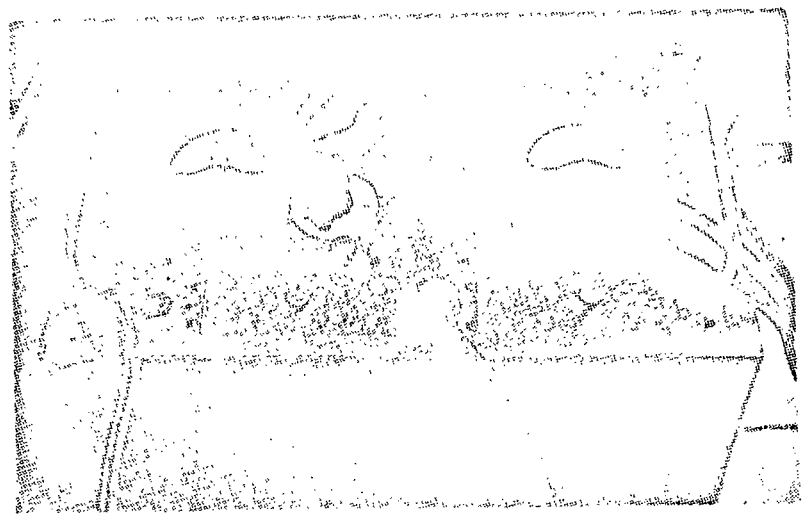

Figure 3. Front panel of the amplifier.

aid the condition not only of the first tubes but also of all succeeding ones is determined. The second potentiometer is equipped with a micrometer motion for very accurate selection of the operating point. The potentiometers of the first two stages have a separate scale. The potentiometers P_4 and P_5 are set only once (during the initial adjustment of the amplifier) and are fastened by screws. It is not desirable to change their positions, but it is possible as a last extreme.

A recorder and milliammeter located on the front panel of the amplifier (Figure 3) serve as indicators of the proper adjustment of the amplifier in our photoelectric set-up. In addition, a microammeter with the aid of which the balance of the photomultipliers is checked, the knobs of all potentiometers, and a milliammeter with which the signals at the output of the amplifier are controlled are mounted on the front panel of the amplifier.

The adequacy of the given circuit consists in the longevity of the amplifier, tubes, resistors, and capacitors, which exist under a very low voltage.

The power supply unit, i.e., a neon regulator, is mounted like the amplifier and the delay unit on a separate chassis. The power supply unit basically consists of the following elements: a power transformer, half-wave diodes, neon voltage regulators, and assorted capacitors, resistors, and choke coils.

In the case of photoelectric recording of star transits it is necessary to keep under control the amplifier's delay, which appears to be one of the main elements in the reduction of the observation [1-3]. The amount of delay is determined mainly by the size of the time constant of the electrometer tube /56 input. The delay of the photoelectric unit for square-wave signals is determined with the aid of a neon lamp mounted in a special adaptor which is attached to the objective of the main tube of the transit instrument during the determination of the delay. The main circuit diagram of the delay unit is shown in Figure 4.

Both photomultipliers in opposed phases respond to flashes of the neon tube, and their effects are mutually cancelled. Therefore, during determinations of the delay of the photomultiplier they are alternately switched off. A record of the star transits was made with the help of a single-pen dynamic recorder; the tube of the transit instrument served as the finder.

To check the operation of the photoelectric adapter a series of experimental observations was carried out at the Main Astronomical Observatory of the USSR Academy of Sciences at Pulkovo. The APM-10, No. 560004, transit instrument was mounted in the east meridian hall of the Observatory. The longitude of the pier relative to the center of the Observatory [1] was

$$\Delta\lambda = -0^{s}.088.$$

The results of the experimental observations showed the complete appropriateness of the photoelectric adapter for operation.

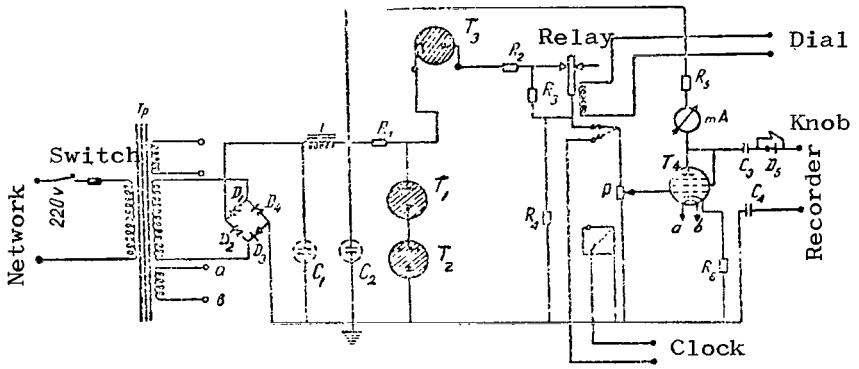

Figure 4.

Results of the observations and their analysis. From February to September 1965, 55 time corrections K_1 were determined by us. Each correction was calculated on the basis of observations of 10 time stars on the average, and the azimuth of the transit instrument was determined from two-three equatorial stars. The stars were not observed at lower culmination.

The observations were carried out in the following way: the filaments of the amplifier's tubes were turned on one and a half hours before the start of the observations and the anodes of the last three stages were turned on 15-20 minutes prior to the start. The inclination of the horizontal axis of the transit instrument was checked, and if necessary it was corrected. Prior to and after the observations the delay of the photoelectric set-up was determined. It was determined with the aid of special devices [1,3]. An adapter with a neon tube was attached for this purpose to the objective of the transit instrument. The clock switch was turned on, which gave second flashes of the neon

tube, from which the adjustment of the amplifier was carried out. /57

The correct adjustment was achieved when the difference in closings, indicated by the flash of the neon tube in front of the objective and the increase in output current of the photoelectric amplifier, was equal to the difference in the corresponding openings upon extinction of the neon tube and a decrease in the output current.

The observations of the stars were carried out near the meridian in the usual order, as for the visual transit instruments. With the help of a circle-finder the tube was approximately directed at the star with an accuracy of one minute; and when the image of the star appeared in the field of view of the tube-finder, the guiding was corrected by a micrometer screw. The star passed through 6-7 gaps and the same number of contacts was registered on the recorder's tape. The position of the instrument was changed in the middle of the observations of each star. The inclination of the instrument was determined from the readings of a suspended level.

Adjustment of the amplifier was carried out prior to the observing with the help of the potentiometers P_2 and P_3, i.e., the null point of the amplifier was found: a position of the potentiometer at which the indicator of the milliameter began to "jump around". This denoted that the grid of the last tube was open. At the start and at the end of the observations the air temperature was determined. A thermometer was located in the pavilion not far from the instrument. The following circumstances were taken into account in making up the program for the photoelectric observations:

a) for an investigation of the operation of the photoelectric adaptor at various zenith distances a rather wide zone in declination of the stars was selected, namely:

$$-9^\circ < \delta < +55^\circ \text{ or } 14^\circ < z < 50^\circ;$$

b) to simplify the process of reduction only stars of the FK4 catalogue were observed, for which the apparent places are given at 10-day intervals for the meridian of Greenwich [13]. Stars from magnitude 0.1 to 6.3 were included in our program.

Marking of the recorder's tape was carried out by the Pulkovo method, i.e., by illumination of the record from below. The tapes were measured on

the comparator [3] by the "shadow method", in which the second marks on the tape are made to coincide not with the comparator's indicator but with its shadow. Having brought contact into coincidence with contact symmetrically with respect to their edges, we get the average instant of a record of star transits to an accuracy of $0^s.1$; we obtained from the measurements of the tape the average instant of a record with an accuracy of $0^s.01$ and then from the calculations, to $0^s.001$. In contrast to the generally accepted reduction, corrections for the delay are introduced into the times of the observations of a star. Since a "Rhode and Schwartz" clock, K_1, which ran on mean solar time, was used during the observations, the times obtained were converted from mean time to sidereal time.

We obtained the delay time of the amplifier for square-wave signals with the aid of signals from the neon tube. It is connected with the time constant (Θ) of the amplifier's input. Determining Θ and knowing the value of S_E, i.e., the diameter of the image of an equatorial star for stars of any declination, we find the value of α [1,3] from the equation

$$\alpha = S_E \sec \delta/\pi\Theta$$

The diameter of the image of an equatorial star for our instrument is /58

$$S_E = 1^s.35.$$

From the argument α we find $1 - t/\Theta$, where $t = \Theta\alpha \operatorname{arc\,tn}(1/\alpha)$, and $\Theta = 0^s.162$.

Multiplying $1 - t/\Theta$ by Θ, we obtain the value of the delay for stars of various declinations. This value is applied to the time of the transits, and the full value of the delay is applied to the final value of the average time correction for the evening of observations in question. The quantities Θ and S_E vary insignificantly. Basically, the photoelectric part of the reduction is limited by this process, and the subsequent reduction coincides with that generally accepted.

We present the reduced values of the delay obtained for the stars from the declination argument:

δ	α	$1-\frac{t}{\theta}$	$\Delta\theta$
0°	2.690	0.043	0^s 007
5	2.701	0.042	7
10	2.730	0.041	7
15	2.784	0.039	6
20	2.862	0.037	6
25	2.967	0.036	6
30	3.107	0.033	5
35	3.284	0.028	5
40	3.510	0.026	4
45	3.804	0.021	3
50	4.186	0.019	3
55	4.689	0.015	2
60	5.380	0.011	2
70	7.866	0.005	1
80	15.492	0.002	0

Below are given the values of Θ and λ, where λ is the length of a second on the recorder's tape:

Date	θ	λ_{mm}
24. XI 1964	0^s158	^{3}4.52
7. XII	0.160	34.12
13. XII	0.162	34.35
20. II 1965	0.158	34.55
1. III	0.160	34.50
1. IV	0.162	34.53
12. IV	0.161	34.41
12. V	0.158	34.42
14. V	0.158	34.51
10. VI	0.156	34.50
18. VI	0.154	34.56
21. VIII	0.156	34.40
16. IX	0.161	34.15
18. IX	0.160	34.31

The results of the astronomical determinations of time are presented in the form of the instants of transmission of radio signals of time on the TU2 system. These instants represent the instants of reception of radio signals to which are applied corrections for the delay of the receiving apparatus and for the speed of propagation of the radio waves, a time correction obtained from the astronomical observations, and corrections for the motion of the pole and for the seasonal nonuniformity of the earth's rotation calculated from the data of the International Time Bureau.

The results of the observations at Pulkovo are presented in Table 1, /59 where n is the number of stars; ϵ is the mean square error of a single correction according to the internal convergence; 1-F are the instants of transmission of the signals of the GBR-9^h radio station according to observations with the photoelectric instrument; and Et. time are the instants according to etalon time.

TABLE 1

Date	n	ε	GBR-9h		Difference
			1-F	Et. time	1-F - Et. time
19.VII 1964	12	±0.s009	928	900	+028
23.VII	26	5	917	898	019
24.VII	18	5	909	897	012
18.VIII	20	4	892	883	009
19.VIII	15	4	907	883	024
29.VIII	15	5	915	878	037

From a comparison of the instants obtained on the photoelectric transit instrument with the data of etalon time [14], we find a difference equal on the average to $+0^s.022$, i.e., the instants appeared greater on the photoelectric transit instrument. N. N. Pavlov obtained at Pulkovo a difference of the same order and the same sign, namely $+0^s.034$, with an instrument mounted on the same pier where we carried out our observations. This difference is explained in the paper [1] as an error of average longitude of the ten principal observatories which took part in the derivation of the instants of the time signal transmission. This is affirmed by the fact that the value of Pulkovo's longitude calculated from the instants of the Greenwich Observatory are significantly closer to the determinations of Ya. I. Belyayev and N. I. Dneprovskiy.

The instants obtained by us at the Pulkovo Observatory are also calculated relative to the radio station (GBR-10h). Thus if the observed difference is considered a correction to the accepted longitude of the site of the observations, then the value of the longitude of the Pulkovo Observatory is $2^h01^m18^s.588 \pm 0^s.004$ according to our observations. It is very close to the determinations of N. N. Pavlov. For comparison we present the values of Pulkovo's longitude obtained by various observers:

Observer	λ_P	Method of observations
Ya. I. Belyayev N. I. Dneprovskiy	$2^h01^m18^s.566 \pm 0^s.001$	Visual
N. N. Pavlov	2 01 18.599 ± 0.004 2 01 18.580 ± 0.004	Photoelectric
T. Sh. Nuraliyev	2 01 18 588 ± 0.004	"

This agreement gives us the right to assume that there are no significant systematic (instrumental) errors in our set-up. Consequently, the difference obtained by us is the correction to the accepted longitude of the Pulkovo Observatory.

Fifty-five time corrections were obtained by the author at the Tashkent Astronomical Observatory in 1965. The results are presented in Table 2; here n and ε have the same values as in Table 1, but the instants are referred to the signals supplied by RVM-14^h. In Table 3 the instants determined on the photoelectric transit instrument 1-F (2nd column) and calculated according to etalon time on the TU2 system (3d column) are given. The difference between these instants is presented in the last column.

TABLE 2

/60

Date, 1965		n	ε	RVM-14^h 1-F
February	2	15	$\pm 0^s.007$	988
	4	12	7	000
	5	19	6	027
	22	30	5	023
	25	21	5	019
	26	16	5	004
	27	23	5	031
March	4	10	8	011
	5	13	4	023
	8	15	3	017
April	1	9	5	009
	4	13	7	014
	7	21	4	013
	11	12	5	008
	12	13	4	994
	19	5	9	994
	25	16	5	003
	26	20	5	999
	27	11	7	000
	28	17	6	994
	29	12	3	996
May	3	15	5	013
	10	7	7	999
	12	18	5	009
	14	11	7	002
	17	13	6	005
	26	10	5	007
	28	10	5	991
May	29	12	$\pm 0^s.008$	009
June	1	10	8	011
	2	14	5	006
	3	12	4	012
	4	10	5	012
	15	7	7	988
	16	12	4	994
	17	10	6	000
	18	10	6	993
	18	10	6	996
	23	11	7	997
	26	11	3	970
September	10	4	11	049
	12	8	11	041
	12	6	9	028
	12	6	5	030
	16	6	9	027
	18	6	13	043
	20	6	5	035
	21	8	10	018
	21	9	6	024
	22	6	10	028
	22	9	8	022
	28	6	10	015
	28	5	8	019
	29	8	8	009
	29	7	7	013

TABLE 3

Date, 1965		RVM-14^h 1-F	RVM-14^h Et.time	Difference 1-F-Et. time
February	2	988	019	−031
	4	000	018	−018
	5	027	018	+009
	22	023	011	+012
	25	019	010	+009
	26	004	010	−006
	27	031	010	+021
March	4	011	008	003
	5	023	008	015
	8	017	006	011
April	1	009	994	015
	4	014	992	022
	7	013	991	022
	11	008	989	019
	12	994	989	005
	19	994	986	008
	25	003	986	017
	26	999	985	014
	27	000	984	016
	28	994	984	010
	29	996	984	012
May	3	013	983	030
	10	999	981	018
	12	009	980	+029

Date, 1965		RVM-14^h 1-F	RVM-14^h Et.time	Difference 1-F-Et. time
	14	002	979	+023
	17	005	978	027
	26	007	972	035
	28	991	971	020
	29	009	970	039
June	1	011	968	043
	2	006	967	039
	3	012	967	045
	4	012	966	046
	15	988	960	028
	16	994	960	034
	17	000	959	041
	18	994	958	036
	23	997	957	040
	26	970	956	014
September	10	049	010	039
	12	033	008	025
	16	027	005	022
	18	043	003	040
	20	035	002	033
	21	021	001	020
	22	025	000	025
	28	017	995	022
	29	011	994	+017

Graphs (Figure 5) are presented on the basis of the data of Tables 2 and 3; in them 1-F is denoted by a solid line, the first transit instrument (1) by a dashed line, and the etalon time by a dot-dash line. The differences presented in Table 3 were compared with similar differences from the etalon time data [15]; with the exception of some dates they gave good agreement. Therefore the quantities which characterized the accuracy of the astronomical time determination are calculated by us on the basis of etalon time. /61

The quantities which we obtained from 55 time corrections observed by the author with the 1-F instrument and from 38 time corrections found by E. A. Sanakulov by the visual method with instrument 1 are indicated below:

Instrument	σ	m_u	m'_u	m_σ
1— F	+0^{s}021	±0.014	±0.009	±0.011
1	0.008	0.018	0.016	0.008

It is evident from this that the observations on the photoelectric instrument give great accuracy in the random sense and low accuracy in the systematic sense.

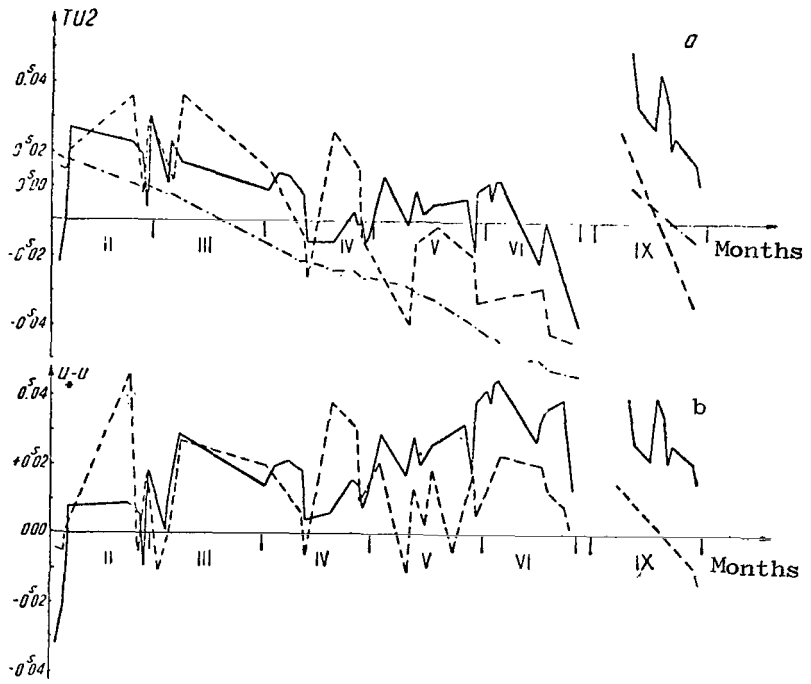

Figure 5. a - Graph of the instants of RVM-14 on the TU2 system; b - graph of the difference of the time correction (U_* - U).

In addition, we compared the instants obtained on the photoelectric and visual transit instruments; the results are presented in Table 4, which is compiled on the basis of observations carried out in the course of 25 total evenings. Then from the equation

$$\varepsilon = \pm \sqrt{\frac{\Sigma v^2}{n}}$$

the average error of the given series is calculated. For the photoelectric instrument its value was equal to $\pm 0^s.015$, and for the visual instrument, $\pm 0^s.022$. This indicates that the dispersion of the differences of the observed corrections referred to the TU2 system, and the corrections taken from the bulletin of etalon time is two times less for the photoelectric record than for the visual. /62

TABLE 4

Date, 1965		RVM-14h 1-F	RVM-14h 1	1-F-1
February	2	988	016	−028
	4	000	015	−015
	5	027	020	+007
	22	023	036	−013
	25	019	008	+011
	26	004	026	−022
	27	031	030	+001
March	5	023	012	+011
April	8	038	036	+002
	1	009	015	−006
	11	008	996	+012
	12	994	984	+010

Date, 1965		RVM-14h 1-F	RVM-14h 1	1-F-1
	19	994	026	−032
	26	999	015	−016
	27	000	996	+004
May	10	999	971	028
	12	009	994	015
	17	005	998	007
	28	991	990	001
	29	009	977	032
June	15	988	981	007
	16	994	981	013
	18	994	968	026
	23	997	966	031
September	28	015	976	+039

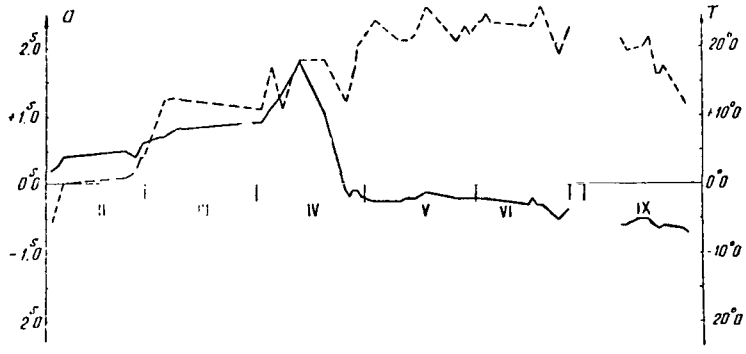

Figure 6.

Dependence of the azimuth variation of the instrument on temperature.

Observations with a duration of about two hours were carried out once a day over a period of one year. The readings of a thermometer mounted in the pavilion where the observations were made were noted twice (before and after the program of observations) and their average was taken. To illustrate the effect of temperature on the azimuth variation of the instrument, the average azimuth values and temperatures during the evening which are presented in Table 5 were used. On the basis of these data a graph is presented in Figure 6 of the azimuth variation of the instrument as a function of temperature, where the azimuth variation is indicated by a solid line and the temperature variation by a dotted line.

It is obvious from Table 5 that over the period of observations from April 25 to September 29, 1965, the temperature varied within the limits from +11.5° to +26.2°, and the azimuth within the limits from $-0^s.088$ to $-0^s.658$. Over the entire period the temperature varied within the limits of -5.5° to +26.2° and the azimuth, within the limits of $-0^s.088$ to $+1^s.782$. /63 Thus for the two periods under discussion a temperature variation by 1°C corresponds to an azimuth change of $+0^s.04$ and $+0^s.06$, respectively.

Starting from April 1965 we controlled the variation of the inclination of the instrument's horizontal axis with the help of a special device (Figure 7). Such a device is used on the PPI-1 photoelectric transit instrument in the Time Division of the Main Astronomical Observatory [16]. At the Astronomical Institute this device is mounted on the rear part of the pier under the mount of the transit instrument. Observations were carried out with a small inclination. Sometimes the inclination was controlled at the time of the observations, which had practically no effect on the instrument's azimuth. It follows from Figure 6 that a decrease of azimuth corresponds to an increase of temperature and vice versa. This can be explained as a deformation of the pier and its foundation [3], since a heating up of the instrument would have appeared rapidly [17].

TABLE 5

Date, 1965		T°	a
February	2	− 5.5	$+0^s.186$
	4	− 2.3	0.349
	5	− 0.1	0.360
	22	+ 1.0	0.484
	25	1.8	0.370
	26	3.8	0.520
	27	3.8	0.601
March	4	10.9	0.718
	5	12.3	0.726
	8	12.5	0.788
April	1	11.2	0.941
	4	17.1	1.139
	7	10.9	1.264
	11	16.6	1.691
	12	17.6	1.782
	19	18.1	+1.038
	25	11.8	−0.108
	26	14.3	0.165
	27	16.5	0.088
	28	19.9	0.123
	29	26.6	0.212
May	3	24.4	0.247
	10	20.5	0.264
	12	20.9	0.162
	14	+22.0	−0.212
	17	+25.6	$0^s.137$
	26	21.2	0.225
	28	22.7	0.189
	29	21.5	0.180
June	1	24.1	0.211
	2	23.9	0.196
	3	24.9	0.188
	4	24.1	0.215
	15	23.3	0.296
	16	23.5	0.202
	17	25.2	0.288
	18	26.2	0.318
	23	18.8	0.496
	26	23.4	0.343
September	10	21.5	0.554
	12	19.5	0.594
	16	19.7	0.534
	18	21.6	0.514
	20	16.2	0.644
	21	15.8	0.654
	22	17.3	0.604
	28	11.8	0.652
	29	+11.5	−0.658

Determination of the correction to the accepted longitude of the Astronomical Institute of the Uzbek SSR Academy of Sciences. The longitude of the pier of the first transit instrument is taken as the longitude of the Astronomical Institute, i.e.

$$\lambda_T = 4^h\ 37^m\ 10^s.470.$$

This value of the longitude was obtained by V. P. Shcheglov as a result of the reduction of observations of the Time Division of the Tashkent Astronomical Observatory of the Uzbek SSR Academy of Sciences which were carried out from 1932 to 1939 [7] on the International Time Bureau system. Consequently, the longitude of the photoelectric transit instrument is

$$\lambda_{1-F} = 4^h\ 37^m\ 10^s.807.$$

But from the papers of V. P. Shcheglov and B. V. Yasevich [18,19], a significant /64 change in the value of the longitude of the Astronomical Institute of $+0^s.015$ is evident, i.e., a different value of the longitude was obtained on the etalon time system; the observations were carried out on the same APM-10 No. 560004 instrument and on the same pier where the photoelectric observations were made. In addition, such a change in the value of the longitude of the Astronomical Institute is confirmed by the data of the International Time Bureau, where $d\lambda = 0^s.018$ [20].

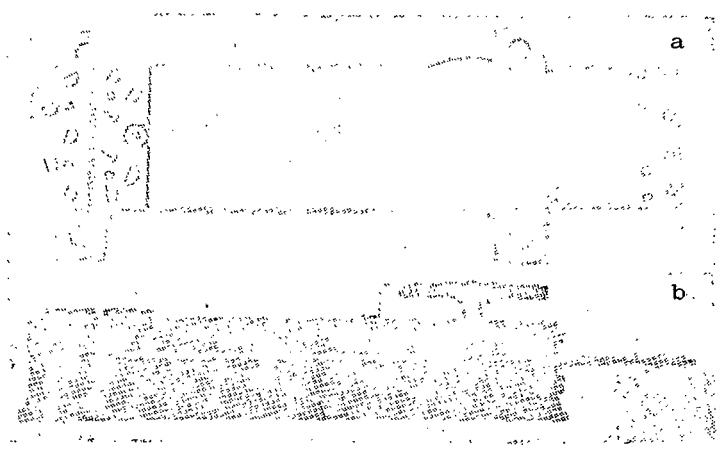

Figure 7. Device for determining the inclination:
a - top view; b - side view.

The quantities indicated above were obtained from visual observations. Corrections to the accepted longitude from the material of the photoelectric observations were calculated from the equation

$$d\lambda = \text{Et. time} - K_1 - U_1,$$

where

Et. time is the etalon time at the average instants of the transmissions of radio signals;

K_1 are the readings of the "Rhode and Schwartz" clock at the time of reception of the time signals;

U_1 is the observed correction of time on the TU2 system.

As a result they obtained $+0^s.021$ as the correction to the longitude of the Astronomical Institute.

If we denote the mean square error of a single correction to the accepted longitude by $\varepsilon_{d\lambda}$ and the final correction by $\varepsilon_{0d\lambda}$, then we obtain

$$\varepsilon_{d\lambda} = \pm 0^s.014, \quad \varepsilon_{0d\lambda} = \pm 0^s.001.$$

Thus according to the material of the photoelectric observations of star transits, the longitude of the Astronomical Institute takes the value

$$\lambda_T = 4^h 37^m 10.491 \pm 0^s.001.$$

Consequently, the longitude of the pier of the photoelectric transit instrument is

$$\lambda_{1-F} = 4^h 37^m 10^s.828.$$

Determination of the difference in longitudes Tashkent - Pulkovo. /65

The material used in the derivation of the longitudes of Tashkent and Pulkovo are not equivalent with respect to the number of observed nights; the value of the longitude of Tashkent was derived from 48 nights, and the value of the longitude of Pulkovo from 6 nights. The observations at Tashkent were reduced to the center of the pier of the first transit instrument of the Astronomical Institute, whose longitude is taken as the longitude of Tashkent. At Pulkovo, the observations were reduced to the center of the circular hall of the main building of the Pulkovo Observatory, through which passes the Pulkovo meridian.

The derivation of the difference in longitudes Tashkent - Pulkovo gave us the possibility of checking the value of the longitude of Tashkent relative to Greenwich determined by the longitude of Pulkovo. The longitude of the Pulkovo Observatory was determined with great accuracy relative to Greenwich in 1925 by the Pulkovo astronomer Ya. I. Belyayev and N. I. Dneprovskiy [21,22]. Its value was the following:

$$\lambda_P = 2^h01^m18.566 \pm 0^s.001.$$

The values of the longitudes of Tashkent and Pulkovo were calculated on the assumption that the systematic errors inherent in the instrument remained constant in the course of the entire period of the work. We also made such an assumption relative to the systematic errors of the instants of etalon time [23].

The difference obtained by us in the longitudes Tashkent - Pulkovo has the form

$$\Delta\lambda = 2^h35^m51^s.903 \pm 0^s.004.$$

With the help of this difference, the value of Tashkent's longitude relative to Greenwich was obtained by the author from the longitude of Pulkovo based on the various determinations of it [1,20,21,24]:

Observer	λ_P	Year
Ya. I. Belyayev and N. I. Dneprovskiy	$2^h01^m18^s.566$	1925
N. N. Pavlov	2 01 18.580	1946
V. M. Vasil'yev	2 01 18.556	1953
N. Stoyko	2 01 18.572	1963

From these four determination of Pulkovo's longitude, taken by us to have equal weight, its average value was derived:

$$\lambda_P = 2^h01^m18^s.568 \pm 0^s.005$$

Then for Tashkent's longitude we have

$$\lambda_T = \overline{\lambda}_P + \Delta\lambda = 4^h37^m10^s.471 \pm 0^s.006.$$

This value agrees to an accuracy of $0^s.001$ with the value of Tashkent's longitude

obtained by V. T. Shcheglov [7], which attests to the absence of significant systematic errors in the longitude difference Tashkent - Pulkovo which we determined from observations with the photoelectric transit instrument and also attests to the stability of the longitude of the Astronomical Institute.

And so, thanks to the southern location of the Astronomical Institute, the record of faint stars is obtained without the fine subdivisions of the contact edges which is encountered at observatories with northern latitudes, particularly during the period of white nights. The contact obtained in pure form excludes accidental errors in the marking of the tape.

A good record of faint stars permits observations of the stars which /66
are observed with the photographic zenith tube. Thanks to this, one can compare the material obtained with various instruments.

REFERENCES

1. Pavlov, N. N., Trudy GAO, Series II, Vol. 59, Lemingrad, 1946.

2. Brandt, V. E., Trudy TsNIIGAIK, Issue No. 112, Moscow, 1956.

3. Dolgov, P. N., Opredeleniye vremeni passazhnym instrumentom v meridiane [Determination of Time by a Transit Instrument on the Meridian], Moscow, 1952.

4. Yasevich, B. V., Trudy TAO, Series II, Vol. 10, Tashkent, AN UzSSR Press, 1964.

5. Vasil'yev, A. S., Proceedings of the AN SSSR, Series 6, Vol. 19, Leningrad, 1925.

6. Suvorova, Ye. V., Proceedings of the AN UzSSR, Physico-Mathematical Series, Vol. 6, 1964, 79-82.

7. Shcheglov, V. P., Yubileynyy sbornik, posvyashchennyy dvadtsatipyatiletiyu UzSSR [Jubilee Collection in Honor of the 25th Anniversary of the UzSSR], AN UzSSR Press, 1949, 102-112.

8. Platonov, Yu. P., Sukhov, V. B., Proceedings of the GAO, Vol. 21, Issue 2, Leningrad, No. 161, 1958.

9. Pavlov, N. N., Trudy 12-oy vsesoyuznoy astrometricheskoy konferentsii [Transactions of the 12th All-Union Astrometric Conference], Leningrad, 1957.

10. Zverev, M. S., Uspekhi astronomicheskikh nauk [Advances in Astronomical Science], Vol. 6, Moscow, 1954.

11. Brandt, V. E., Trudy 10-y vsesoyuznoy astrometricheskoy konferentsii [Transactions of the 10th All-Union Astrometric Conference], Leningrad, 1954.

12. Bonch-Bruyevich, A. M., Primeneniye elektronnyikh lamp v eksperimental'noy fizike [Application of Electron Tubes in Experimental Physics], Moscow, 1956.

13. Apparent Places of Fundamental Stars, Heidelberg, 1965.

14. Etalonnoye vremya v sredniye momenty peredach radiosignalov [Etalon Time at the Average Instants of Radio Signal Transmissions], Moscow, 1964 (July-August).

15. Etalonnoye vremya v sredniye momenty peredach radiosignalov [Etalon Time at the Average Instants of Radio Signal Transmissions], Moscow, 1965 (February-September).

16. Chzhen Chzhun-Lyan, Proceedings of the GAO, Vol. 23, Issue 1, Leningrad, 1962, No. 171.

17. Fedorov, Ye. P., O prichinakh izmeneniy naklonnosti osi i azimuta meridiannykh instrumentov [Causes of Variations in the Inclination of the Axis and the Azimuth of Meridian Instruments], Transactions of the Pultava Gravimetric Observatory, Kiev, 1950.

18. Shcheglov, V. P., Sovremennyye dvizheniya zemnoy kory [Recent Movements of the Earth's Core], AN USSR Press, Moscow, 1963, No. 1.

19. Shcheglov, V. P., Yasevich, B. V., Vrashcheniye zemli [Rotation of the Earth], Kiev, 1963.

20. Stoyko, A., Bulletin Horaire, No. 6 (Series H), Paris, 1963.

21. Belyayev, Ya. I., Dneprovskiy, N. I., Trudy GAO, Series 2, Vol. 34, Leningrad, 1928.

22. Yazev, N. N., Pavlov, N. N., Trudy GAO, Series 2, Vol. 42, Leningrad, 1933.

23. Yasevich, B. V., Trudy TAO, Series 2, Vol. 8, Tashkent, AN UzSSR Press, 1961.

24. Vasil'yev, V. M., Proceedings of the GAO, Vol. 19, Issue 3, Leningrad, 1953, No. 150.

DIFFERENTIAL CATALOGUE OF RIGHT ASCENSIONS OF 102 STARS OF THE TASHKENT WIDE ZENITH ZONE

E. A. Sanakulov

ABSTRACT. The author presents a differential catalogue of the right ascensions of 102 stars ranging in declination from 25° to 53°. His data are referred to the FK4 system. The observations were carried out at the Tashkent Astronomical Observatory with the Askania Works No. 85951 transit instrument, which has an objective 100 mm in diameter, a focal length of 1000 mm, a magnification of 100, and a horizontal axis 650 mm in length.

The stars were divided into hour groupings and observed visually by the group method, since 122 reference stars, 48 equatorial stars, and 12 northern stars were included in the program in addition to the 102 program stars. A sighting mark 80.3 m north of the transit pavilion was used to check on the instrument's azimuth. Transit data was recorded by a writing chronograph. A quartz clock was used as a time reference check. Data from 117 nights from October 1964 to June 1966 were used in the final reduction. On the average each program star was observed 19 times. The mean square error of a single determination of the right ascension of a catalogue star was $\pm 0^{s}.023$ for the zenith zone.

A comparison of the author's catalogue with FK4 by means of the GC reveals a systematic error as large as $0^{s}.01$, which he explains as being due to an accumulation of accidental errors and the inaccuracy of the catalogues. He considers his catalog to be of comparable accuracy to the GC.

The author also determined the corrections to the right ascensions of the 12 northern stars in his program and gives a differential catalogue for them based on the FK4 system. He also investigated the effect on the right ascensions determined for the program stars of using a combination of observations of northern and zenith stars to determine the instrument's azimuth rather than equatorial and zenith stars. He found that the system of right ascensions of the program stars was the same in both cases, so only the catalogue based on the latter combination is given.

In connection with the developing problem of detailed study of the non- /67
uniformity of the earth's rotation, significant difficulties have arisen regarding the accuracy of right ascensions of stars of the fundamental catalogue. Therefore the results of observations of Service Time are used for improving the fundamental reference system [1-3], for which a program of observations including, in particular, observations of northern stars at both culminations was set up. The list of stars compiled by B. V. Yasevich [4] was used as the basis of the program.

Included in the program were 285 stars which were distributed in declination in the following way: 122 reference zenith stars ($+25° < \delta < +52°$), 102 program stars ($+25° < \delta < +53°$), 48 equatorial stars ($-17° < \delta < +15°$), 12 northern stars ($+75° < \delta < +80°$), and the pole star for determining the absolute azimuth. The northern stars were observed at both culminations.

To improve the right ascensions it was necessary to solve two problems: the differential determinations of the right ascensions of 102 stars on the FK4 system and the derivation of the absolute catalogue of right ascensions of zenith stars. Only the solution of the first of these is discussed in the present article.

The instrument and its survey. The observations were carried out with the Askaniya Works No. 85951 transit instrument. A detailed description of a similar instrument is given in the paper [5]. The basic characteristics of the instrument are the following: the diameter of the objective is 100 mm, the focal distance is 1000 mm, the length of the horizontal axis is 650 mm, and the magnification is 100^{X}. It was mounted in a wooden pavilion in 1932. The internal dimensions of the pavilion are: 2.9 m along the meridian, 4.2 m in the vertical direction, and the height of the floor is 2.2 m. The pavilion is slid open forming a slit with a width of 1.5 m. At a distance of 80.3 m to the north from it is situated a sighting mark, protected by a frame stall. The lens for the sighting mark is situated within the pavilion on a masonry pier at a distance of 2.34 m from the instrument.

In 1962, the author, along with T. Nuraliyev, investigated the suspended level by the method of A. S. Vasil'yev [6] with the Herbst testing machine. The quality of the grinding of the vial appeared to be satisfactory. A value

of a division of $\tau = 1\overset{s}{.}146$ was obtained; it agrees well with the value of $\tau = 1\overset{s}{.}14$ found by V. T. Beda in 1957. The temperature coefficient of the level was not determined, but since the investigations, which were carried out at various times at various temperatures, gave the same results, one can assume that it is small. /68

They obtained a value of a revolution of the micrometer screw from observations of near-polar stars; it is equal to $R = 6\overset{s}{.}845 \pm 0\overset{s}{.}010$. The backlash of the micrometer screw was determined three times by aiming the moving bisector at the fixed filament [5]; it was found to be very small, smaller than the accidental errors of the determination, and was taken equal to zero. The width of the micrometer's contact K was found in August 1963 and 1964 with the aid of a telephone [5]. It was found to be equal to $K = 0\overset{s}{.}056$. In February 1966 they investigated the width of the micrometer's contact with the aid of a telephone and also on the basis of star observations [5]. In the first case, they obtained a value of $0\overset{s}{.}030$, but from the observations of 22 stars they obtained $K = 0\overset{s}{.}032$. Therefore from January 1966 the time corrections obtained were calculated with a new value of the contact width equal to $K = 0\overset{s}{.}031$.

In the interval between investigations the time corrections were calculated taking into account interpolated values of the contact width. The pivots of the transit instrument were investigated in December 1963 by the contact method with the help of Uverskiy's interferometer. The calculations were carried out by the method of Moreau-Verbaandert [7]. Investigations showed that although the average deviation of the figure of the pivots from the ideal circle attains 1μ, however for both pivots the depressions and protrusions are symmetrical. Therefore the correction to the inclination for the incorrectness of the figure of the pivots does not exceed $0\overset{s}{.}006$, and $0\overset{s}{.}004$ in the azimuth. Upon reduction of our observations these corrections were not taken into account.

Program of observations. The list of stars was divided into hour groupings. Each group contained from 7-12 near-zenith stars, 4 equatorial stars, and one northern star.

For comparison of the method of A. A. Nemiro [1] with the classical

method of determining the absolute azimuth, the polar star was included in the program. But daytime observations were not obtained because of poor visibility. The choice of groups was carried out in such a way that the total of the azimuthal coefficients of the stars of the zenith zone would be close to zero. The observations were carried out visually by the group method [1]. Each evening they observed the four groups. Before and after the observations they took readings of the sighting mark both for a positive and a negative rotation of the micrometer screw, making ten aimings. The program was made up so that at the start and at the end of each group a pair of equatorial stars were observed necessarily in various orders of observations.

A writing chronograph running on sidereal time was the recording device. A Rhode and Schwartz quartz clock K_1 running on mean solar time served as the operating clock. Before and after the observations of each group, reading of the chronograph and the quartz clock were compared with each other. The variation of the chronograph was taken into account for each group separately, and the instants of transits of stars were referred to the common start of the observations. The observations were carried out from October 1964 to June 1966 (140 nights in all).

For the final reduction and derivation of the right ascension corrections the material of 117 nights or 468 time corrections were used. The observations were carried out with a reversal of the instrument in the middle of the observations of each star and by two revolutions of the micrometer screw; 18 pairs of contacts were recorded. For zenith and equatorial stars, 10 pairs of sym- /69
metrical contacts were selected, and for northern stars from 18 to 21 pairs. Before and after the observation of each star, readings of the level were taken. Prior to the start of the observations, if it was required, the inclination of the instrument was adjusted. In the course of an evening, the inclination always decreased within the limits of 3 to 7 half-divisions of the level.

Metal grids were used to reduce the brightness of the stars. The observations of all stars were distributed equally between the two orders of observations EW and WE. The setting of the tube was always done in zenith distance by a positive rotation of the micrometer screw. On the average they observed each program star 19 times, with 12 being the minimum number of observations and 22

the maximum. The mean square error of a single determination of the right ascension of a catalogue star for the zenith zone is equal to $\pm 0^s.023$.

Reduction of the observations and derivation of the catalogue. The values of the apparent right ascensions of the stars were taken from the tables of the ITA and "Apparent Places of Fundamental Stars" FK4, and for the program stars these values were calculated from the corresponding catalogue [8-12].

The instants of star transits obtained were corrected for the variation in azimuth of the instrument during the course of a given evening; the azimuth was determined from readings of the sighting mark. It was assumed that the variation in the azimuth is proportional to the time [13]. The azimuth of the instrument was calculated from a combination of observations of a group of fundamental stars with each equatorial star from the equation

$$a = \frac{u'_s - u'_z}{A_s - A_z}, \tag{1}$$

where

u'_s is the preliminary time correction found from the observations of the equatorial star without taking into account the azimuth of the instrument;

u'_z is the average correction obtained from the observations of the group of reference stars without taking into account the azimuth; and

A_s and A_z are the azimuthal coefficients of an equatorial star and the average azimuthal coefficient of the group of reference stars.

They obtained a separate value of the instrument's azimuth for each equatorial star; nevertheless they calculated from the four equatorial stars an average value for each group. They found a time correction u_{ref} based on the reference stars for each group. The right ascensions of the program stars were calculated from the equation

$$\alpha_{prog,\, i} = u_{ref} + T_i, \tag{2}$$

where

$$T_i = (t_i + A_i \delta a_i) + B_i\, b + A_i\, a + (m) \sec \delta_i; \tag{3}$$

t_i is the instant of the record of the star's transit;

A_i and B_i are the Mayer coefficients;

a is the instrument's azimuth;

δa_i is the correction for azimuth variation determined from the readings of the sighting mark; and

$(m) \sec \delta_i$ is the correction for the width of the contact, backlash, and diurnal aberration;

$$(m) = \frac{R}{2}(M_x + K) - 0^s.021 \cos \varphi. \tag{4}$$

The corrections of the right ascensions of the program stars were calculated on the system of the corresponding catalogue. In order to exclude error dependent on the order of the observations, they found initially the average value for each order of observations $\Delta\alpha_{EW}$, $\Delta\alpha_{WE}$, and then took their arithmetical mean: /70

$$\Delta\alpha = \frac{\Delta\alpha_{EW} + \Delta\alpha_{EW}}{2}. \tag{5}$$

They found the error in the determination of the right ascension of each star from the equation

$$\varepsilon_\alpha = \pm \frac{1}{2} \sqrt{\bar{\varepsilon}_1^2 + \bar{\varepsilon}_2^2}; \tag{6}$$

here

$$\bar{\varepsilon}_1 = \pm \sqrt{\frac{\sum v_{EW}^2}{n_1 (n_1 - 1)}}; \quad \bar{\varepsilon}_2 = \pm \sqrt{\frac{\sum v_{WE}^2}{n_2 (n_2 - 1)}};$$

v_{EW} and v_{WE} are the deviations of the corrections to the right ascension from their average value in the case of the orders EW and WE;

n_1 and n_2 are the numbers of observations of each star for the orders EW and WE, respectively.

The errors of the average result of the observations for each star are given in a separate column of the catalogue. On the average, they amount to $\pm 0^s.005$ for a single star.

The square errors of a single observation averaged over time and reduced to the equator were calculated from the equation

$$\varepsilon_\vartheta = \pm \sqrt{\frac{\sum (\varepsilon_1^2 + \varepsilon_2^2)\cos^2 \delta}{k}}, \qquad (7)$$

where

k is the number of program stars in the group;

$$\varepsilon_1 = \pm \sqrt{\frac{\sum v_{EW}^2}{n_1 - 1}}; \quad \varepsilon_2 = \pm \sqrt{\frac{\sum v_{WE}^2}{n_2 - 1}}.$$

On the average, the square error of a single observation reduced to the equator is $\pm 0^s.024$.

Comparison of the catalogue obtained with other catalogues.

All the stars of our catalogue (Appendix 1) are in the GC. It has 78 stars in common with KGZ, 44 with N30, 59 with $FK4_{supp}$, 79 with the differential catalogue of E. V. Suvorova (Suv), and 34 with ITA catalogue [14]. We compared our catalogue with the catalogues listed and with FK4 by means of the GC, KGZ, and N30. For this, they compared the FK4 catalogue with GC, KGZ and N30 based on the reference stars. They averaged the differences in right ascensions over five-degree zones in declination. The systematic differences obtained for all the catalogues are presented in Table 1[1] (n is the number of common stars).

It is evident from the table that upon comparison of our catalogue with FK4 by means of the GC the systematic error reaches $0^s.01$, and by means of KGZ and N30, $0^s.02$. It is most probable that these differences are explained by an accumulation of accidental errors and the inaccuracy

1. In all tables the values of quantities are given in $0^s.001$.

of the catalogues, and that the accuracy of our catalogue is comparable with the accuracy of the KGZ and GC.

A comparison of the catalogue presented with others with respect to /71
$\Delta\alpha_\alpha$ is presented after the exclusion of $\Delta\alpha_\delta$ from the differences in the right ascensions. Smoothed [13,15] systematic differences of the type $\Delta\alpha_\alpha$ are given in Table 2.

TABLE 1

δ	C - GC		FK4 - GC		C - KGZ		FK4-KGZ		C - N30	
	Δα	n	Δα	n	Δα	n	Δα	n	Δα	n
25—30	—29	5	—19	8	—10	4	— 6	8	+ 4	3
30—35	—23	16	—19	20	+ 3	13	— 6	20	+23	7
35—40	— 1	28	—16	22	+ 3	20	—10	21	— 1	13
40—45	—20	22	—17	29	—12	17	— 7	28	—25	11
45—50	—26	23	—20	38	—14	17	— 8	38	—33	4
50—55	—13	8	—20	5	+ 9	7	—10	8	— 8	6

δ	FK4 - N30		Comparison of the catalogue with FK4 through			C-FK4 supp		C - Suv	
	Δα	n	KGC	GC	N30	Δα	n	Δα	n
25—30	— 2	8	— 4	—10	+ 6	+23	3	— 9	2
30—35	— 4	20	+ 9	— 4	+27	+25	11	+ 4	15
35—40	—13	22	+13	+15	+12	— 9	3	—10	20
40—45	—15	29	— 5	— 3	—10	—21	15	—11	18
45—50	—12	38	— 6	— 6	—21	—24	11	— 5	18
50—55	—24	5	+19	+ 7	+16	+ 8	6	—10	6

TABLE 2

α	Comparison with FK4 through			C-FK4 supp	C - Suv
	GC	N30	KGZ		
0—3	— 3	— 7	—5	+10	+ 3
3—6	— 3	—20	—5	— 9	+ 1
6—9	+ 5	0	—3	— 1	— 6
9—12	— 3	+10	—2	— 2	— 9
12—15	+ 5	+ 7	+7	+10	— 9
15—18	+ 6	+13	—9	+ 2	— 1
18—21	—14	— 3	—5	— 7	+ 1
21—24	+ 2	—13	+2	—14	+21

TABLE 3

m	Catalogue minus				
	GC	KGC	N30	FK4 supp	Suv
0—4	—	—	—	—	—
4—5	—4	—5	—6	+4	+2
5—6	—2	—3	—1	0	0
6—7	+6	+4	+6	—1	+2

The errors which depend on the brightness of the stars were determined in the following manner. Initially, the systematic differences of the form $\Delta\alpha_\delta$ and then the averages for each hour $\Delta\alpha_\alpha$ were excluded from the differences in right ascensions "our catalogue minus a comparable one" for the common stars; the remaining differences were grouped according to stellar magnitudes; the systematic differences of the form $\Delta\alpha_m$ are indicated in Table 3.

Determination of the corrections of the right ascensions of northern stars. Since the Kyustner series were not observed by us, we calculated the corrections to the right ascensions of northern stars for the control of systematic errors of the type $\Delta\alpha_\delta$. Using the observational material, we determined the right ascensions of 12 northern stars with declination 75° to 80° and α Ursae Minoris. In this case the fine corrections were determined from /72 zenith stars and the azimuth from equatorial stars. The calculations were carried out the same as indicated above.

Each northern star was observed an average of 43 times; the minimum number of observations was 32, and the maximum number was 47. The corrections in right ascensions were determined separately for the upper and lower culminations. In order to exclude errors dependent on the order of the observations, the average corrections to the right ascensions were initially calculated for each order of the observations and then the simple average was taken. The final corrections to the right ascensions of the northern stars were determined as the arithmetic averages of the corrections in right ascensions obtained from the upper and lower culminations:

$$\Delta\alpha = \frac{\Delta\alpha_{up} + \Delta\alpha_{low}}{2}. \qquad (8)$$

The accuracy was estimated in the same way as for the zenith stars. The differential catalogue of northern stars obtained on the FK4 system is given in Appendix 2. The catalogue of northern stars was compared with FK4 and N30. The comparison of our catalogue with the catalogues indicated above with respect to $\Delta\alpha_\delta$ is given below (n is the number of common stars):

Catalogue differences	$\Delta\alpha_\delta$	n
C - FK4	- 81	12
C - N30	-105	12
FK4 - N30	- 24	12

It follows from this that upon the calculation of the azimuth from equatorial stars the right ascensions of northern stars are determined with significant systematic errors. We present the systematic differences, arranged by threes, of the type $\Delta\alpha_\delta$ obtained from a comparison of our catalogue with others:

α	C —FK4	C —N30	FK4—N30
0—3	— 8	0	+ 8
3—6	+21	+ 7	—14
6—9	+18	—15	—32
9—12	+17	—11	—28
12—15	+10	—16	—26
15—18	—12	+16	+29
18—21	—24	+17	+42
21—24	—20	+32	+52

Effect of a chance of the azimuthal stars on the right ascensions of the program stars. The question of the choice of stars for the determination of the time corrections is discussed in a series of papers [16-20]. M. S. Zverev [16], investigating the choice of reference stars for the relative determination of right ascensions, constructed graphs of the Aurell type and established the fact that upon a decrease in the systematic errors in both the instrumental and the personal nature of the observation it is necessary to work with narrow zones in declination. In this case the weights of the right ascensions practically reach the maximum value (0.8). M. S. Zverev recommends, for the best determination of azimuth, combinations of observations of upper and lower culminations of stars with declinations from +70° to +80°.

One can observe equatorial or northern stars as "azimuthal" stars to obtain the right ascensions of stars. Equatorial stars have the following advantages over northern stars: more exact right ascensions, small accidental error upon recording a transit across the meridian, and a large speed of /73
transit across the meridian.

We found the azimuth from the combination of observations of equatorial and zenith stars, and observations of northern stars were initially not investigated. Therefore it was necessary to find out how the systematic errors of the differential catalogue are changed if the azimuth is determined from a combination of observations of northern and zenith stars. The average correction based on a group of reference zenith stars was calculated from the equation

$$u^{S}_{ref} = u'_z - A_z a_S. \tag{9}$$

If the azimuth was found from northern stars, then

$$u^{N}_{ref} = u'_z - A_z a_N. \tag{10}$$

where

u'_z is the time correction based on the reference stars without taking into account the azimuth of the instrument;

A_z is the average azimuthal coefficient of the group of reference zenith stars; and

a_S and a_N are the azimuth of the instrument calculated from northern and southern stars.

Subtracting (9) from (10), we obtain

$$u^{N}_{ref} - u^{S}_{ref} = A_z(a_S - a_N). \tag{11}$$

The right ascensions of the program stars were calculated from the equation

$$\alpha_{prog} = T + u^{S}_{ref} + A_{prog} a_S. \tag{12}$$

Then one can obtain for the case where the azimuth is determined from northern stars:

$$\alpha_{prog} = T + u^{N}_{ref} + A_{prog} a_N, \tag{13}$$

where

T is the instant of transit of the star across the meridian corrected for the inclination, contact width, backlash, diurnal aberration, and the variation in azimuth found from readings of the sighting mark.

From (11) to (13) we obtain

$$\Delta\alpha_N = \Delta\alpha_S + [A_{prog}(a_N - a_S) - A_z(a_N - a_S)]. \tag{14}$$

The difference $a_N - a_S$ based on opposite culminations are given in Table 4. Since like culminations of northern stars take place as a rule in two hours, and the reduction was carried out for hour groups, the averages (given in parentheses) were calculated from the adjacent values $a_N - a_S$.

The systematic nature of the culmination difference is evident from the table. This is confirmed by the observations of A. Kadyrov [21], who obtained for northern stars at upper culminations

$$a_N - a_S = -0^s.034.$$

Evidently, this systematic difference does not depend on the instrument nor on the observer, and it seems to us that it is explained by the systematic errors in the right ascensions of northern stars or the effect of local conditions. The effect of $a_N - a_S$ on the right ascension of the program stars is shown in Table 5 [the values $\Delta\alpha_\delta$ were calculated from Eq. (14)], from which it is evident that the northern "azimuthal" stars are observed only in one culmination, and the system of right ascension of the program stars /74 differs with respect to $\Delta\alpha_\delta$ from the system obtained when locating the azimuth from equatorial stars. In the case of the observation of northern stars at both culminations, these systems practically coincide.

TABLE 4

Group	$a_N - a_S$			A_m
	Upper culm.	Lower culm.	Average	
1	(−35)	+16	−10	+ 36
2	−45	(+39)	− 3	− 65
3	(−30)	+62	+16	+ 23
4	(−30)	+30	0	− 12
5	−15	(+24)	+ 4	− 50
6	(−24)	+18	− 3	+ 31
7	−33	(+19)	− 7	+ 3
8	(−14)	+20	+ 3	− 47
9	+ 6	(+26)	+16	−112
10	(+ 4)	+33	+18	+ 51
11	+ 3	(+28)	+16	+ 44
12	(− 6)	+23	+ 8	− 30
13	−16	(+14)	− 1	− 78
14	(−21)	+ 4	− 8	+ 5
15	−26	(+20)	− 3	−110
16	−50	(+20)	−15	+ 53
17	(−26)	+35	+ 4	− 51
18	− 2	(+38)	+18	− 9
19	(−20)	+42	+11	+ 51
20	−39	(+18)	−10	− 46
21	(−54)	− 6	−30	+ 28
22	−68	(+18)	−25	+ 48
23	(−46)	+41	− 2	+ 72
24	−25	(+28)	+ 2	+ 42
Average	−26	+25	0	− 5

Thus a second version of the differential catalogue of right ascensions was obtained. It was compared with the catalogues GC, KGZ, and also with FK4 through the catalogues GC and KGZ. The systematic difference of the type $\Delta\alpha_\delta$, obtained upon comparison of our catalogue with FK4 through GC and

TABLE 5

δ	$\Delta\alpha_\delta = \Delta\alpha_N - \Delta\alpha_S$		
	Upper culm.	Lower culm.	Average
25—30	— 3	+7	+2
30—35	— 3	+5	+1
35—40	— 2	+2	0
40—45	+ 1	0	0
45—50	+ 4	—5	0
50—55	+11	—9	+1

KGZ, respectively, is presented in Tables 6 and 7.

And so, upon the determination of the azimuth and the combination of observations of zenith and northern stars, significant systematic errors arise which are excluded upon the observation of northern stars at both culminations. Then the system of right ascensions of the program stars is found to be the same as for the calculation of the azimuth from a combination of zenith and equatorial stars. Therefore the first version of our catalogue is published (the azimuth was determined from zenith and equatorial stars). /75

Derivation of right ascensions of equatorial stars. If the azimuth is found from a combination of observations of zenith and northern stars, then one can find the right ascensions of the equatorial stars. Since the equatorial stars enter into FK4, the corrections to them permit a control of the system of our instrument. Initially, the azimuth was calculated from equatorial and zenith stars. The corrections to the right ascensions of equatorial stars were obtained from the equation

$$\Delta\alpha_S = u^S_{ref} - u_{prog(s)} + A_{prog(s)}a_s, \qquad (15)$$

where

u^S_{ref} is the time correction based on zenith stars;

$u_{prog(s)}$ is the time correction based on an equatorial star without taking into account the instrument's azimuth; and

$A_{prog(s)}$ is the azimuthal coefficient of an equatorial star.

The average for both orders of observation were obtained to exclude errors dependent on the order of observation, $\Delta\alpha_s$. The final corrections to the right ascensions of the equatorial stars were calculated from Eq. (14). On the average, each equatorial star was observed 23 times; the minimum number of observations was 19 and the maximum number was 27. The estimate of

TABLE 6

δ	n	Azimuth according to equatorial stars		Azimuth according to northern stars						FK4 - GC
				Upper culm.		Lower culm.		Average		
		C-GC	C-FK4	C-GC	C-FK4	C-GC	C-FK4	C-GC	C-FK4	
25–30	5	–29	–10	–31	–12	–22	– 3	–26	– 8	-19
30–35	16	–23	– 4	–26	– 7	–17	+ 2	–21	– 2	-19
35–40	28	– 1	+15	– 3	+13	+ 1	+17	– 1	+15	-16
40–45	22	–20	– 3	–19	– 2	–21	– 4	–20	– 3	-17
45–50	23	–26	– 6	–22	– 2	–31	–11	–26	– 6	-20
50–55	8	–13	+ 7	– 2	+18	–22	– 2	–12	+ 8	-20

TABLE 7

δ	n	Azimuth according to equatorial stars		Azimuth according to northern stars						FK4 - KGC
				Upper culm.		Lower culm.		Average		
		C-KGZ	C-FK4	C-KGZ	C-FK4	C-KGZ	C-FK4	C-KGZ	C-FK4	
25–30	4	–10	– 4	–12	– 6	0	+ 6	– 6	0	-6
30–35	13	+ 3	+ 9	0	+ 6	+ 9	+15	+ 4	+10	-6
35–40	20	+ 3	+13	+ 1	+11	+ 5	+15	+ 3	+13	-10
40–45	17	–12	– 5	–11	– 4	–12	– 5	–12	– 5	-7
45–50	17	–14	– 6	– 9	– 1	–19	–11	–14	– 6	-8
50–55	7	+ 9	+19	+21	+31	+ 1	+11	+11	+21	-10

accuracy was made the same way as for the zenith stars. The mean square error of a determination of the right ascension of a single star is $\pm 0^s.004$. /76

The differential catalogue of right ascensions obtained for 48 equatorial stars is given in Appendix 3. It was compared with the FK4 and N30 catalogues. The systematic difference of the type $\Delta\alpha_\delta$ (n is the number of stars) and the smoothed systematic difference of the type $\Delta\alpha_\alpha$ are presented in Tables 8 and 9. The catalogues obtained for near-equa-

TABLE 8

δ		C - FK4			C-N30	FK4-N30	n
		Upper culm.	Lower culm.	Average			
−15	−20	−47	− 4	−26	−37	−11	3
−10	−15	−19	+22	+ 2	−10	−11	3
− 5	−10	−22	+19	− 2	−16	−14	10
0	− 5	−18	+21	+ 2	− 8	−10	12
0	+ 5	−18	+ 9	− 5	−15	−10	8
+ 5	+10	−11	+17	+ 3	− 6	− 9	11
+10	+15	+ 3	+22	+12	+ 5	− 7	1

torial stars agrees well with respect to $\Delta\alpha_\delta$ (Table 8) with the FK4 system (with the exclusion of the stars farthest from the equator). The systematic difference with the N30 catalogue of the type $\Delta\alpha_\delta$ reaches a large value.

TABLE 9

α	C - FK4			C - N30	FK4 - N30
	Upper culm.	Lower culm.	Average		
0— 3	− 7	+3	−2	+1	+3
3— 6	+ 5	+7	+4	+6	0
6— 9	+10	+3	+6	+4	−2
9—12	+11	+2	+6	+4	−3
12—15	+ 4	0	+2	0	−1
15—18	− 1	0	−2	−1	0
18—21	− 6	−1	−4	−2	+2
21—24	− 6	+2	−3	+2	+4

This is explained by the fact that with respect to $\Delta\alpha_\delta$ the N30 system differs from the FK4 system for the equatorial zone. It is evident from Table 9 that our catalogue differs little with respect to $\Delta\alpha_\alpha$ from the FK4 and N30 catalogues, which indicates a sufficient reliability in the determination of the right ascensions.

REFERENCES

1. Nemiro, A. A., Proceedings of the GAO, 1957, No.157.

2. Pavlov, N. N., Proceedings of the GAO, 1958, No.161.

3. Nemiro, A. A., Pavlov, N. N., AZh, Vol. 36, No. 5, 1959.

4. Suvorova, Ye. V., Tsirkulyar TAO [Circular of the Tashkent Astronomical Observatory], "Fan" Press of the UzSSR, 1965, No. 340.

5. Dolgov, P. N., Opredeleniye vremeni passazhnym instrumentom v meridiane [Determination of Time by a Transit Instrument on the Meridian], Moscow, GITTL, 1952.

6. Vasil'yev, A. S., Proceedings of the AN USSR, Series VI, Vol. 19, 1925.

7. Sanakulov, E. A., Proceedings of the AN UzSSR, Math-Physics Series, 1966, No.2.

8. Kopff, A., Supplement to the FK3 Catalog, published by the Astronomical Computing Institute, Heidelberg. /77

9. Veröffentlichungen des Astronomischen Rechen, Instituts [Publications of of the Astronomical Computing Institute], Heidelberg, No. 11, 1965.

10. Zimmerman, N. V., Trudy GAO, Series 2, Vol. 61, 1948.

11. Boss, B., General Catalogue of 33342 Stars, Volumes 1 - 5, Washington, 1937.

12. Morgan, H. R., Catalogue of 5268 Standard Stars, 1950.0, based on the normal system N30, Astronomical Papers, Vol. 13, Part 3, 1952.

13. Yasevich, B. V., Trudy TAO, Series 2, Vol. 10, 1964.

14. Zhelezhyak, M. B., Mal'kova, A. G., Rumyantseva, L. I., Appendix to the ITA Bulletin, AN USSR, Vol. 10, No.2(115), 1965.

15. Kalikhevich, A. S., Proceedings of the GAO, No. 171, 1962.

16. Zverev, M. S., AZh, Vol. 25, No. 4, 1949.

17. Brandt, V. E., Trudy TsNIIGAIK, No. 64, 1949.

18. Shteins, K. A., AZh, Vol. 30, No. 5, 1953.

19. Pil'nik, T. P., AZh, Vol. 33, Nos. 2 and 5, 1956.

20. Petrov, G. M., Proceedings of the GAO, No. 161, 1958.

21. Kadyrov, A., Proceedings of the AN UzSSR, Math-Physics Series, 1959, No. 5.

APPENDIX 1

/78

Catalogue number				m	δ_{1960}	$\alpha_{1960.0}$	E_r 1960+	ε_α	n	C - KGC	C - GC	C - N30	C-$FK4_{supp}$	C - Suv	C - ITA
KGZ	GC	N 30	$FK4_{supp}$												
40	488	74	2022	5.7	+52° 50′	$00^h\ 22^m 55^s.892$	4.95	±4	19	+24	+11	+23	+31	+20	+30
43	546	—	2027	5.2	44 10	26 04.197	4.94	4	20	− 9	−41	—	+39	+32	+38
49	611	—	—	6.1	33 22	29 17.816	4.93	6	21	+62	+63	—	—	+26	—
74	812	138	2043	5.4	39 14	38 56.592	4.94	6	20	+ 9	+ 1	− 4	+ 5	+ 9	—
158	1541	263	—	6.6	39 16	01 14 59.309	5.01	5	19	−11	−16	−18	—	—	—
181	1850	311	2100	6.3	34 36	29 50.272	5.01	5	20	+19	+26	+33	+38	+ 5	—
197	2025	341	—	4.9	40 23	38 12.530	5.00	6	20	−19	−25	−34	—	−50	−19
284	2813	—	—	5.6	49 58	02 18 18.527	5.11	5	20	+ 3	−21	—	—	− 5	—
290	2902	—	2165	4.9	50 06	22 56.568	5.09	4	22	+31	+18	—	+11	+12	+11
305	3103	—	—	5.6	34 31	33 20.695	5.10	6	21	−14	+ 4	—	—	+ 4	—
—	3161	—	—	6.3	37 55	35 58.443	5.16	7	16	—	+81	—	—	—	—
333	3356	572	—	4.6	29 05	35 31.282	5.09	4	21	− 3	−12	−21	—	—	+ 6
384	3791	—	—	4.8	39 28	03 08 41.924	5.27	6	22	−16	−18	—	—	− 2	—
397	3923	—	—	5.4	43 53	15 05.301	5.31	6	20	27	−48	-	—	−14	—
440	4287	—	—	4.3	48 04	33 38.162	5.29	6	21	−67	−63	—	—	−37	−48
449	4387	—	—	5.6	37 27	38 31.186	5.31	5	20	− 8	−37	—	—	—	—
576	5359	—	2325	5.3	31 21	04 23 33.240	5.47	4	22	− 6	−38	—	+ 8	+30	—
606	5609	—	2338	4.5	41 11	33 54.765	5.45	5	22	+ 3	+27	—	− 7	− 4	—
643	5932	—	—	5.6	42 31	49 57.892	5.47	6	22	−33	−63	—	—	−11	—
661	6064	1060	—	5.0	37 50	56 32.229	5.49	6	21	+ 3	−12	−38	—	—	—
692	6311	1106	—	5.6	46 55	05 07 43.933	5.50	5	18	+ 6	−15	−49	—	+27	+20
719	6556	1145	2400	6.1	41 46	18 58.309	5.49	5	21	−37	−46	−50	−28	−33	—
—	6922	—	2417	6.0	47 41	32 14.514	5.51	6	20	—	− 6	—	−47	0	—
—	7066	1216	2425	6.0	31 20	38 00.487	5.49	4	21	—	−126	−27	−18	−11	—
857	7888	—	2470	6.0	32 42	06 09 42.865	5.55	6	19	−53	−124	—	+47	− 5	—
—	8082	1359	—	6.6	35 16	16 13.215	5.55	4	20	—	−48	− 4	—	− 2	—
—	8411	—	2496	6.0	46 43	27 03.715	5.55	6	20	—	−60	—	−22	− 2	—
—	8474	—	2500	5.6–6.2	32 29	29 50.567	5.55	6	20	—	−48	—	− 8	+ 6	—
931	8751	—	2517	5.2	44 34	40 10.372	5.55	5	20	−26	−44	—	−19	−20	−19
953	8931	1485	2527	5.0	41 50	47 56.316	5.55	5	20	−30	−46	−23	0	—	—
984	9405	1556	2549	6.5	33 54	07 05 35.943	5.53	4	18	+23	− 4	+14	+26	+ 9	—
1010	9769	—	2567	5.6	45 18	18 23.950	5.51	3	19	−25	−50	—	−25	−29	−25

APPENDIX 1 (Cont.)

KGC	Catalogue number			m	δ_{1960}	$\alpha_{1960.0}$	E_r 1960+	ε_α	n	C - KGC	C - GC	C - N30	C-$FK4_{supp}$	C - Suv	C - ITA
	GC	N 30	$FK4_{supp}$												
1052	10257	1723	2592	4.9	34 41	35 33.431	5.51	5	19	−28	−44	+ 5	+20	− 8	—
1064	10377	—	2599	5.3	50 32	41 02.780	5.51	5	19	− 8	−17	—	+ 5	−23	—
—	10579	—	—	6.0	33 20	48 28.243	5.51	5	19	—	−44	—	—	—	—
1116	11163	—	2641	5.6	29 47	08 10 40.308	5.49	5	17	− 6	−44	—	+28	− 2	+27
—	11534	—	2660	6.3	45 47	24 49.812	5.49	5	18	—	+ 8	—	− 3	−27	—
1170	12037	2040	2690	6.1	30 51	42 54.419	5.47	6	18	− 3	−22	+53	+66	+ 2	—
1180	12221	2079	2700	5.2	43 53	49 16.175	5.49	6	17	− 4	− 46	−40	−15	−16	−15
—	12341	—	2706	5.9	40 21	53 55.076	5.47	4	18	—	−12	—	−61	−29	—
1233	12799	2206	2738	5.7	46 59	09 14 50.676	5.47	6	17	−28	−47	−30	− 9	−12	− 9
1248	13051	—	2751	5.6	45 47	26 03.172	5.47	4	17	−11	+11	—	−40	−11	—
1271	13265	—	2765	5.7	31 21	34 20.711	5.47	5	17	−11	−39	—	0	−17	0
1283	13372	2314	2773	5.5	39 56	39 32.022	5.48	4	16	+11	0	− 7	+15	−14	+15
1323	13985	2425	2817	6.1	37 36	10 08 50.907	5.56	5	15	+38	+26	+33	+55	+ 8	—
—	14154	—	2827	6.2	48 36	16 58.183	5.58	4	14	—	−67	—	−50	—	—
—	14377	—	2838	6.5	45 25	26 12.336	5.62	9	13	—	+ 1	—	−51	—	−51
1384	14897	2559	2863	6.1	28 11	47 42.026	5.54	5	16	−22	−35	+16	+20	−16	—
1391	14974	2565	2870	4.8	43 24	51 41.039	5.54	5	16	−12	−16	−46	−21	—	−20
1440	15625	—	2908	5.1	43 42	11 20 38.212	5.62	4	17	−26	−43	—	−24	−36	−24
—	15857	—	2923	6.3	37 02	31 48.883	5.62	6	17	—	−14	—	−40	−51	—
1484	16199	—	—	5.8	35 09	47 37.170	5.62	4	17	−14	−25	—	—	−61	—
1534	16906	2862	2994	5.0	51 47	12 22 05.219	5.60	6	18	+16	− 1	− 3	+14	—	+14
1538	16964	2879	2999	4.6	28 29	24 56.724	5.60	7	18	− 7	−13	+16	+21	—	—
—	17231	—	3013	6.3	36 10	37 20.264	5.60	5	18	—	−39	—	−14	+ 7	—
1579	17430	—	—	5.9	37 44	48 16.764	5.60	3	18	+56	+ 48	—	—	−20	+68
1640	18171	—	—	5.9	46 14	13 24 33.710	5.68	6	18	+ 3	+ 1	—	—	− 7	—
—	18283	3086	—	6.2	42 19	29 31.660	5.68	5	18	—	−40	−12	—	—	—
1661	18421	3107	—	4.9	36 30	35 40.595	5.68	3	17	− 3	−28	+13	—	−23	—
1676	18636	3138	3094	5.6	38 45	45 16.215	5.61	5	18	− 6	−29	− 4	+13	—	—
1730	19345	3253	3136	6.3	30 37	14 18 23.661	5.71	4	21	+26	+19	+20	+25	+11	—
1738	19519	3279	3144	6.2	36 22	26 37.013	5.68	4	20	+24	+ 6	+38	+50	—	—
1750	19668	3305	3155	5.9	49 33	33 15.606	5.64	6	19	−38	−46	−27	−12	−36	−12
1763	19841	3330	3166	5.8	40 38	42 11.267	5.67	6	21	−16	−45	+ 2	+15	−15	+14
1811	20380	3418	3197	5.8	50 12	15 07 03.218	5.69	7	18	−37	−51	−22	− 6	−51	− 7
—	20651	—	—	5.9	44 35	19 18.734	5.67	6	20	—	+47	—	—	+14	—
1938	21800	—	—	5.7	36 32	16 10 20.179	5.70	4	21	− 3	−10	—	—	−10	—
1967	22108	—	3296	5.5	37 29	23 58.540	5.70	4	21	+17	+14	—	−14	+13	—
1972	22172	3690	3303	5.0	41 58	27 19.581	5.70	5	21	+ 6	− 2	+10	− 3	− 8	—
1983	22251	—	—	5.6	45 41	30 34.800	5.70	7	21	−13	−62	—	—	—	—
—	23229	—	—	6.0	49 47	17 10 38.886	5.70	4	21	—	−21	—	—	− 5	—
2061	23374	3855	—	4.8	37 20	16 17.351	5.69	6	19	−23	−37	+ 6	—	+17	+20
2073	23544	3878	—	4.5	37 11	22 18.013	5.71	3	20	−29	−31	− 2	—	−14	−19

APPENDIX 1 (Cont.) /80

Catalogue number															
KGC	GC	N 30	$FK4_{supp}$	m	δ_{1960}	$\alpha_{1960.0}$	E_r 1960+	ε_α	n	C - KGC	C - GC	C - N30	C-$FK4_{supp}$	C - Suv	C - ITA
2107	23879	3920	3397	5.8	30°49′	$17^h35^m05^s.307$	5.69	4	18	+ 6	− 6	+60	+68	+36	—
—	24067	—	3408	6.6	44 06	41 54.254	5.69	4	20	—	−29	—	−44	—	—
2187	24787	—	—	5.9	36 27	18 08 35.367	5.70	6	20	+ 3	− 2	—	—	—	—
—	24874	—	3451	5.9	38 46	11 44.637	5.70	5	18	—	+29	—	−93	−131	−92
2203	25085	4081	3458	5.1	49 05	20 31.120	5.70	6	18	−11	−34	−25	−17	—	—
2210	25137	4089	3463	5.0	39 29	22 54.616	5.70	6	18	−11	−18	− 6	+ 3	− 5	—
2221	25340	—	—	5.4	30 31	31 18.093	5.70	4	18	+14	+ 9	—	—	−11	—
2244	25643	—	—	5.5	31 53	42 21.317	5.70	4	18	+12	+12	—	—	−12	—
—	25757	4171	—	5.8	52 57	45 49.364	5.66	8	16	—	−78	−18	—	—	−16
2296	26181	—	—	5.1	46 53	19 00 18.398	5.71	8	17	+26	+20	—	—	+ 2	—
—	26690	—	3545	6.3	35 07	19 05.346	5.64	4	17	—	−13	—	−41	0	—
2383	27249	—	3575	5.0	45 26	39 36.066	5.64	7	17	−21	−69	—	+ 9	+ 1	+ 9
—	27401	—	—	5.7	25 17	46 02.500	5.64	4	17	—	−40	—	—	—	—
2409	27492	4391	3584	5.6	40 30	49 14.846	5.64	5	17	− 1	+ 6	−30	−40	− 3	—
2434	27724	4423	3599	5.2	36 56	58 27.073	5.64	4	17	+ 3	− 1	−14	− 4	+14	—
2513	28642	—	—	5.6	46 33	20 32 36.147	5.65	5	18	+ 4	− 8	—	—	−16	− 4
2553	29036	—	—	4.9	45 58	47 34.384	5.65	7	18	−42	−53	—	—	—	—
2563	29150	4626	—	4.7	44 14	51 49.747	5.65	5	18	+13	−10	+ 2	—	+ 7	+ 8
2629	30013	—	—	5.5	46 32	21 23 31.353	5.47	5	17	−27	−40	—	—	+60	−34
2664	30391	4786	3733	5.3	51 00	40 40.235	5.47	6	19	−15	−34	+12	+11	−23	+11
2758	31252	—	—	4.6	46 20	22 19 22.139	5.32	6	20	+ 4	−10	—	—	+ 3	− 9
—	31824	—	—	6.0	37 12	46 20.839	5.33	5	21	—	+85	—	—	—	—
2818	31896	—	—	5.2	43 06	50 13.510	5.33	6	19	+11	+ 1	—	—	+41	—
2838	32039	5058	3838	6.4	52 26	57 25.967	5.34	7	21	+54	+45	−42	− 4	+ 8	− 5
2864	32288	5098	3857	5.8	43 20	23 08 35.839	5.16	5	20	+ 6	+11	−28	−24	−54	−25
2879	32432	—	—	5.0	48 48	15 52.969	5.18	7	21	− 2	−12	—	—	+ 5	—
2903	3 703	—	—	5.3	39 01	29 19.136	5.16	7	22	+11	+ 6	—	—	+61	− 1
—	33063	—	3914	5.9	36 12	47 39.871	5.14	6	21	—	+48	—	−57	+ 6	—
—	33211	—	3923	6.0	42 26	55 01.431	5.18	7	22	—	+18	—	−76	− 3	—

NOTE 1. ε_α - the mean square error of the right ascensions of stars; n - number of observations.

2. Star 25757 was incorrectly determined as a program star.

CATALOGUE OF NORTHERN STARS

Number FK4	m	δ_{1960}	$\alpha_{1960.0}$	Er 1960+	ε_α	n	C−FK4	C−N 30
41	5.7	+79° 28′	01h08m44.s560	5.34	±30	46	— 51	— 68
Nb	2.1	89 05	55 41.331	5.42	303	45	−1.515	−1.554
173	6.0	75 52	04 43 25.019	5.56	19	41	— 89	−130
260	4.8	77 02	06 54 15.784	5.64	22	43	−105	−152
310	5.7	75 53	08 14 34.162	5.57	20	40	+ 22	— 42
395	5.0	75 55	10 31 44.754	5.39	29	36	— 60	−132
454	5.1	77 50	12 10 20.805	5.36	28	47	— 71	−101
550	2.2	74 19	14 50 47.813	5.44	22	47	−110	−138
590	4.3	77 55	15 45 26.449	5.49	27	48	−101	−147
675	5.0	76 58	17 51 14.135	5.66	25	45	— 26	— 78
734	6.0	79 31	19 24 08.134	5.50	34	32	−126	— 34
795	5.9	77 58	21 06 19.663	5.46	33	43	−158	−113
893	3.4	77 24	23 37 41.012	5.34	34	37	— 96	−122

APPENDIX 3

CATALOGUE OF EQUATORIAL STARS

FK 4	m	δ_{1960}	$\alpha_{1960.0}$	Er 1960+	ε_α	n	C−FK 4	C−N 30
1002	4.7	−05° 56′	00h03m17.s231	5.02	±4	26	— 3	+10
1022	4.9	−01 22	50 57.711	4.94	4	26	— 6	−15
36	4.4	+07 41	01 00 51.824	4.96	5	23	+ 2	— 9
1019	5.3	−03 53	40 42.034	5.06	3	24	0	0
60	4.5	+08 57	43 16.683	5.04	4	27	— 3	— 9
104	4.0	−09 03	02 54 28.305	5.20	4	25	+14	+ 4
107	2.8	+03 56	03 00 11.119	5.18	3	27	+ 7	— 6
149	3.2	−13 37	56 09.687	5.37	3	27	0	−14
1111	5.2	−01 40	59 30.256	5.39	3	26	— 3	— 19
1140	4.7	+15 21	05 02 16.857	5.50	2	26	+12	+ 5
188	2.9	−05 08	05 52.820	5.48	4	27	— 6	−26
1161	5.2	+00 33	56 46.066	5.52	4	26	−14	−22
230	5.7	+04 10	06 02 51.450	5.50	3	25	— 6	−23
1181	5.8	−08 21	58 28.369	5.54	4	22	+19	−21
271	4.1	−15 34	07 01 56.838	5.57	5	22	−14	−18
304	5.1	−03 34	57 44.214	5.48	4	22	+14	+12
(1097)	4.5	−06 14	08 00 11.066	5.52	3	22	(+2)	—
1235	5.8	−00 20	59 55.364	5.48	5	21	+21	+ 8
347	3.8	+02 29	09 12 17.061	5.42	4	19	−14	−11
378	4.9	+08 14	58 06.034	5.49	3	19	+14	+ 6
1261	4.7	−12 52	10 03 10.514	5.49	6	20	+16	+ 6
1284	5.0	+03 50	58 29.693	5.57	2	20	+ 4	−15
418	4.7	+07 33	11 02 57.127	5.54	2	19	+12	— 7
1311	4.6	+06 50	58 49.362	5.61	3	22	+ 4	— 6
450	5.3	+08 57	12 03 10.178	5.59	3	21	0	−10
484	3.7	+03 37	53 35.022	5.62	3	21	−10	−22
1336	5.9	−03 36	57 35.699	5.59	2	22	— 3	−15
1355	5.2	−08 30	13 39 30.516	5.60	4	19	+ 5	— 8
1357	5.7	−15 59	42 20.029	5.70	3	19	— 9	−36
1393	5.7	00 00	14 55 30.014	5.68	3	25	— 6	−11
1394	4.8—5.9	−08 22	58 49.835	5.66	3	26	−13	−31
1417	4.7	−14 10	15 55 56.694	5.68	4	25	−11	−21
1420	5.6	−08 18	58 37.814	5.68	3	26	−12	−23
633	3.4	+09 26	16 55 46.260	5.69	4	25	+14	+ 4
1445	5.0	−04 10	58 56.862	5.69	3	25	+18	+ 3
673	3.5	−09 46	17 56 49.349	5.70	3	24	— 7	−17
680	3.7	+09 33	18 05 27.080	5.70	3	23	+ 6	+ 6

FK 4	m	δ_{1960}	$\alpha_{1960.0}$	Er 1960+	n_α	n	C − FK 4	C − N 30
717	3.6	−04° 57′	19h04m07s.520	5.67	4	22	+ 8	− 7
1500	5.4	−08 00	10 30.497	5.68	4	21	0	−17
1524	5.6	+07 10	20 02 11.042	5.65	2	23	− 6	−10
756	3.4	−00 56	09 14.441	5.65	3	21	−12	−26
800	4.1	+05 05	21 13 49.432	5.57	2	23	−15	−20
1561	4.3	−17 00	20 01.236	5.56	4	21	−54	− 57
1580	6.4	−04 34	56 49.813	5.42	3	21	− 3	−20
827	3.2	−00 31	22 03 43.752	5.40	3	24	− 6	− 7
1602	4.6	+03 36	23 01 50.401	5.26	3	25	0	− 4
1603	4.7	+09 12	04 59.254	5.24	4	24	+ 2	−10
1630	4.7	−06 14	59 54.491	5.01	4	23	−13	−24

NOTE. Star 1097 is from the KGZ catalogue in the ITA System.

INVESTIGATION OF THE PIVOTS OF THE TASHKENT MERIDIAN CIRCLE

O. S. Tursunov

ABSTRACT. The pivots of the Tashkent meridian circle were investigated by two methods: 1) with an axial microscope-micrometer and 2) with a Type IKPV interferometer. The first method consists of mounting a glass plate marked with reference gaps separated by 2-3 microns on one of the pivots and measuring with a microscope-micrometer the change in position of the two geometrical axes of the instrument with respect to each other. By this means the deviation of the pivots from their ideal circular shape is determined. It was found that one of the pivots of the meridian circle has an ellipticity in its working cross section which causes most of the errors, namely, from $-0^{s}.042$ to $+0^{s}.042$ in azimuth, from $-0^{s}.018$ to $+0^{s}.019$ in the inclination of the axis, and from $-0^{s}.042$ to $+0^{s}.038$ in collimation. Because of the alignment of the "pits" on the pivots they had almost no effect on the results from the microscope-micrometer investigation.

The investigation using the Type IKPV contact interferometer is affected by the interaction of the interferometer probe with the pivot such that the presence of "pits" on the pivots results in strong distortion of the corrections determined at the points of interaction of the supports with the "pits". The interferometer results using flat and spherical probes agree well except at places where the "pits" are situated. A comparison of the interferometer results with the microscope-micrometer results reveals satisfactory agreement. An increase in the separation of the supports reduced the depth of the "pits" on the pivots from 5-7 microns to 1-2 microns, but the fact is that they still remained.

It was found that the corrections to the observed right ascensions of the stars in the Kyustner series for stars situated in ten-degree belts from -20° to +90° in declination agreed, upon reversal of their signs to give corrections to the instrument's system, with corrections found from the microscope-micrometer and interferometer investigations of the irregularities in the working cross sections of the instrument's pivots.

Investigations of the pivots of the Tashkent meridian circle were carried /83
out in 1955 by N. F. Bykov and Gun-Der Kim by Challis' method [1] and also in 1962 by I. N. Boroditskiy according to the modified Podobed method with the use

of an interferometer [2]. It is evident from these investigations that the pivots have sharply expressed "pits" in their working cross section which reach 5 to 7 microns. In February 1963 the supports of the instrument were extended by 10 mm, by which the transition to the new working cross sections was accomplished, i.e., to new pivots. The necessity of their investigation arose in connection with this and with the completion of the papers in the "Bright Stars" program.

Investigation of the pivots with an axial microscope-micrometer.

The method of investigation of the pivots with the aid of an axial microscope-micrometer by which the author was guided is expounded in the papers [1,3-5]. The essence of this method reduces to the determination of the positions with respect to height of the two geometrical axes of rotation of the instrument's tube; the first axis passes through the "center of gravity" of the working cross sections of the pivots and is fastened tightly to the physically-horizontal axis of the instrument, and the second is fixed relative to the supports. The position of the first geometrical axis changes relative to the second due to the incorrectness of the figure of the pivots. These variations can be displayed if one mounts a glass plate with a circular micromark on one of the pivots close to its center and illuminates it through the second pivot. The position of the micromark is measured with the aid of a microscope-micrometer for various positions of the instrument's tube in altitude. Thus one can investigate the deviations of the shape of the pivots from the circular.

To determine the inaccuracies of the pivots we introduce two systems of coordinates: a fixed one and a movable one. As the origin of both systems we take the center of gravity of the n positions of a point in the plane of the working cross section of the pivot. The directions of the axis of the fixed system of coordinates are the following: X is towards the southern point in the horizontal plane and Y is towards the zenith. The movable system of coordinates has its axes directed as follows: ξ is parallel to the projection of the optical axis of the instrument on the XY plane and the η axis is distant by an angle of 90° from the ξ axis in the direction of a positive angle of setting of the tube, which runs from the south point through the zenith, from 0° to 360°.

Upon setting the tube of the instrument at an angle h_i to the horizontal plane the position of the observed point is determined by the coordinates x_i, y_i, and the angle between the ξ and X axes is determined by the angle h_i.

The transformation formulas from the measured coordinates x_i, y_i to the ξ_i, η_i coordinates are:

$$\left.\begin{aligned}\xi_i &= x_i \cos h_i + y_i \sin h \\ \eta_i &= -x_i \sin h_i + y_i \cos h_i\end{aligned}\right\} \quad (1) \qquad /84$$

From the known ξ_i and η_i we find their average values, i.e.,

$$\xi_0 = \frac{1}{n}\sum_{i=0}^{i=n-1} \xi_i \text{ and } \eta_0 = \frac{1}{n}\sum_{i=0}^{i=n-1} \eta_i.$$

We have in the case of inaccurate pivots

$$\left.\begin{aligned}\Delta\xi_i &= \xi_i - \xi_0 \\ \Delta\eta_i &= \eta_i - \eta_0\end{aligned}\right\}, \quad (2)$$

where

$\Delta\xi_i$ and $\Delta\eta_i$ are small quantities of the order of the deviations of a pivot from a circular shape. They are also the coordinates of the center of the pivot.

We take the conditions

$$\left.\begin{aligned}\sum_{i=0}^{i=n-1} \Delta\xi_i = 0 \\ \sum_{i=0}^{i=n-1} \Delta\eta_i = 0\end{aligned}\right\} \quad (3)$$

for them in the ξ, η system.

Then the Eqs. (1) to (3) give

$$\left.\begin{aligned}\xi_0 &= \frac{1}{n}\sum_{i=0}^{i=n-1} x_i \cos h_i + \frac{1}{n}\sum_{i=0}^{i=n-1} y_i \sin h_i \\ \eta_0 &= -\frac{1}{n}\sum_{i=0}^{i=n-1} x_i \sin h_i + \frac{1}{n}\sum_{i=0}^{i=n-1} y_i \cos h_i\end{aligned}\right\} \quad (4)$$

From the measured x_i, y_i and the known h_i one can obtain by Eqs. (1) and (4) ξ_i, η_i and ξ_0 and η_0, and from them $\Delta\xi_i$ and $\Delta\eta_i$. Knowing the least mobile points, the centers of both the pivots at one and the same position of the instrument, and also the distance L between the working cross sections of the pivots, one can determine the corrections for the error in the pivots:

correction to collimation

$$\Delta\xi_{i,\,\theta} = \Delta\xi^{w}_{i,\,\theta} - \Delta\xi^{0}_{i,\,\theta}, \tag{5}$$

corrections to azimuth and slope of the instrument's axis

$$\left.\begin{aligned} \Delta x_{i,\,\theta} &= \Delta\xi_{i,\,\theta}\cos h_i - \Delta\eta_{i,\,\theta}\sin h_i \\ \Delta y_{i,\,\theta} &= \Delta\xi_{i,\,\theta}\sin h_i + \Delta\eta_{i,\,\theta}\cos h_i \end{aligned}\right\} \tag{6}$$

where the index θ corresponds to the position of the instrument's circle. The final corrections for inaccuracies in the figures of the pivots are determined from the equation

$$\Delta c_{i,\,\theta} = \varkappa\Delta\xi_{i,\,\theta} \tag{7}$$

or

$$\left.\begin{aligned} \Delta k_{i,\,\theta} &= \varkappa\Delta x_{i,\,\theta} \\ \Delta i_{i,\,\theta} &= \varkappa\Delta y_{i,\,\theta} \end{aligned}\right\} \tag{8}$$

here $\varkappa = \mu/15L \sin 1''$; μ is the value of a revolution of the screw of the microscope-micrometer in the same linear measure as L. /85

Axial microscope-micrometer and micromark. The choice of a micromark is the basic difficulty in the investigation of pivots by this method. This is complicated by the fact that for the reliable determination of a position of a micromark in a microscope with large magnification ($\sim$ 400 to 500 times) a circular mark whose diameter does not exceed 5 microns is suitable. There exist many different methods of obtaining such micromarks.

In our case, gaps in a polyethylene aluminized film representing circular objects of 2-3 microns were used. The film with the gaps was placed between two glasses in a specially prepared mounting which was set in the working cross section of the pivot. The glass plate nearest to the face of the pivot had a scale with divisions of 0.1 mm, which made it possible to determine the value of the screw revolutions.

The measuring apparatus consisted of a microscope-micrometer with two screws and a system for attaching it. We mounted the microscope-micrometer and the cases of the micrometer of the Repsold measuring device outside of the objective with the aid of three Duraloy tubes: one with a length of 815 mm and two with a length of 150 mm. The exterior diameter of the short tubes is equal to the interior diameter of the main one. An objective is braced in one of the short tubes and a micrometer case on the other. The presence of the objective tube and the tube with the micrometer case permits carrying out relatively easily focusing on the image of the micromark.

The microscope-micrometer was simply placed in a 1½-inch iron tube with a length of 760 mm with the help of four bolts positioned not far from its ends. At each end two bolts were fastened at opposite points of a diameter in the horizontal plane and two others in the vertical plane. With the help of these bolts the average position of the filament of the micrometer was set close to the center of the pivot's cross section. The iron tube was fastened at one end to the opening of the spurious supports, and at the other end, to the instrument's pier by brackets made of angle iron. Illumination of the micromark was carried out through the instrument's axis; therefore the prisms mounted for the axial illumination of the filaments of the ocular micrometer of the main tube of the instrument were removed in advance from the instrument chamber.

Measurement of the coordinates of the micromark and their accuracy.

In the investigation of the pivots by Challis' method it is important to have a stable mount for the microscope-micrometer, but it is difficult to obtain it because of the awkwardness of our set-up. Therefore we used a relative method of measurements of the micromark's coordinates [1]. With the help of a level of minute accuracy attached to the upper area of the micrometer case, the movable filament of its ocular reticle in the y coordinate was brought to a horizontal position. In addition, the observations of the level's bubble permitted exclusion of appreciable rotational motion of the microscope-micrometer, and its shifts had the nature of translational motion. Measurements of the coordinates of the mark were carried out by us with the relative method, the same as in the investigation of the pivots made in 1955, i.e., the coordinates of the micromark were measured at successive points situated around the circle: 0°, 10°, 0°, 20°, 0° ..., 0°, 350°, 0°;

in other words, the tying-in came for a position of the micromark at a circle reading of 0°.

The coordinates measured by three methods relative to the position of the mark when the circle reading was 0° are given in Appendix 1 in columns 2 to 4. N. F. Bykov called this system of readings the tie-in system. The coordinates /86
obtained relative to the center of gravity of 36 positions of the point are located in columns 5 to 7, and the average value of each coordinate from the three methods is given in the last column. The coordinates relative to the center of gravity are given in the main coordinate system XY. The average value of the coordinate x in Appendix 1 is referred to the western pivot in a "circle east" position of the instrument.

The numerical average values of the coordinates are presented in Appendix 2 and expressed in revolutions of the screws of the micrometer. The mean square error of a single determination of a coordinate was calculated from the equation

$$m_0 = \pm \sqrt{\frac{\Sigma v^2}{(s-1)n}}, \qquad (9)$$

where

v is the deviation of individual values of the coordinate x or y from their arithmetical average of the three methods;

s is the number of methods; and

n is the number of positions of the observed point in a single method.

Below are presented the values of the mean square error of a single determination of a coordinate at corresponding positions of the instrument, which do not exceed 0.24 microns:

Position of the instrument	Investigated pivot	$m_0(x)$	$m_0(y)$
Circle east	Western	$\pm 0^d.006$	$\pm 0^d.007$
	Eastern	±0.009	±0.010
Circle west	Western	±0.008	±0.007
	Eastern	±0.009	±0.010

Results of the investigations. To determine the corrections for irregularities of the pivots it is necessary to know the quantities Δx_i, Δy_i or $\Delta \xi_i$, which, if L and h_i are known, permits the calculation from Eqs. (1) to (8) of Δk, the correction to the azimuth, Δi, the correction to the slope, or

Δc, the correction to collimation. The average values of the coordinates x_i and y_i (Appendix 2), from which sinusoids of the first order were excluded beforehand, serve as the original data for their determination. The quantity $\varkappa$ is assumed to be equal to $0^s.447$.

In Table 1 are presented the final corrections for the irregularities of the pivots expressed in thousandths of a second of time. We also calculated the corrections for the irregularities of the pivots from the measurements of M. F. Bykov (Table 2). According to the data of Tables 1 and 2, similar corrections are obtained for the azimuth, the inclination of the axis, and the collimation of the Tashkent meridian circle due to the effect of irregularities of the figure of the pivots (Table 3).

Similar corrections are obtained as the average arithmetic value based on the determinations of both observers. The mean square error of a single determination of a similar correction for corresponding positions of the instrument is given below:

Position of the instrument	$m_0(\Delta k)$	$m_0(\Delta i)$	$m_0(\Delta c)$
Circle east	$\pm 0^s.006$	$\pm 0^s.004$	$\pm 0^s.005$
Circle west	± 0.004	± 0.003	± 0.003

The results of the investigations show that one of the pivots of the meridian circle has an ellipticity in its working cross section, which primarily causes large amounts of the errors: from $-0^s.042$ to $+0^s.042$ in azimuth, from $-0^s.018$ to $+0^s.019$ in the inclination of the axis, and from $-0^s.042$ to $0^s.038$ in collimation.

Investigation of the pivots with the aid of an interferometer. /87

Recently astronomers of domestic observatories have been applying the Type IKPV contact interferometer for the investigation of the pivots of instruments. In this regard, they are using the Moreau-Verbaandert [6-9] and the Podobed [2,10,11] methods, modifying them somewhat. The insufficiencies of the Moreau-Verbaandert method are noted in the papers [7,8]. The determination of the corrections by the Podobed method is associated with some difficulties in the preparation of the probe with a strictly specified angle of shear or in the modified version of this method, with the

TABLE 1

h	Circle reading		Circle east			Circle west		
	Circle east	Circle west	Δk	Δi	Δc	Δk	Δi	Δc
8°41′	140°	310°	—33	0	—33	—40	—15	—42
18 41	150	300	—28	— 3	—28	—32	+ 2	—29
28 41	160	290	—13	+ 4	— 9	—30	— 2	—27
38 41	170	280	+ 5	+13	+12	— 6	0	— 5
48 41	180	270	+14	+ 3	+11	— 4	— 3	— 5
58 41	190	260	+29	+ 2	+17	+ 7	+ 5	+ 9
68 41	200	250	+35	— 5	+ 8	+14	— 6	— 1
78 41	210	240	+25	— 8	— 3	+34	+ 2	+ 9
88 41	220	230	+40	— 9	— 8	+49	—15	—14
98 41	230	220	+36	— 5	—10	+38	+ 2	— 4
108 41	240	210	+27	— 3	—12	+27	+ 8	— 1
118 41	250	200	+18	+ 6	— 4	+28	+ 5	— 9
128 41	260	190	— 4	+ 5	+ 6	+18	+ 6	— 6
138 41	270	180	—21	+15	+26	+ 6	+ 1	— 4
148 41	280	170	—34	+11	+35	—15	+ 7	+17
158 41	290	160	—29	+ 5	+29	—20	+ 4	+20
168 41	300	150	—39	— 7	+37	—21	+ 3	+22
178 41	310	140	—41	—17	+41	—32	— 7	+32
188 41	320	130	—36	—13	+38	—37	— 6	+38
198 41	330	120	—20	+ 2	+18	—33	+ 1	+31
208 41	340	110	—11	+ 8	+ 6	—34	— 4	+32
218 41	350	100	0	+ 6	— 4	—21	— 4	+18
228 41	0	90	+21	+ 3	—16	—11	—11	+15
238 41	10	80	+25	+ 4	—16	+ 6	— 7	+ 3
248 41	20	70	+39	— 4	—10	+24	— 6	— 3
258 41	30	60	+39	— 3	— 5	+33	+ 1	— 7
268 41	40	50	+47	—13	+12	+47	— 9	+ 8
278 41	50	40	+30	—18	+23	+32	+ 6	— 1
288 41	60	30	+24	+13	— 4	+36	+10	+ 3
298 41	70	20	+ 4	+11	— 8	+34	+19	— 1
308 41	80	10	0	+12	— 9	+18	+ 9	+ 4
318 41	90	0	—27	+10	27	+ 4	+ 8	— 2
328 41	100	350	—30	— 2	—25	—10	+ 2	—10
338 41	110	340	— 15	— 2	—41	—26	— 7	—21
348 41	120	330	—43	— 5	—41	—26	— 2	—25
358 41	130	320	— 7	— 6	— 7	—45	—11	—45

very accurate adjustments of the interferometer between its positions by the angle specified earlier. On account of this, the corrections for the irregularities of the pivots determined by this method are not completely free from the effect of interaction of the probe with the pivot.

The removal of the interferometer beyond the working cross section also affects the sizes of the corrections. In the presence of "pits" on the pivots, the interferometer gives strongly distorted results for the corrections at the places of interaction of the supports with the "pits" of the pivots [2].

The method of investigating the pivots with the help of an interferometer which was applied by us is also not free of the effect of the interaction of the probe with the pivot. However, it is simple in practical application and

trouble-free both in the measurements and in the reduction. The simplified method expounded on above is taken as its basis. This method was proposed by N. F. Bykov, and worked out and described by the author. /88

We introduced in the plane of the working cross section of the pivot two coordinate systems fixed relative to the supports and with a common origin. The system of coordinates XY is the same as above, and the system of coordinates Z,T is rotated with respect to the first by an angle of 45°. The interferometer is set up in the direction of the Z and T axes. At these positions of the interferometer we would be measuring the diameter of the pivot situated between the support and the probe at specified positions of the tube altitude.

The radii of the pivot at the corresponding n positions of the tube in altitude are at one and the same position of the interferometer:

$$R_i = r_0 + \Delta r_i, \tag{10}$$

where

$i = 0.1..., n - 1$, and r_0 is the average value of R_i. The transfer to the tie-in system gives the system of equations:

$$R_i - r_0 - \Delta r_0 = \Delta r_i - \Delta r_0; \tag{11}$$

here Δr_i are the deviations of the corresponding radius with respect to the radius of the circle at the tube setting in altitude determined by a circle reading of 0°. This deviation is equal to half the difference of the readings of the interferometer at the corresponding i-th setting of the instrument on the circle and at the setting characterized by a reading of 0°. The condition /89

$$\Delta r_i = 0 \tag{12}$$

is fulfilled in the case of correct pivots. But since this condition is not fulfilled in practice, then the inequalities

$$\left.\begin{aligned} dz_i &= \Delta z_i - \Delta z_0 \\ dt_i &= \Delta t_i - \Delta t_0 \end{aligned}\right\}, \tag{13}$$

come in, where

$$\Delta z_0 = \frac{1}{n}\sum_{i=0}^{i=n-1} \Delta z_i \text{ and } \Delta t_0 = \frac{1}{n}\sum_{i=0}^{i=n-1} \Delta t_i.$$

TABLE 2

h	Circle reading		Circle east			Circle west		
	Circle east	Circle west	Δk	Δl	Δc	Δk	Δl	Δc
8°41′	140°	310°	−20	− 6	−21	−40	− 3	−40
18 41	150	300	−17	− 3	−17	−32	+ 5	−29
28 41	160	290	− 7	− 4	− 8	−30	+ 8	−22
38 41	170	280	+ 6	− 5	+ 2	−21	0	−16
48 41	180	270	+11	0	+ 7	− 9	+11	+ 2
58 41	190	260	+12	−11	− 3	+15	− 1	+ 7
68 41	200	250	+30	+ 1	+10	+29	+ 2	+12
78 41	210	240	+32	+ 5	+11	+34	− 2	+ 5
88 41	220	230	+32	− 7	− 6	+40	−20	−19
98 41	230	220	+22	− 1	− 4	+31	+ 2	− 3
108 41	240	210	+16	+ 1	− 4	+28	+20	+10
118 41	250	200	+14	+ 5	− 2	+24	+16	+ 3
128 41	260	190	− 7	+ 8	+11	+20	− 1	−13
138 41	270	180	−18	+ 2	+15	0	+ 7	+ 5
148 41	280	170	−16	− 2	+13	− 9	+ 2	+ 9
158°41′			−24	0	+22	−18	+ 5	+19
168 41	290°	160°	−25	0	+25	−27	+ 6	+28
178 41	300	150	−34	− 3	+31	−29	−20	+29
188 41	310	140	−27	− 4	+27	−32	−12	+33
198 41	320	130	−23	− 3	+23	−28	+ 4	+25
208 41	330	120	−12	+ 3	+ 9	−27	+ 2	+23
218 41	340	110	+ 6	+ 4	− 7	−11	+ 5	+ 5
228 41	350	100	+13	− 1	− 8	− 9	− 2	+ 7
238 41	0	90	+33	− 4	−14	0	− 1	+ 1
248 41	10	80	+29	+ 1	−11	+13	+ 6	−10
258 41	20	70	+40	+ 4	−12	+28	+ 4	− 9
268 41	30	60	+35	− 7	+ 6	+35	− 9	+ 8
278 41	40	50	+14	−12	+14	+24	+ 6	− 2
288 41	50	40	+ 7	− 3	+ 5	+33	+ 5	+ 6
298 41	60	30	0	+ 2	− 2	+51	+19	+ 8
308 41	70	20	− 3	+ 7	− 7	+24	+10	+ 7
318 41	80	10	−11	+ 4	−11	+ 7	+ 7	+ 1
328 41	90	0	−27	+ 8	−27	− 7	− 4	− 4
338 41	100	350	−24	+ 3	−23	−18	− 1	−17
348 41	110	340	−20	+10	−22	−34	− 3	−33
358 41	120	330	−30	− 1	−30	−38	−12	−38
	130	320						

TABLE 3

h	Circle reading		Circle east			Circle west		
	Circle east	Circle west	Δk	Δi	Δc	Δk	Δi	Δc
8°41′	140°	310′	−26	− 3	−27	−40	− 9	−41
18 41	150	300	−22	− 3	−22	− 32	+ 4	−29
28 41	160	290	−10	0	− 8	−30	+ 3	- 24
38 41	170	280	+ 6	+ 4	+ 7	−14	0	−10
48 41	180	270	+12	+ 2	+ 9	− 6	+ 4	− 2
58 41	190	260	+20	− 4	+ 7	+11	+ 2	+ 8
68 41	200	250	+32	− 2	+ 9	+21	− 2	+ 6
78 41	210	240	+28	− 2	− 4	+34	0	+ 7
88 41	220	230	+36	− 8	− 7	+44	−18	−16
98 41	230	220	+29	− 3	− 7	+34	+ 2	− 4
108 41	240	210	+22	− 1	− 8	+28	+14	+ 5
118 41	250	200	+16	+ 6	− 3	+26	+10	− 3
128 41	260	190	− 6	+ 6	+ 8	+19	+ 2	−10
138 41	270	180	−20	+ 8	+20	+ 3	+ 4	0
148 41	280	170	−25	+ 4	+24	−12	+ 4	+13
158 41	290	160	−26	+ 2	+26	−19	+ 4	+20
168 41	300	150	−32	− 4	+31	−24	+ 4	+25
178 41	310	140	−38	−10	+38	−30	−14	+30
188 41	320	130	−32	− 8	+32	−34	− 9	+36
198 41	330	120	−22	0	+20	−30	+ 2	+28
208 41	340	110	−12	+ 6	+ 8	−30	− 1	+28
218 41	350	100	+ 3	+ 5	− 6	−16	0	+12
228 41	0	90	+17	+ 1	−12	−10	− 6	+11
238 41	10	80	+29	0	−15	+ 3	− 4	+ 2
248 41	20	70	+34	− 2	−10	+18	0	− 6
258 41	30	60	+40	0	− 8	+30	+ 2	− 8
268 41	40	50	+41	−10	+ 9	+41	− 9	+ 8
278 41	50	40	+22	−15	+18	+28	+ 6	− 2
288 41	60	30	+16	+ 5	0	+34	+ 8	+ 4
298 41	70	20	+ 2	+ 6	− 5	+42	+19	+ 4
308 41	80	10	− 2	+10	− 8	+21	+10	+ 6
318 41	90	0	−19	+ 7	−19	+ 6	+ 8	0
328 41	100	350	−28	+ 3	−26	− 8	− 1	− 7
338 41	110	340	−34	0	−32	−22	− 4	−19
348 41	120	330	−32	+ 2	−32	−30	− 2	−29
358 41	130	320	−18	− 8	−18	−42	−12	42

The coordinates Δz_0 and Δt_0 determine the center of gravity of the figure of the working cross section of a pivot in the ZT system. In order to obtain /90 the smallest shifts of the center of the pivot in the ZT system of coordinates, the conditions

$$\left.\begin{aligned}\sum_{i=0}^{i=n-1} dz_i &= 0\\ \sum_{i=0}^{i=n-1} dt_i &= 0\end{aligned}\right\} \tag{14}$$

should be fulfilled. It is easy to transform from the ZT system of coordinates to the XY system of coordinates, using the equations for rotation of the axes by an angle α

$$\left.\begin{aligned}\Delta x_i &= dz_i \cos\alpha - dt_i \sin\alpha\\ \Delta y_i &= dz_i \sin\alpha + dt_i \cos\alpha\end{aligned}\right\}. \tag{15}$$

Then Δx_i and Δy_i determine the least shifts of the center of the pivot in the fundamental system of coordinates X,Y. Knowing Δx_i and Δy_i for both pivots at one and the same position of the instrument and the distance between the working cross sections of the pivots L one can determine the effect of the irregularities of the pivots on the azimuth and on the slope of the instrument's axis from the equations

$$\left.\begin{aligned}\Delta x_{i,\theta} &= \left(dz^w_{i,\theta} - dz^0_{i,\theta}\right)\cos\alpha - \left(dt^w_{i,\theta} - dt^0_{i,\theta}\right)\sin\alpha\\ \Delta y_{i,\theta} &= \left(dz^w_{i,\theta} - dz^0_{i,\theta}\right)\sin\alpha + \left(dt^w_{i,\theta} - dt^0_{i,\theta}\right)\cos\alpha\end{aligned}\right\}. \tag{16}$$

To obtain the corrections for collimation we use the equation

$$dc_{i,\theta} = \Delta x_{i,\theta}\cos h_i + \Delta y_{i,\theta}\sin h_i. \tag{17}$$

Since the angle between the two systems of coordinates is $\alpha = 45°$, then the Eqs. (15) are simplified and take the form

$$\left.\begin{aligned}\Delta x_i &= \frac{\sqrt{2}}{2}\left(dz_i - dt_i\right)\\ \Delta y_i &= \frac{\sqrt{2}}{2}\left(dz_i + dt_i\right)\end{aligned}\right\}. \tag{18}$$

Eqs. (18) can be considered as operating at one and the same value of a division of the interferometer. The final equations for calculation of

the corrections for the pivot irregularities are:

$$\left.\begin{aligned}\Delta k_{i,\,\theta} &= \varkappa\left[\left(dz^{w}_{i,\,\theta} - dz^{0}_{i,\,\theta}\right) - \left(dt^{w}_{i,\,\theta} - dt^{0}_{i,\,\theta}\right)\right]\\ \Delta i_{i,\,\theta} &= \varkappa\left[\left(dz^{w}_{i,\,\theta} - dz^{0}_{i,\,\theta}\right) + \left(dt^{w}_{i,\,\theta} - dt^{0}_{i,\,\theta}\right)\right]\end{aligned}\right\} \qquad (19)$$

or

$$\Delta c_{i,\,\theta} = \varkappa dc_{i,\,\theta}, \qquad (20)$$

where $\varkappa = \frac{\mu}{15\sqrt{2}L\sin 1''}$; L is the distance between the working cross sections of the pivots; and μ is the value of a division of the interferometer in the same linear measure as L.

Interferometer set-up, the measurements, and their accuracy.

The measurements were carried out with a contact interferometer of the IKPV system whose description can be found in [10]. To attach the interferometer we used a channel bar screwed onto the metal pedestal which supports the circles /91 of the reading micrometer. Two rack devices from a biological microscope were attached to the channel bar. The circles of the reading microscopes were removed during the investigation of the pivots. The rack devices were mounted on the channel bar in such a way that their translational motion agreed with the direction to the center of the pivot and the center of the support, i.e., the interferometer's probe, the center of the working cross section of the pivot, and the center of the support should be situated on a single straight line.

Prior to working, the interferometer, which was installed in a tube of the rack device, was attached with a bolt. The rack device permitted the smooth raising and lowering of the interferometer with the probe. After contact of the probe with the pivot the rack device was attached with a locking bolt. One could judge as to the reliability of the interferometer attachment from the condition of the interference fringes.

Upon working with the interferometer the lines of the spectrum did not oscillate relative to the scale. The zero point varied in time due to temperature and mechanical effects on the mounting, but the relative method excluded it completely. The reading of the interferometer scale was carried out at positions of the instrument's tube set in altitude through a 10° rotation to this and the other side. Differences in the readings of the direct and reverse runs

were not detected. The relative method of measurements also excludes the error in closing the cycle.

The value of a division of the interferometer was equal to 0.1 or 0.2 micron for a flat probe and 0.2 micron for a spherical one, and it was controlled during the process of observing (it was determined before and after the measurements). A flat jeweled tip with a diameter of 5 mm and a spherical tip with a diameter of 3 mm and a radius with a curvature of 14 mm were used as probes.

The average values of the corresponding coordinates in microns found by the three methods of measurement of the interferometer scale using a flat probe are given in Appendix 5.

The measurements were carried out by two methods with the spherical probe located at the middle of the working cross section. The average values of the corresponding coordinates in microns obtained with the spherical probe of the interferometer are given in Appendix 6. The error of a single measurement in this method for the flat and the spherical probes are identical on the average and equal to ±0.03 micron. The errors of a single measurement of the coordinates of the center of gravity of the cross section of the pivots with the interferometer at two settings and also at corresponding positions of the instrument and the investigated pivot are given in Table 4.

A sinusoid of the first power in h_i could appear in the measured coordinates of the center of gravity, which should not be due to irregularities of the pivots. In our interferometer set-up, the value of the amplitude of the first harmonic was so small that practically no perceptible effect on the results appeared. The amplitudes obtained by us for the first harmonics are given in Table 5.

The corrections for the irregularities of the pivots to the azimuth, inclination of the axis, and collimation of the instrument obtained with the use of the flat and the spherical interferometer probes in thousandths of a second of time are given in Tables 6 and 7. Comparing the corresponding corrections of these tables among each other, one notices good agreement of the results; the discrepancies arise mainly at places where the "pits" are situated.

The combined corrections for the pivot irregularities of the instrument obtained from the data of Tables 6 and 7 are given in Table 8. The square

TABLE 4

/92

Diameter of the interferometer's probe	Position of the instrument	Investigated pivot	$m_0(Z)$ microns	$m_0(T)$ microns
5 mm	Circle east	Western	±0.030	±0.021
		Eastern	±0.039	±0.027
	Circle west	Western	±0.025	±0.030
		Eastern	±0.036	±0.025
3 mm	Circle east	Western	±0.029	±0.019
		Eastern	±0.033	±0.029
	Circle west	Western	±0.032	±0.015
		Eastern	±0.033	±0.042

TABLE 5

Diameter of the interferometer's probe	Position of the instrument	Investigated pivot	Amplitudes of the first harmonics	
			Along the Z-axis	Along the T-axis
5 mm, flat	Circle east	Western	0.07	0.06
		Eastern	0.11	0.03
	Circle west	Western	0.03	0.07
		Eastern	0.02	0.04
3 mm, spherical	Circle east	Western	0.04	0.04
		Eastern	0.03	0.11
	Circle west	Western	0.03	0.06
		Eastern	0.02	0.01

TABLE 6

h	Circle reading		Circle east			Circle west		
	Circle east	Circle west	Δk	Δi	Δc	Δk	Δi	Δc
8°41′	140°	310°	−28	−22	−31	−41	−26	−44
18 41	150	300	− 9	− 8	−10	−30	− 5	−30
28 41	160	290	− 9	− 3	− 9	−20	− 1	−17
38 41	170	280	+ 2	− 2	0	−10	0	− 8
48 41	180	270	+12	0	+ 8	− 1	+ 2	+ 1
58 41	190	260	+19	+ 2	+12	+ 8	+ 2	+ 6
68 41	200	250	+22	+ 5	+13	+ 1	+ 6	+ 6
78 41	210	240	+18	+13	+16	+25	+ 1	+ 6
88 41	220	230	+51	−14	−13	+60	−20	−19
98 41	230	220	− 3	−24	−23	− 1	−24	−24
108 41	240	210	+12	+ 4	0	+17	+ 1	− 4
118 41	250	200	+ 8	+ 7	+ 2	+18	+11	+ 1
128 41	260	190	− 3	+ 6	+ 7	+10	+11	+ 2
138 41	270	180	−12	+ 7	+14	+ 3	+13	+ 6
148 41	280	170	−18	+ 8	+20	− 4	+14	+11
158 41	290	160	−22	+ 8	+23	−16	+14	+20
168 41	300	150	−34	+19	+37	−12	+11	+14
178 41	310	140	− 7	− 8	+ 7	+ 1	−11	− 1
188 41	320	130	−38	−22	+41	−51	−25	+54
198 41	330	120	−18	− 1	+17	−27	0	+26
208 41	340	110	− 8	+ 3	+ 6	−20	+ 8	+14
218 41	350	100	+ 3	+ 2	− 4	−12	+ 3	+ 7
228 41	0	90	+12	0	− 8	− 3	− 2	0
238 41	10	80	+19	+ 2	−11	+ 8	+ 1	− 5
248 41	20	70	+30	− 2	− 9	+18	+ 7	−13
258 41	30	60	+25	+ 4	− 1	+26	− 3	− 2
268 41	40	50	+58	−15	+14	+58	−19	+16
278 41	50	40	+11	− 6	+14	+11	−10	+12
288 41	60	30	+ 4	− 6	+ 6	+14	− 2	+ 6
298 41	70	20	+ 8	+ 8	− 3	+20	+10	+ 1
308 41	80	10	− 1	+ 6	− 5	+11	+ 9	0
318°41′	90°	0°	−10	+10	−13	+ 2	+ 8	− 4
328 41	00	350	−15	+ 8	−17	0	+ 8	− 4
338 41	110	340	−22	+ 5	−22	−18	+ 6	−19
348 41	120	330	−41	+16	−43	−27	+10	−28
358 41	130	320	0	− 1	0	− 4	−17	− 4

TABLE 7

h	Circle reading of the instrument		Circle east			Circle west		
	Circle east	Circle west	Δk	Δi	Δc	Δk	Δi	Δc
8°41′	140°	310°	−31	−25	−34	−34	−18	−36
18 41	150	300	−17	− 6	−18	−20	− 7	−21
28 41	160	290	− 8	− 6	−10	−15	− 4	−15
38 41	170	280	+ 4	− 6	− 1	− 7	− 3	− 7
48 41	180	270	+13	− 6	+ 4	+ 1	− 3	− 2
58 41	190	260	+17	− 1	+ 8	+10	− 5	+ 1
68 41	200	250	+20	+ 2	+ 9	+19	+ 5	+12
78 41	210	240	+21	+10	+14	+13	+ 7	+ 9
88 41	220	230	+33	− 4	− 3	+29	0	+ 1
98 41	230	220	+23	− 2	− 5	+27	− 5	− 9
108 41	240	210	+13	0	− 4	+22	0	− 7
118 41	250	200	+14	+ 6	+ 1	+22	+ 3	− 8
128 41	260	190	+ 3	+ 8	+ 4	+13	+ 5	− 4
138 41	270	180	− 7	+ 6	+ 9	+ 7	+ 6	− 1
148 41	280	170	−13	+ 5	+14	− 3	+ 4	+ 5
158 41	290	160	−18	+ 6	+19	−13	+ 3	+13
168 41	300	150	−35	+18	+38	−32	+18	+35
178 41	310	140	−21	0	+21	−26	+ 6	+26
188 41	320	130	−31	−23	+34	−27	− 5	+27
198 41	330	120	−17	− 3	+17	−28	− 8	+29
208 41	340	110	− 5	− 2	+ 5	−16	− 6	+17
218 41	350	100	+ 2	− 5	+ 2	−10	− 8	+13
228 41	0	90	+11	− 7	− 2	0	− 7	+ 5
238 41	10	80	+18	− 6	− 4	+ 9	− 8	+ 2
248 41	20	70	+21	− 1	− 7	+14	− 1	− 4
258 41	30	60	+15	+ 8	−11	+12	+10	−12
268 41	40	50	+33	− 9	+ 8	+28	+ 2	− 3
278 41	50	40	+24	− 2	+ 7	+23	− 3	+ 6
288 41	60	30	+15	− 8	+12	+20	− 4	+10
298 41	70	20	+12	+ 6	+ 1	+22	+ 5	+ 6
308 41	80	10	+ 3	+ 8	− 4	+13	+ 5	+ 4
318 41	90	0	− 7	+ 8	−11	+ 5	+ 4	+ 1
328 41	100	350	−15	+ 6	−16	− 4	0	− 5
338 41	110	340	−23	+ 6	−24	−12	− 1	−11
348 41	120	330	−40	+19	−43	−34	+15	−36
358 41	130	320	−28	− 4	−28	−26	+ 9	−26

TABLE 8

/94

h	Circle reading		Circle east			Circle west		
	Circle east	Circle west	Δk	Δi	Δc	Δk	Δi	Δc
8°41′	140°	310′	−30	−24	−32	−38	−22	−40
18 41	150	300	−13	− 7	−14	−25	− 6	−26
28 41	160	290	− 8	− 4	−10	−18	− 2	−16
38 41	170	280	+ 3	− 4	0	− 8	− 2	− 8
48 41	180	270	+12	− 3	+ 6	0	0	0
58°41°	190°	260°	+18	0	+10	+ 9	− 2	+ 4
68 41	200	250	+21	+ 4	+11	+10	+ 6	+ 9
78 41	210	240	+20	+12	+15	+19	+ 4	+ 8
88 41	220	230	+42	− 9	− 8	+44	−10	− 9
98 41	230	220	+10	−13	−14	+13	−14	−16
108 41	240	210	+12	+ 2	− 2	+20	0	− 6
118 41	250	200	+11	+ 6	+ 2	+20	+ 7	− 4
128 41	260	190	0	+ 7	+ 6	+12	+ 8	+ 1
138 41	270	180	−10	+ 6	+12	+ 5	+10	+ 2
148 41	280	170	−16	+ 6	+17	− 4	+ 9	+ 8
158 41	290	160	−20	+ 7	+21	−14	+ 8	+16
168 41	300	150	−34	+18	+38	−22	+14	+24
178 41	310	140	−14	− 4	+14	−12	− 2	+12
188 41	320	130	−34	−22	+38	−39	−15	+40
198 41	330	120	−18	− 2	+17	−28	− 4	+28
208 41	340	110	− 6	0	+ 6	−18	+ 1	+16
218 41	350	100	− 1	− 2	− 1	−11	− 2	+10
228 41	0	90	+12	− 4	− 5	− 2	− 2	+ 2
238 41	10	80	+18	− 2	− 8	+ 8	− 4	− 2
248 41	20	70	+26	− 2	− 8	+16	+ 3	− 8
258 41	30	60	+20	+ 6	− 6	+19	+ 3	− 7
268 41	40	50	+46	−12	+11	+43	− 8	+ 6
278 41	50	40	+18	− 4	+10	+17	− 6	+ 9
288 41	60	30	+10	− 7	+ 9	+17	− 3	+ 8
298 41	70	20	+10	+ 7	− 1	+21	+ 8	+ 4
308 41	80	10	+ 1	+ 7	− 4	+12	+ 7	+ 2
318 41	90	0	− 8	+ 9	−12	+ 4	+ 6	− 2
328 41	100	350	−15	+ 7	−16	− 2	+ 4	− 4
338 41	110	340	−22	+ 6	−23	−15	+ 2	−15
348 41	120	330	−40	+18	−43	−30	+12	−32
358 41	130	320	−14	− 8	−14	−15	− 4	−15

TABLE 9

h	Circle reading		Circle east			Circle west		
	Circle east	Circle west	Δk	Δl	Δc	Δk	Δl	Δc
8°41′	140°	310°	−28	−14	−30	−39	−16	−40
18 41	150	300	−18	− 5	−18	−28	− 1	−28
28 41	160	290	− 9	− 2	− 9	−24	0	−20
38 41	170	280	+ 4	0	+ 4	−11	− 1	− 9
48 41	180	270	+12	0	+ 8	− 3	+ 2	− 1
58 41	190	260	+19	− 2	+ 8	+10	0	+ 6
68 41	200	250	+26	+ 1	+10	+16	+ 2	+ 8
78 41	210	240	+24	+ 5	+ 5	+26	+ 2	+ 8
88 41	220	230	+39	− 8	− 8	+44	−14	−12
98 41	230	220	+20	− 8	−10	+24	− 6	−10
108 41	240	210	+17	0	− 5	+24	+ 7	0
118 41	250	200	+14	+ 6	0	+23	+ 8	− 4
128 41	260	190	− 3	+ 6	+ 7	+16	+ 5	− 6
138 41	270	180	−15	+ 7	+16	+ 4	+ 7	+ 1
148 41	280	170	−20	+ 5	+20	− 8	+ 6	+10
158 41	290	160	−23	+ 4	+24	−16	+ 6	+18
168 41	300	150	−33	+ 7	+34	−23	+ 9	+24
178 41	310	140	−26	− 7	+26	−21	− 8	+21
188 41	320	130	−33	−15	+35	−36	−12	+38
198 41	330	120	−20	− 1	+18	−29	− 1	+28
208°41′	340°	110°	− 9	+ 3	+ 7	−24	0	+22
218 41	350	100	+ 1	+ 2	− 4	−14	− 1	+11
228 41	0	90	+14	− 2	− 8	− 6	− 4	+ 6
238 41	10	80	+24	− 1	−12	+ 6	− 4	0
248 41	20	70	+30	− 2	− 9	+17	+ 2	− 7
258 41	30	60	+30	+ 3	− 7	+24	+ 2	− 8
268 41	40	50	+44	−11	+10	+42	− 8	+ 7
278 41	50	40	+20	−10	+14	+22	0	+ 4
288 41	60	30	+13	− 1	+ 4	+26	+ 2	+ 6
298 41	70	20	+ 6	+ 6	− 3	+32	+14	+ 4
308 41	80	10	0	+ 8	− 6	+16	+ 8	+ 4
318 41	90	0	−14	+ 8	−16	+ 5	+ 7	− 1
328 41	100	350	−22	+ 5	−21	− 5	+ 2	− 6
338 41	110	340	−28	+ 3	−28	−18	− 1	−17
348 41	120	330	−36	+10	−38	−30	+ 5	−30
358 41	130	320	−16	− 8	−16	−28	− 6	−28

error of a single determination of these corrections is as follows:

Position of the instrument	$m_0(\Delta k)$	$m_0(\Delta i)$	$m_0(\Delta c)$
Circle east	$\pm 0^s.007$	$\pm 0^s.003$	$\pm 0^s.005$
Circle west	± 0.009	± 0.009	± 0.008

/95

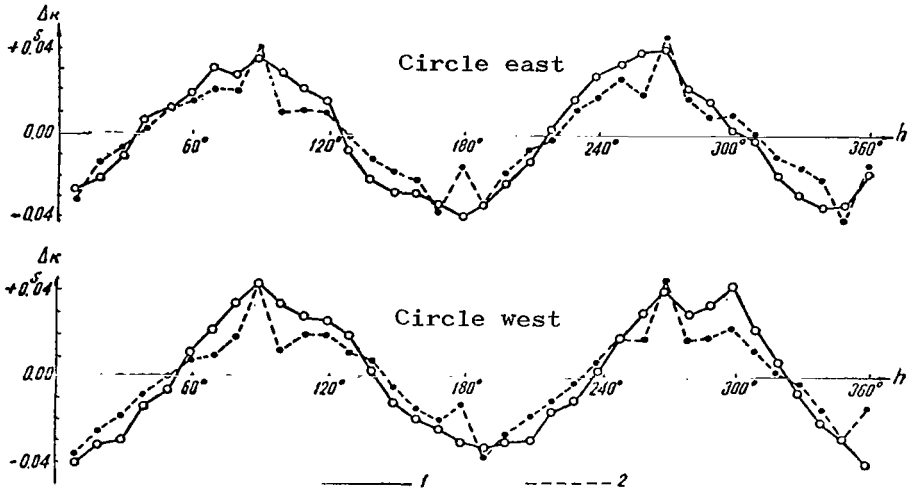

Figure 1. Corrections for irregularities in the pivot figures to the instrument's azimuth obtained during the investigation with the microscope-micrometer (1) and with the interferometer (2).

Comparison of the results of the investigation. Comparing the values of the corrections among themselves which were obtained with the microscope-micrometer and with the interferometer, one comes to the conclusion that their values are in completely satisfactory agreement.

The correction for the irregularity of the figure of the pivots obtained as the arithmetic average based on the values of the corrections of Table 3 and 8 are given in Table 9. The mean square error of a single determination of this correction is given below:

/96

Position of the instrument	$m_0(\Delta k)$	$m_0(\Delta i)$	$m_0(\Delta c)$
Circle east	$\pm 0^s.004$	$\pm 0^s.004$	$\pm 0^s.004$
Circle west	± 0.005	± 0.004	± 0.004

These corrections are presented in Figures 1 to 3.

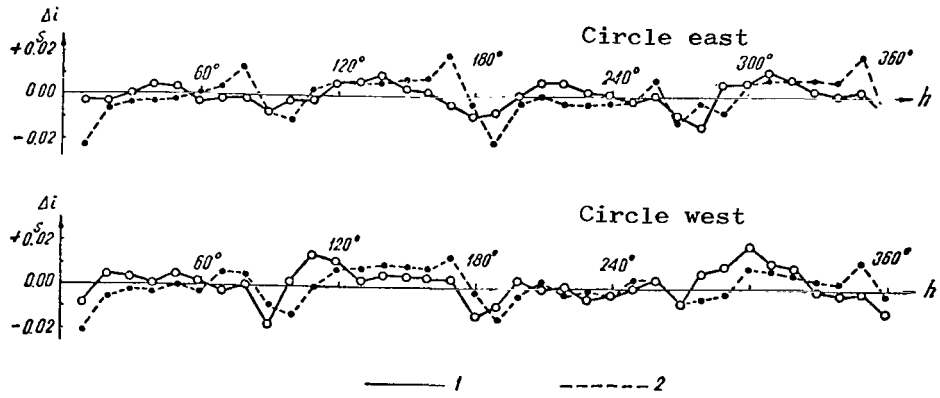

Figure 2. Corrections for irregularities in the pivot figures to the inclination of the instrument's axis obtained from the investigation with the microscope-micrometer (1) and with the interferometer (2).

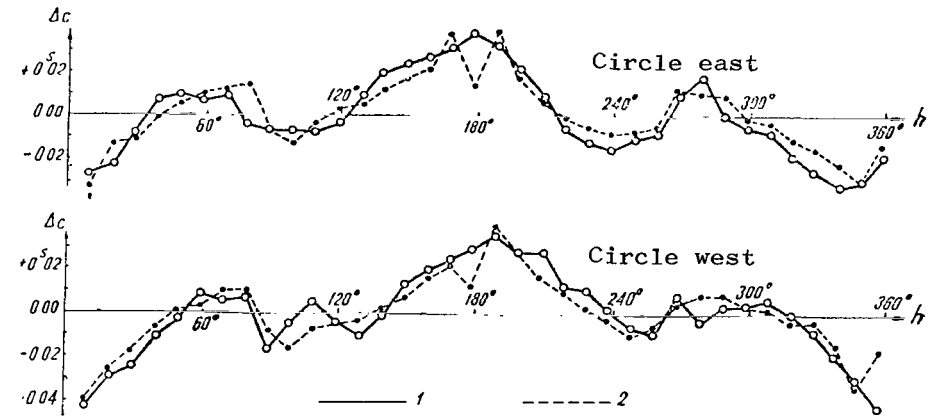

Figure 3. Corrections for irregularities in the pivot figures to the instrument's collimation obtained from the investigation with the microscope-micrometer (1) and with the interferometer (2).

A comparison of the results of the 1965 and 1967 investigations by the Challis method and the results of 1962 and 1967 using an interferometer shows that the ellipticity of the working cross section of one pivot of the Tashkent meridian circle primarily affects the corrections for irregularities of the figure. The difference of the semiaxes of the cross section of this pivot reach 2.8 microns.

The differences in the results of the investigation by the Challis method are given in Appendices 3 and 4; the values of the corrections of the 1967 investigation are presented for intervals of 15° by a linear interpolation. /97 These differences show satisfactory agreement, notwithstanding the fact that the investigations refer to different working cross sections of the pivot. Because of the alignment of the "pits" they have almost no effect on the results of the investigations using the micrometer, which is quite evident in Figures 4 to 6.

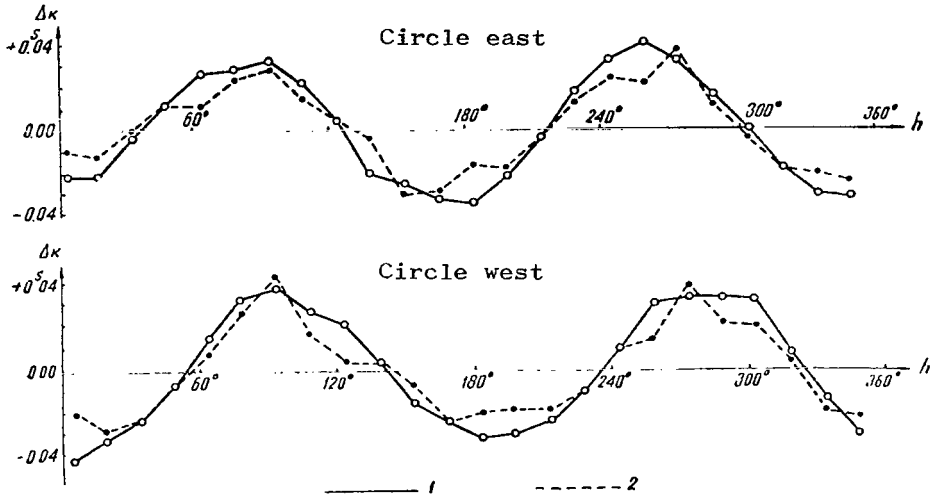

Figure 4. Corrections for irregularities in the pivot figures to the instrument's azimuth obtained from the investigation with the microscope-micrometer in 1955 (2) and 1967 (1).

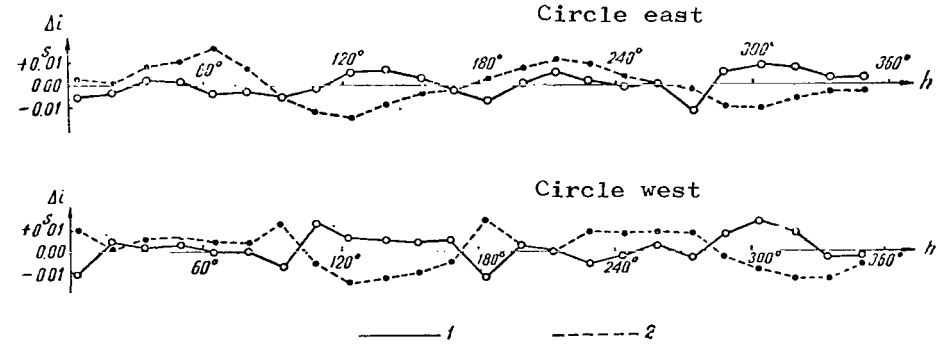

Figure 5. Corrections for irregularities in the pivot figures to the inclination of the instrument's axis obtained from the investigation with the microscope-micrometer in 1955 (2) and 1967 (1).

The differences in the results of the investigation obtained with the interferometer are presented in Appendices 7 and 8. These differences are taken from the 1967 investigations completed by the method described above and the 1962 investigation completed by the modified Podobed method. The agreement of the results of the investigation using the interferometer is somewhat worse than the investigations carried out with the microscope-micrometer. In using the interferometer the "pits" are not excluded from the results. It is evident from Appendices 7 and 8 that in the presence of "pits" on the pivots the interferometer distorts the results of the observations at least at 8 points of the 36, since trouble spots comprised an interval of arc of the circle greater than 20°. /98

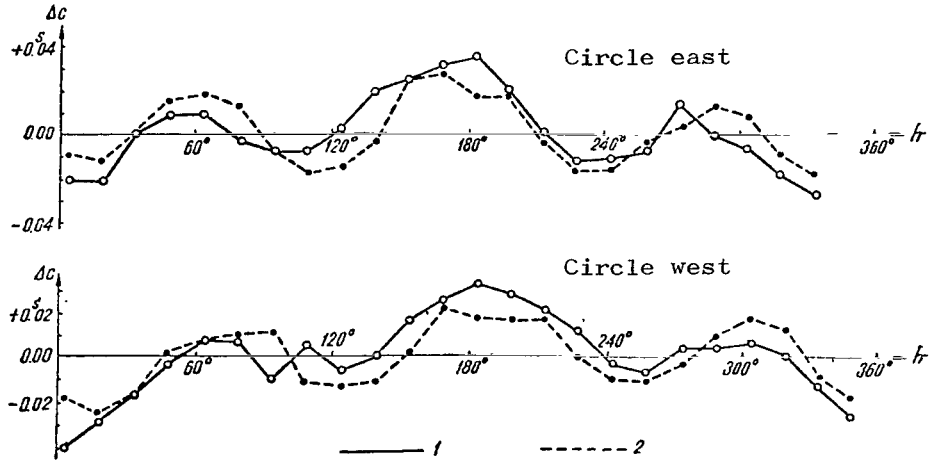

Figure 6. Corrections for irregularities in the pivot figures to the instrument's collimation obtained from the investigation with the microscope-micrometer in 1955 (2) and 1967 (1).

In spite of the separation of the supports, the "pits" remained on the pivots, but their depth decreased from 5-7 to 1-2 microns. These "pits" on the working cross section were evidently formed by the superposed level where it hangs on the instrument's axis. The curves of the corrections for pivot irregularities obtained from the investigations with the interferometer are presented in Figures 7 to 9.

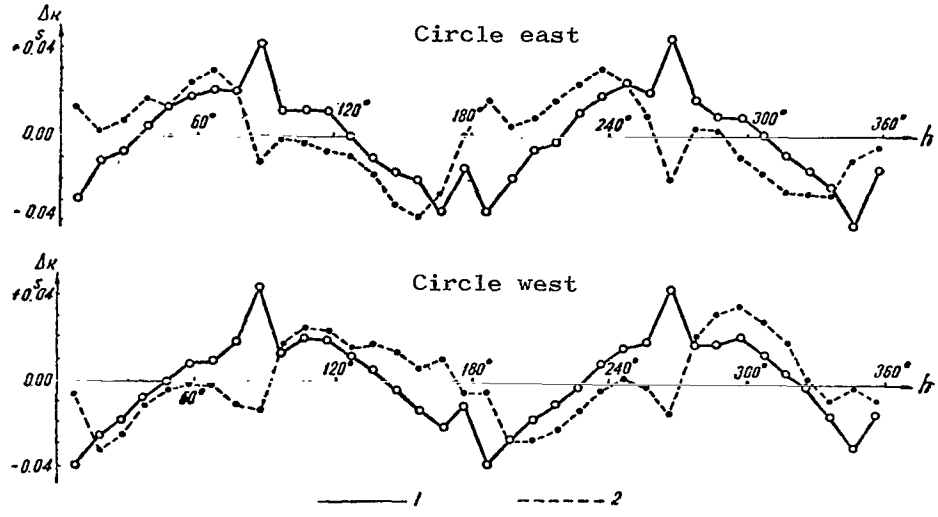

Figure 7. Corrections for irregularities of the pivot figures to the instrument's azimuth obtained from the investigation with the interferometer in 1962 (2) and 1967 (1).

In the observation of stars based on the program of the "Bright Stars" catalogue the Kyustner series [13] were observed in right ascension. As a result the errors $\Delta\alpha_\delta \cos\delta$ were obtained for the stars situated in ten-degree belts from -20° to + 90° in declination. Having changed the signs of $\Delta\alpha_\delta \cos\delta$ to the reverse, they obtained corrections for the instrument's system and compared them with the corrections for irregularity in the figure of the pivots from the investigations carried out with the microscope-micrometer and with the interferometer. The corrections for the system of the instrument obtained as a result of observations of the stars and the average final corrections to the collimation obtained at both positions of the instrument are presented in Table 10. /99

These results attest to the satisfactory agreement of the corrections of the type $\Delta\alpha^\delta \cos\delta$ with the corrections for irregularities of the pivots.

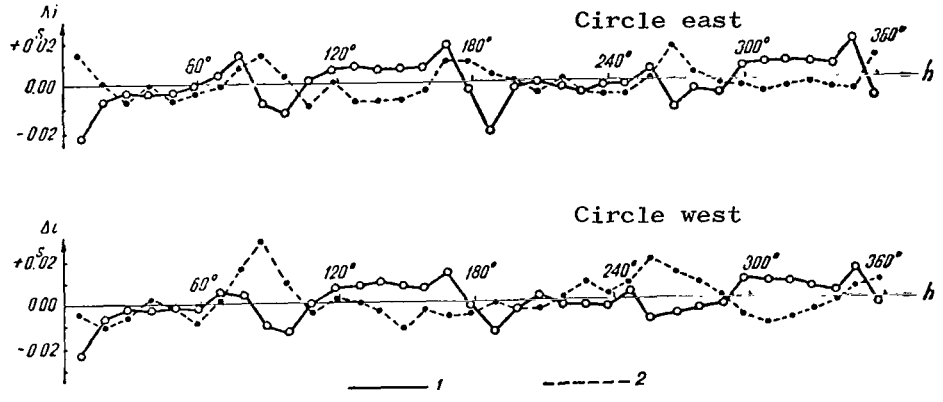

Figure 8. Corrections for irregularities in the pivot figures to the inclination of the instrument's axis obtained from the investigation with the interferometer in 1962 (2) and 1967 (1).

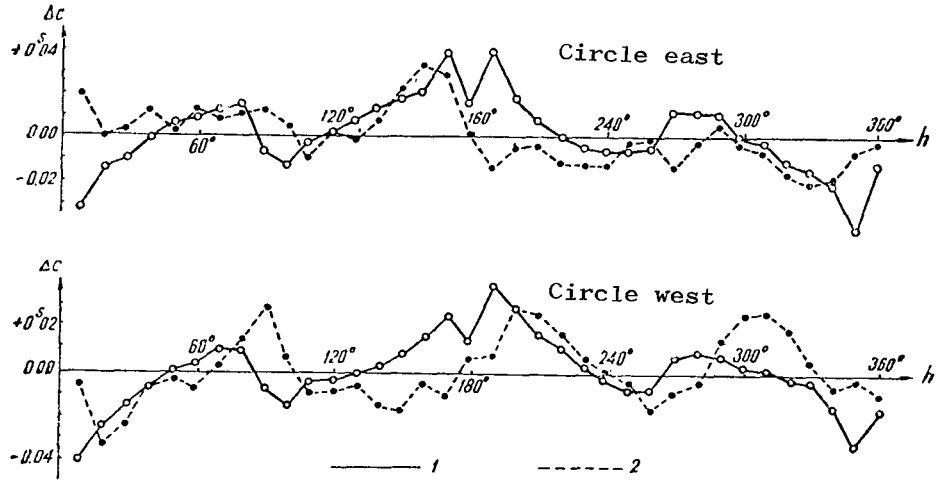

Figure 9. Corrections for irregularities in the pivot figures to the instrument's collimation obtained with the interferometer in 1962 (2) and 1967 (1).

TABLE 10

/100

Declination belt	Corrections for error of the pivots		
	From observations of stars	From measurements: From microscope-micrometer	From measurements: With interferometer
From −10° to −20°	$-0^s.007$	$-0^s.014$	$-0^s.011$
0 −10	−0.006	−0.004	−0.003
0 +10	+0.004	+0.001	+0.001
+10 +20	+0.005	+0.003	+0.005
+20 +30	+0.005	−0.001	+0.008
+30 +40	0.000	−0.010	−0.002
+40 +50	−0.007	0.013	−0.015
+50 +60	−0.021	−0.008	−0.011
+60 +70	−0.017	−0.007	−0.005
+70 +80	−0.009	−0.007	−0.002
+80 +90	+0.001	−0.001	+0.002

APPENDIX 1

Circle reading	Tie-in system: Method 1	Tie-in system: Method 2	Tie-in system: Method 3	Fundamental system: Method I	Fundamental system: Method II	Fundamental system: Method III	Average value of the coordinate x
0°	0	0	0	−5.886	−5.886	−5.887	−5.886
10	+ 0.476	+ 0.478	+ 0.471	−5.410	−5.408	−5.416	−5.411
20	+ 1.096	+ 1.104	+ 1.101	−4.790	−4.782	−4.786	−4.786
30	+ 1.875	+ 1.866	+ 1.858	−4.011	−4.020	−4.029	−4.020
40	+ 2.764	+ 2.765	+ 2.761	−3.122	−3.121	−3.126	−3.123
50	+ 3.712	+ 3.711	+ 3.704	−2.174	−2.175	−2.183	−2.177
60	+ 4.753	+ 4.755	+ 4.741	−1.133	−1.131	−1.146	−1.137
70	+ 5.811	+ 5.814	+ 5.812	−0.075	−0.072	−0.075	−0.074
80	+ 6.889	+ 6.876	+ 6.889	+1.003	+0.990	+1.002	+0.998
90	+ 7.916	+ 7.909	+ 7.911	+2.030	+2.023	+2.024	+2.026
100	+ 8.879	+ 8.881	+ 8.884	+2.993	+2.995	+2.997	+2.995
110	+ 9.768	+ 9.770	+ 9.765	+3.882	+3.884	+3.878	+3.881
120	+10.565	+10.557	+10.556	+4.679	+4.671	+5.669	+4.673
130	+11.206	+11.194	+11.201	+5.320	+5.308	+5.314	+5.314
140	+11.696	+11.697	+11.691	+5.810	+5.811	+5.804	+5.808
150	+12.015	+12.007	+12.016	+6.129	+6.121	+6.129	+6.126
160	+12.139	+12.142	+12.145	+6.253	+6.256	+6.258	+6.256
170	+12.090	+12.087	+12.091	+6.204	+6.201	+6.204	+6.203
180	+11.836	+11.827	+11.838	+5.950	+5.941	+5.951	+5.947
190	+11.421	+11.435	+11.422	+5.535	+5.549	+5.535	+5.540
200	+10.822	+10.828	+10.824	+4.936	+4.942	+4.937	+4.938
210	+10.058	+10.058	+10.059	+4.172	+4.172	+4.172	+4.172
220	+ 9.171	+ 9.186	+ 9.194	+3.285	+3.300	+3.307	+3.297
230	+ 8.174	+ 8.193	+ 8.188	+2.288	+2.307	+2.301	+2.299
240	+ 7.107	+ 7.114	+ 1.126	+1.221	+1.228	+1.239	+1.229
250	+ 5.993	+ 6.007	+ 6.016	+0.107	+0.121	+0.129	+0.119
260	+ 4.867	+ 4.875	+ 4.878	−1.019	−1.011	−1.009	−1.013
270	+ 3.776	+ 3.771	+ 3.784	−2.110	−2.115	−2.103	−2.109
280	+ 2.769	+ 2.760	+ 2.773	−3.117	−3.126	−3.114	−3.119
290	+ 1.851	+ 1.861	+ 1.855	−4.035	−4.025	−4.032	−4.031
300	+ 1.059	+ 1.053	+ 1.051	−4.827	−4.833	−4.836	−4.832
310	+ 0.420	+ 0.418	+ 0.419	−5.466	−5.468	−5.468	−5.467
320	− 0.048	− 0.056	− 0.049	−5.934	−5.943	−5.936	−5.937
330	− 0.322	− 0.318	− 0.315	−6.208	−6.204	−6.202	−6.205
340	− 0.406	− 0.403	− 0.401	−6.292	−6.289	−6.288	−6.290
350	− 0.304	− 0.304	− 0.296	−6.190	−6.190	−6.183	−6.188

APPENDIX 2

/101

Circle reading	Circle east				Circle west			
	Eastern pivot		Western pivot		Eastern pivot		Western pivot	
	x	y	x	y	x	y	x	y
0°	+0.511	+2.230	−5.886	−2.070	+1.781	−0.313	−2.284	+1.586
10	+0.871	+2.104	−5.411	−3.055	+1.848	−0.014	−1.974	+1.966
20	+1.241	+1.930	−4.786	−3.955	+1.828	+0.276	−1.594	+2.276
30	+1.550	+1.693	−4.020	−4.714	+1.771	+0.588	−1.197	+2.518
40	+1.822	+1.389	−3.123	−5.375	+1.633	+0.866	−0.750	+2.678
50	+2.034	+1.065	−2.177	−5.840	+1.457	+1.139	−0.246	+2.754
60	+2.181	+0.667	−1.137	−6.084	+1.218	+1.357	+0.222	+2.780
70	+2.246	+0.281	−0.074	−6.192	+0.948	+1.544	+0.690	+2.694
80	+2.269	−0.117	+0.998	−6.102	+0.643	+1.683	+1.129	+2.537
90	+2.202	−0.524	+2.026	−5.847	+0.314	+1.755	+1.536	+2.285
100	+2.089	−0.876	+2.995	−5.397	−0.021	+1.783	+1.907	+1.991
110	+1.888	−1.223	+3.881	−4.788	−0.364	+1.758	+2.224	+1.625
120	+1.643	−1.551	+4.673	−4.038	−0.646	+1.681	+2.451	+1.220
130	+1.430	−1.833	+5.314	−3.195	−0.936	+1.547	+2.619	+0.747
140	+1.020	−2.052	+5.808	−2.188	−1.201	+1.357	+2.728	+0.264
150	+0.644	−2.183	+6.126	−1.134	−1.405	+1.142	+2.739	−0.205
160	+0.271	−2.263	+6.256	−0.035	−1.572	+0.894	+2.650	−0.677
170	−0.11'	−2.316	+6.203	+1.028	−1.695	+0.599	+2.492	−1.142
180	−0.493	−2.246	+5.947	+2.068	−1.738	+0.321	+2.263	−1.561
190	−0.879	−2.105	+5.540	+3.070	−1.750	−0.002	+1.971	−1.941
200	−1.226	−1.904	+4.938	+3.960	−1.709	−0.316	+1.601	−2.264
210	−1.557	−1.665	+4.172	+4.718	−1.624	−0.613	+1.190	−2.503
220	−1.803	−1.364	+3.297	+5.350	−1.482	−0.902	+0.746	−2.796
230	−2.008	−1.041	+2.299	+5.812	−1.300	−1.133	+0.304	−2.801
240	−2.159	−0.667	+1.229	+6.1'0	−1.129	−1.354	−0.160	−2.770
250	−2.240	−0.295	+0.119	+6.215	−0.892	−1.510	−0.662	−2.687
260	−2.262	+0.115	−1.013	+6.141	−0.632	−1.673	−1.108	−2.532
270	−2.215	+0.490	−2.109	+5.866	−0.368	−1.745	−1.516	−2.305
280	−2.106	+0.879	−3.119	+5.421	0.064	−1.774	−1.886	−1.992
290	−1.904	+1.240	−4.031	+4.802	+0.220	−1.750	−2.224	−1.630
300	−1.667	+1.560	−4.832	+4.020	+0.523	−1.673	−2.474	−1.204
310	−1.384	+1.828	−5.467	+3.117	+0.805	−1.519	−2.660	−0.764
320	−1.044	+2.038	−5.937	+2.148	+1.054	−1.358	−2.754	−0.295
330	−0.673	+2.188	−6.205	+1.136	+1.309	−1.134	−2.751	+0.215
340	−0.289	+2.270	−6.290	+0.071	+1.511	−0.889	−2.694	+0.677
350	+0.105	+2.267	−6.188	−1.033	+1.668	−0.607	−2.522	+1.155

APPENDIX 3

Circle east

h	Correction to the azimuth			Correction to the inclination			Correction to the collimation		
	1967	1955	Difference	1967	1955	Difference	1967	1955	Difference
3°41′	−22	−10	−12	−6	+ 2	− 8	−22	−10	−12
18 41	−22	−12	−10	−3	0	− 3	−22	−11	−11
33 41	− 2	− 2	0	+2	+ 8	− 6	0	+ 2	− 2
48 41	+12	+12	0	+2	+11	− 9	+ 9	+16	− 7
63 41	+26	+10	+16	−3	+17	−20	+ 8	+19	−11
78 41	+28	+23	+ 5	−2	+ 8	−10	− 4	+13	−17
93 41	+32	+29	+ 3	−6	− 4	−10	− 7	− 6	− 1
108 41	+22	+15	+ 7	−1	−14	+13	− 8	−18	+10
123 41	+ 5	+ 3	+ 2	+6	−16	+22	+ 2	−15	+17
138 41	−20	− 5	−15	+8	−10	+18	+20	− 3	+23
153 41	−26	−30	+ 4	+3	− 3	+ 6	+25	+26	− 1
168 41	−32	−29	− 4	−4	− 4	0	+31	+27	+ 4
183 41	−35	−16	−19	−9	+ 3	−11	+35	+16	+19
198 41	−22	−20	− 2	0	+ 8	− 8	+20	+16	+ 4
213 41	− 4	− 4	0	+6	+11	− 5	+ 1	− 3	+ 4
228 41	+17	+13	+ 4	+1	+10	− 9	−12	−17	+ 5
243°41′	+32	+24	+ 8	− 1	+ 4	− 5	−12	−15	+ 3
258 41	+40	+21	+19	0	+ 1	− 1	− 8	− 5	− 3
273 41	+32	+37	− 5	−12	− 1	−11	+14	+ 3	+11
288 41	+16	+11	+ 5	+ 5	−11	+16	0	+14	−14
303 41	0	− 4	+ 4	+ 8	−12	+20	− 6	+ 8	−14
318 41	−19	−19	0	+ 7	− 8	+15	−19	− 9	−10
333 41	−31	−21	−10	+ 2	− 3	+ 5	−29	−18	−11
348 41	−32	−23	−11	+ 2	− 4	+ 6	−32	−22	−10

APPENDIX 4

/102

Circle west

h	Correction to the azimuth			Correction to the inclination			Correction the collimation		
	1967	1955	Difference	1967	1955	Difference	1967	1955	Difference
3°41′	−41	−18	−23	−10	+10	−20	−42	−17	−25
18 41	−32	−27	− 5	+ 4	+ 1	+ 3	−29	−26	− 3
33 41	−22	−23	+ 1	+ 2	+ 6	− 4	−17	−16	− 1
48 41	− 6	− 5	− 1	+ 4	+ 6	− 2	− 2	+ 2	− 4
63 41	+16	+ 9	+ 7	0	+ 4	− 4	+ 7	+ 8	− 1
78 41	+34	+28	+ 6	0	+ 4	− 4	+ 7	+ 9	− 2
93 41	+39	+45	− 6	− 8	+14	−22	−10	+11	−21
108 41	+28	+16	+12	+14	− 6	+20	+ 5	−11	+16
123 41	+22	+ 4	+18	+ 6	−15	+21	− 6	−14	+ 8
138 41	+ 3	+ 2	+ 1	+ 4	−14	+18	0	−11	+11
153 41	−16	− 6	−10	+ 4	−10	+14	+16	+ 1	+15
168 41	−24	−23	− 1	+ 4	− 5	+ 9	+25	+22	+ 3
183 41	−32	−18	−14	−12	+15	−27	+33	+17	+16
198 41	−30	−18	−12	+ 2	+ 3	− 1	+28	+16	+12
213 41	−23	−19	− 4	0	− 1	+ 1	+20	+17	+ 3
228 41	−10	− 9	− 1	− 6	+ 8	−14	+11	0	+11
243 41	+10	+ 8	+ 2	− 2	+ 8	−10	− 2	−11	+ 9
258 41	+30	+13	+17	+ 2	+ 8	− 6	− 8	−11	+ 3
273 41	+34	+40	− 6	− 2	+ 8	−10	+ 3	− 5	+ 8
288 41	+34	+21	+13	+ 8	− 2	+10	+ 4	+ 9	− 5
303 41	+32	+20	+12	+14	− 9	+23	+ 5	+18	−13
318 41	+ 6	+ 4	+ 2	+ 8	−13	+21	0	+12	−12
333 41	−15	−19	+ 4	− 2	−13	+11	−13	−11	− 2
348 41	−30	−21	− 9	− 2	− 6	+ 4	−29	−20	− 9

APPENDIX 5

Circle reading	Circle east				Circle west			
	Eastern pivot		Western pivot		Eastern pivot		Western pivot	
	dz	*dt*	*dz*	*dt*	*dz*	*dt*	*dz*	*dt*
0°	+0.55	+0.23	+1.03	−0.22	0.00	+0.43	+0.38	+0.71
10	+0.58	+0.24	+1.35	−0.46	−0.35	+0.76	+0.45	+0.71
20	+0.60	+0.05	+1.64	−0.67	−0.62	+1.07	+0.49	+0.68
30	+0.50	−2.05	+1.56	−2.85	−0.90	+1 28	−0.43	+0.68
40	−1.12	−0.35	+0.52	−3.11	−3.48	+1.30	−3.47	+0.54
50	−2.24	+0.52	−2.32	−0.37	−1.84	+0.64	−0.36	−2.29
60	+0.15	+0.57	+0.22	+0.10	−0.23	−0.66	+0.66	−1.78
70	+0.27	+0.54	+0.91	−0.51	+0.02	+0.72	+0.94	+0.32
80	+0.34	+0.61	+0.57	−0.89	+0.53	+0.60	+0.88	+0.34
90	+0.30	+0.49	+0.26	−1.24	+1.00	+0.25	+0.98	+0.45
100	+0.30	+0.59	+0.05	−1.46	+1.27	−0.14	+0.90	+0.43
110°	+0.44	+0.50	−0.20	+1.54	+1.44	−0.41	+0.94	+0.64
120	+0.49	−1.54	−0.46	+0.59	+1.54	−0.68	+0.34	+0.49
130	−0.93	−1.16	−1.58	−1.35	−0.29	−0.82	−3.15	+0.15
140	−1.75	+0.34	−3.66	+0.59	−0.57	−1.73	−0.96	−2.18
150	+0.72	+0.32	−0.34	+0.78	+0.90	−2.02	+0.54	−0.81
160	+0.81	+0.25	−0.32	+0.48	+0.66	−0.31	+0.54	+0.81
170	+0.76	+0.22	+0.77	+0.06	+0.14	+0.06	+0.41	+0.83
180	+0.71	+0.19	+1.17	−0.26	−0.14	+0.43	+0.47	+0.81
190	+0.67	+0.18	+1.43	−0.46	−0.47	+0.76	+0.34	+0.79
200	+0.62	+0.02	+1.64	−0.61	−0,70	+1.09	+0.41	+0.79
210	+0.47	−1.76	+1.64	−1.92	−0.80	+1.26	−0.11	+0.66
220	−1.15	−1.44	+0.22	−2.92	−2.71	+1.34	−3.64	+0.49
230	−1.93	+0.47	−2.95	−0.34	−1.80	+0.68	−0.28	−2.35
240	+0.16	+0.48	+0.79	+0.30	−0.27	−0.35	+0.71	−1.24
250	+0.28	+0.58	+0.85	+0.56	+0.06	+0.64	+0.88	+0.26
260	+0.34	+0.60	+0.46	+0.94	+0.49	+0.52	+0.92	+0.26
270	+0.40	+0.54	+0.18	+1.28	+0.86	+0.14	+0.90	+0.26
280	+0.27	+0.49	−0.08	+1.48	+1.23	−0.16	+0,84	+0.24
290	+0.26	+0.40	−0.24	+1.54	+1.52	−0.47	+0.81	+0.34
300	+0.19	−1.70	−0.40	+0.30	+1.58	−0.62	+0.24	+0.34
310	−1.86	−1.93	−2.44	−1.00	−0.66	−0.78	−3.34	−0.06
320	−1.72	+0.10	−3.92	+0.60	+0.14	−2.39	−0.64	−2.89
330	+0.39	+0.18	−0.34	+0.82	+1.02	−2.10	+0.32	−0.77
340	+0.57	+0.10	+0.38	+0.52	+0.76	−0.33	+0.32	+0.58
350	+0.60	+0.17	+0.79	+0.12	+0.35	+0.04	+0.34	+0.64

APPENDIX 6

/103

Circle reading	Circle east				Circle west			
	Eastern pivot		Western pivot		Eastern pivot		Western pivot	
	dz	*dt*	*dz*	*dt*	*dz*	*dt*	*dz*	*dt*
0°	+0.34	+0.04	+0.52	−0.66	−0.42	+0.32	−0.08	+0.28
10	+0.34	+0.04	+0.84	−0.88	−0.66	+0.64	0.00	+0.36
20	+0.34	−0.16	+1.12	− .04	−0.92	+0.94	+0.08	+0.28
30	+0.28	−1.12	+1.16	−1.36	−0.96	+1.18	−0.32	+0.28
40	+0.04	+0.12	+0.98	−1.48	−1.46	+1.16	−0.76	+0.16
50	−0.78	+0.28	+0.04	−0.72	−0.96	+0.84	+0.16	−0.16
60	0.00	+0.36	+0.52	−0.26	−0.56	−0.20	+0.28	−0.30
70	−0.08	+0.36	+0.62	+0.14	+0.16	+0.44	+0.32	−0.12
80	−0.10	+0.38	+0.32	+0.60	+0.28	+0.48	+0.34	−0.16
90	−0.10	+0.34	−0.04	+0.88	+0.60	+0.08	+0.32	−0.18
100	−0.04	+0.32	−0.38	+1.08	+0.96	−0.22	+0.24	−0.18
110	+0.08	+0.20	−0.56	+1.28	+1.12	−0.44	+0.30	−0.08
120	+0.04	−1.06	−0.78	+1.12	+1.26	−0.74	−0.12	0.00
130	−0.06	−0.48	−1.26	+0.40	+0.98	−0.90	−0.24	−0.08
140	0.00	+0.18	−2.08	+0.40	+0.68	−1.32	−0.12	−0.12
150	+0.28	+0.12	−0.58	+0.52	+0.60	−1.80	+0.04	+0.06
160	+0.32	+0.08	−0.20	+0.10	+0.40	−0.40	0.00	+0.16
170	+0.30	+0.06	+0.20	−0.32	−0.06	−0.04	+0.02	+0.20
180	+0.28	+0.12	+0.56	−0.60	−0.44	+0.34	+0.08	+0.28
190	+0.24	−0.06	+0.84	−0.72	−0.72	+0.58	−0.04	+0.28
200	+0.16	−0.18	+1.02	−0.88	−0.94	+0.92	0.00	+0.24
210	+0.04	−0.80	+1.20	−1.28	−1.00	+1.14	−0.32	+0.16
220	−0.14	+0.06	+1.00	−1.36	−1.40	+1.26	−0.56	+0.04
230	−0.86	+0.22	0.00	−0.70	−0.88	+0.92	+0.08	−0.16
240	−0.08	+0.30	+0.44	−0.20	−0.58	−0.04	+0.18	−0.28
250°	−0.16	+0.44	+0.60	+0.16	−0.58	+0.44	+0.34	−0.08
260	−0.18	+0.36	+0.24	+0.56	+0.16	+0.42	+0.34	−0.18
270	−0.16	+0.38	−0.14	+0.86	+0.48	0.00	+0.36	−0.16
280	−0.18	+0.38	−0.46	+1.08	+0.76	−0.24	+0.40	−0.08
290	−0.20	+0.24	−0.64	+1.16	+1.04	−0.56	+0.28	−0.14
300	−0.18	−0.96	−0.80	+1.06	+1.08	−0.64	+0.06	−0.14
310	−0.40	−0.36	−1.20	+0.44	+0.84	−0.82	−1.12	−0.24
320	−0.38	−0.01	−2.38	+0.24	+0.56	−1.64	−0.10	−0.34
330	+0.06	−0.04	−0.68	+0.48	+0.64	−1.92	−0.08	−0.08
340	+0.16	−0.04	−0.08	+0.08	+0.38	−0.34	−0.12	+0.04
350	+0.28	−0.04	−0.20	−0.34	+0.02	−0.04	−0.12	+0.12

Circle east

h	Correction to the azimuth			Correction to the inclination			Correction to the collimation		
	1967	1962	Difference	1967	1962	Difference	1967	1962	Difference
8°41′	−30	+17	−47	−24	+13	−37	−32	+19	−54
18 41	−13	+ 1	−14	− 7	0	− 7	−14	+ 1	−15
28 41	− 8	+ 6	−14	− 4	− 5	+ 1	−10	+ 3	−13
38 41	+ 3	+16	−13	− 4	0	− 4	0	+12	−12
48 41	+12	+12	0	− 3	− 5	+ 2	+ 6	+ 4	+ 2
58 41	+18	+24	− 6	0	− 2	+ 2	+10	+11	− 1
68 41	+21	+30	− 9	+ 4	− 3	+ 7	+11	+ 8	+ 3
78 41	+20	+20	0	+12	+ 7	+ 5	+15	+11	+ 4
88 41	+42	−12	+54	− 9	+13	−22	− 8	+12	−20
98 41	+10	− 2	+12	−13	+ 4	−17	−14	+ 4	−18
108 41	+12	− 2	+14	+ 2	− 9	+11	− 2	− 9	+ 7
118 41	+11	− 7	+18	+ 6	0	+ 6	+ 2	+ 4	− 2
128 41	0	− 9	+ 9	+ 7	− 9	+16	+ 6	− 1	+ 7
138 41	−10	−17	+ 7	+ 6	− 9	+15	+12	+ 7	+ 5
148 41	−16	−30	+14	+ 6	− 7	+13	+17	+22	− 5
158 41	−20	−36	+16	+ 7	− 5	−12	+21	+32	−11
168 41	−34	−26	− 8	+18	+ 9	+ 9	+38	+28	+10
178 41	−14	0	−14	− 4	+10	+14	+14	+ 1	+13
188 41	−34	+16	−50	−22	+ 4	−26	+38	−16	+54
198 41	−18	+ 6	−24	− 2	0	− 2	+17	− 6	+23
208 41	− 6	+ 8	−14	0	− 1	+ 1	+ 6	− 6	+12
218 41	− 1	+17	−18	− 2	− 1	− 1	− 1	−13	+12
228 41	+12	+24	−12	− 4	− 4	0	− 5	−13	+ 8
238 41	+18	+31	−13	− 2	− 5	+ 3	− 8	−12	+ 4
248 41	+26	+27	− 1	− 2	− 6	+ 4	+ 8	− 4	− 4
258 41	+20	+10	+10	+ 6	+ 1	+ 5	− 6	− 3	− 3
268 41	+46	−20	+66	−12	+17	−29	+11	−17	+28
278 41	+18	+ 4	+14	− 4	+ 4	− 8	+10	− 3	+13
288 41	+10	+ 2	+ 8	− 7	− 2	− 5	+ 9	+ 3	+ 6
298 41	+10	− 9	−19	+ 7	− 2	+ 9	− 1	− 3	+ 2
308 41	+ 1	−17	+18	+ 7	− 5	+12	− 4	− 7	+ 3
318 41	− 8	−25	+17	+ 9	− 3	+12	−12	−17	+ 5
328 41	−15	−25	+10	+ 7	− 1	+ 8	−16	−21	+ 5
338 41	−22	−24	+ 2	+ 6	− 4	+10	−23	−21	− 2
348 41	−40	−10	−30	+18	− 6	+24	−43	− 8	−35
358 41	−14	− 3	−11	− 8	+11	−19	−14	− 3	−11

Circle west

h	Correction to the azimuth			Correction to the inclination			Correction to the collimation		
	1967	1962	Difference	1967	1962	Difference	1967	1962	Difference
8°41′	−38	− 6	−32	−22	− 4	−18	−40	− 6	−34
18 41	−25	−32	+ 7	− 6	− 8	+ 2	−26	−33	+ 7
28 41	−18	−26	+ 8	− 2	− 4	+ 2	−16	−24	+ 8
38 41	− 8	−12	+ 4	− 2	+ 3	− 5	− 8	− 8	0
48 41	0	− 4	+ 4	0	0	0	0	− 2	+ 2
58 41	+ 9	− 2	+11	− 2	− 8	+ 6	+ 4	− 8	+12
68 41	+10	− 2	+12	+ 6	+ 2	+ 4	+ 9	+ 2	+ 7
78 41	+19	−12	+31	+ 4	+16	−12	+ 8	+14	− 6
88 41	+44	−14	+58	−10	+28	−38	− 9	+28	−37
98 41	+13	+16	− 3	−14	+ 9	−23	−16	+ 6	−22
108 41	+20	+24	− 4	0	− 3	+ 3	− 6	−10	+ 4
118 41	+20	+21	− 1	+ 7	+ 1	+ 6	− 4	−10	+ 6
128 41	+12	+14	− 2	+ 8	0	+ 8	− 1	− 8	+ 7
138 41	+ 5	+16	−11	+10	− 4	+14	+ 2	−15	+17
148 41	− 4	+13	−17	+ 9	−14	+23	+ 8	−18	+26
158 41	−14	+ 6	−20	+ 8	− 5	+13	+16	− 7	+23
168 41	−22	+10	−32	+14	− 8	+22	+24	−11	+35
178 41	−12	− 6	− 6	− 2	− 4	+ 2	+12	+ 6	+ 6
188 41	−39	− 6	−33	−15	− 2	−13	+40	+ 6	−34
198 41	−28	− 29	+ 1	− 4	− 3	− 1	+28	+28	0
208 41	−18	−28	+10	+ 1	− 4	+ 5	+16	+26	−10
218 41	−11	−23	+12	− 2	0	− 2	+10	+18	− 8
228 41	− 2	−14	+12	− 2	+ 6	− 8	+ 2	+ 4	− 2
238 41	+ 8	− 4	+12	− 4	+ 2	− 6	− 2	0	− 2
248 41	+16	+ 1	+15	+ 3	+ 6	− 3	− 8	− 6	− 2
258 41	+19	− 2	+21	+ 3	+18	−15	− 7	−18	+11
268 41	+43	−16	+59	− 8	+10	−18	+ 6	−10	+16
278 41	+17	+21	− 4	− 6	+ 6	−12	+ 9	− 3	+12
288 41	+17	+31	−14	− 3	− 2	− 1	+ 8	+12	− 4
298 41	+21	+36	−15	+ 8	−10	+18	+ 4	+26	−22
308 41	+12	+28	−16	+ 7	−14	+21	+ 2	+28	−26
318 41	+ 4	+18	−14	+ 6	−12	+18	− 2	+20	−22
328 41	− 2	+ 2	− 4	+ 4	− 8	+12	− 4	+ 6	−10
338 41	−15	− 8	− 7	+ 2	− 3	+ 5	−15	− 6	− 9
348 41	−30	− 2	−28	+12	+ 2	+10	−32	− 2	−30
358 41	−15	− 8	− 7	− 4	+ 6	−10	−15	− 8	− 7

REFERENCES

1. Bykov, M. F., Kim, G., Trudy tashkentskoy astronomicheskoy observator [Transactions of the Tashkent Astronomical Observatory], Series 2, Vol. 5, 1957.

2. Boroditskiy, I. M., Trudy tashkentskoy astronomicheskoy observator [Transactions of the Tashkent Astronomical Observatory], Series 2, Vol. 10, 1964.

3. Moreau, F., Verbaandert, I., Bulletin astronomique, Ser. 2, Mémoires et variétés, Vol. 13, Paris, 1948.

4. Koval'skiy, A., Issledovaniye figury tsapfov bol'shogo passazhnogo instrumenta Ertelya [Investigation of the Figure of the Pivots of the Large Ertel' Transit Instrument], Proceedings of the Academy of Sciences, Vol. 5, 1896.

5. Yakovkin, A. A., Ob issledovanii tsapf passazhnogo instrumenta [On the Investigation of the Pivots of a Transit Instrument], Trudy 10-y vsesoyuznoy astronomicheskoy konferentsii [Transactions of the 10th All-Union Astronomical Conference], Leningrad, 1954.

6. Villarceau, Yvon, A. I., Annales de l'Observatoire Imperial de Paris, Mémoires, Vol. 7, Paris, 1863.

7. Shishkina, V. N., Izvestiya glavnoy astronomicheskoy observatorii v Pulkove [Proceedings of the Main Astronomical Observatory in Pulkovo], Vol. 22, Issue 1, 1960, No. 166.

8. Gulyayev, A. P., Soobshcheniya GAIsh [Communications of the Shternberg Astronomical Observatory], Moscow, 1964, No. 134.

9. Starostin, A. M., Trudy TsNIIGAK, No. 148, Moscow, 1962.

10. Podobed, V. V., Soobshcheniya GAIsh [Communications of the Shtenberg Astronomical Observatory], Moscow, 1953, No. 94.

11. Gulyayev, A. P., AZh, Vol. 35, No. 1, Moscow, AN USSR Press, 1958.

12. Krupp, N. Ya., Optiko-mekhanicheskiye izmeritel'nyye pribory [Optico-Mechanical Measuring Instruments], Moscow-Leningrad, Mashgiz, 1962.

13. Tursunov, O. S., Tsirkulyar TAO [Circular of the Tashkent Astronomical Observatory (TAO)], Tashkent, 1966, No. 342.

NASA-Langley, 1971 —— 30

"The aeronautical and space activities of the United States shall be conducted so as to contribute . . . to the expansion of human knowledge of phenomena in the atmosphere and space. The Administration shall provide for the widest practicable and appropriate dissemination of information concerning its activities and the results thereof."

—NATIONAL AERONAUTICS AND SPACE ACT OF 1958

NASA SCIENTIFIC AND TECHNICAL PUBLICATIONS

TECHNICAL REPORTS: Scientific and technical information considered important, complete, and a lasting contribution to existing knowledge.

TECHNICAL NOTES: Information less broad in scope but nevertheless of importance as a contribution to existing knowledge.

TECHNICAL MEMORANDUMS: Information receiving limited distribution because of preliminary data, security classification, or other reasons.

CONTRACTOR REPORTS: Scientific and technical information generated under a NASA contract or grant and considered an important contribution to existing knowledge.

TECHNICAL TRANSLATIONS: Information published in a foreign language considered to merit NASA distribution in English.

SPECIAL PUBLICATIONS: Information derived from or of value to NASA activities. Publications include conference proceedings, monographs, data compilations, handbooks, sourcebooks, and special bibliographies.

TECHNOLOGY UTILIZATION PUBLICATIONS: Information on technology used by NASA that may be of particular interest in commercial and other non-aerospace applications. Publications include Tech Briefs, Technology Utilization Reports and Technology Surveys.

Details on the availability of these publications may be obtained from:

SCIENTIFIC AND TECHNICAL INFORMATION OFFICE

NATIONAL AERONAUTICS AND SPACE ADMINISTRATION

Washington, D.C. 20546